PULSED OPTICAL STIMULATION OF LUMINESCENCE FROM QUARTZ

M L Chithambo

A thesis submitted to the University of Edinburgh in fulfilment of the requirements for the degree of Doctor of Philosophy

2000

Abstract

A light emitting diode based pulsing system capable of producing luminescence time–resolved spectra was developed for study of optically stimulated luminescence from quartz and feldspar. The aim of the pulsed optical stimulation method is to separate in time stimulation and detection of luminescence so that luminescence can be measured in the absence of scatter from stimulating light unlike in conventional continuous stimulation where luminescence monitored includes such scatter. Pulsed optical stimulation not only offers the possibility of improvements in signal to background ratio but also the ability to investigate the time dependence of luminescence emission relative to the time of stimulation. Although study of pulsed luminescence has been dominated by laser–based systems, a pulsing system based on light emitting diodes offers, in comparison, advantages of simplicity and economy.

The present system has been used over a wide range of pulse widths (25 ns (FWHM) – 30 μs) and dynamic ranges (40 ns – 64 μs). The system can be adapted for use with a wide range of wavelengths with pulse widths from 25 ns (FWHM) to as long as desired.

Luminescence time–resolved spectra have been recorded from feldspar and quartz. Half lives measured from feldspar range from 25 ns and from quartz, 20 – 28 μs. Properties of luminescence half lives from quartz were studied in detail as a function of experimental parameters such as stimulation time, temperature, radiation dose, and preheating method. The influence of temperature on luminescence intensity was studied for time–resolved spectra recorded at long stimulation times. Explanations are proposed to account for experimental results.

Acknowledgements

I first of all wish to thank my supervisor, Dr R.B. Galloway for his encouragement and support throughout the course of my research. His comments, criticisms and suggestions were beneficial in the work reported in this thesis.

I am also grateful to Mr Harry Napier for technical assistance and for sharing his experience and knowledge of the equipment in the laboratory. I have learnt much from him. His sense of humour, at times, kept me going. Thanks are also due to Mr Paul Harris for keeping the equipment in good repair at all times.

I also wish to thank many friends who made varied and positive contributions to my work. Professor John Monteith read some parts of this thesis and made useful comments on style for which I am grateful. I also wish to thank Moira Kirwan for her encouragement. Peter, Janet and Frank Kirwan were always helpful and for this, I am very grateful. I also wish to thank Rev. Sandy Young and the Session of the Mayfield Salisbury Church of Scotland as well as the World Mission for kindly extending to myself and my family use of the church house flat at 18 West Mayfield.

Finally, I thank my wife, Bertha, and children, Sungeni, Tamani and N'lamwai for being good.

Dedication

I dedicate this thesis to my parents.

Contents

Chapter 1

Introduction

1.1 Luminescence

Luminescence occurs as a result of stimulation of a mineral which has previously been exposed to ionizing radiation. When stimulation is by heating, the luminescence is called thermoluminescence. Optically stimulated luminescence is when the stimulation is by light. The underlying physics of luminescence stimulation is that defects in a crystal lattice act as charge traps and recombination centres. Ionizing radiation energy can move charges to these traps which are metastable. Subsequent stimulation then de-traps the charges and luminescence is emitted when the charges make a transition to a lower energy state.

Applications of luminescence phenomena are based on the premise that the intensity of luminescence depends on the amount of radiation that the sample has been exposed to. Radiation dosimetry measurements are made on this assumption. Archaeological and geological dating are possible because of the presence in minerals of traps which are able to retain their charge for thousands of years. The age calculated relates to some event which last

emptied the traps such as firing in case of pottery or exposure to sunlight in the case of wind blown sediments as further exposure to sunlight is impossible because of subsequent deposits. Applications of luminescence to dating do not usually include cases where irradiation is followed by nearly instantaneous emission of light such as fluorescence or phosphorescence.

The application of optically stimulated luminescence was first introduced by Huntley *et al* [1] who used the 514 nm line from an argon ion laser to stimulate luminescence from sedimentary quartz. The aim of that work was to test the method for dating and ever since a major application of optically stimulated luminescence has been to dating. In dating, the age is calculated from the relationship between absorbed radiation dose (Equivalent dose) and the radiation dose rate from surrounding soil:

$$Age = \frac{Equivalent\,dose\,(Gy)}{Radiation\,dose\,rate\,(Gy/year)}$$

The sample radiation dose rate can be measured in the laboratory. Optically stimulated luminescence measurements are made to determine the equivalent dose. In principle, this is done by estimating the standard laboratory irradiation that produces the same signal as the natural radiation.

There are two methods of measuring optically stimulated luminescence, the traditional one of continuous optical stimulation, the other, pulsed optical stimulation is a relatively new and potentially better method and is the main subject of this thesis.

1.2 Continuous optical stimulation

Optically stimulated luminescence measurements have normally been performed using continuous optical stimulation. In this method, the stimulating

light is on continuously and the luminescence is monitored in the presence of the stimulating light at a different wavelength. To reduce the background signal due to scattered stimulating light may require the use of two sets of filters; band pass filters to transmit the luminescence and reject scattered light and often also long pass filters to restrict the wavelength range of the luminescence stimulating light.

Since the work of Huntley *et al* [1] where green light was used, there has been research on alternative stimulating light sources at different wavelengths some of which have been adopted for stimulation of luminescence from quartz and feldspar. Examples include the use of infrared light filtered from a Xe-lamp by Hütt *et al* [2], infrared light emitting diodes by Poolton and Bailiff [3], green light emitting diodes by Galloway [4], and more recently blue light emitting diodes by Hong and Galloway [5] and by Bötter-Jensen *et al* [6]. The two main wavelengths for optical stimulation of luminescence are green light which is effective with quartz and feldspar and infrared light which is most appropriate for feldspar [7].

1.3 Pulsed optical stimulation

The aim of the pulsed optical stimulation method is to separate in time the stimulation and detection of luminescence so that luminescence can be measured in the absence of scatter from stimulating light.

There are two possible reasons for using pulsed stimulation of luminescence, one to improve the signal to background ratio and the other to investigate the time dependence of luminescence emission relative to the time of stimulation. An improved signal to background ratio is achievable [8, 9] as the luminescence signal is recorded in the absence of scatter from the

luminescence stimulating light. It only becomes necessary to select the stimulating pulse width that experimentally offers the best signal to background ratio. Apart from an improved signal to background ratio, luminescence time–resolved spectra can be recorded which can be resolved into various components with associated lifetimes [10, 11] which may aid an understanding of the physical processes responsible for luminescence. In addition, by separating in time the stimulation of the source and the detection of luminescence, the method provides a potential for detecting luminescence in emission bands which are close to the wavelength used to induce the luminescence.

The option of pulsing as a luminescence stimulating method was discussed by Sanderson and Clark [12] who used pulses (10 ns width) from an N_2 dye laser to stimulate luminescence from alkali feldspars. The stimulation wavelength selected was 470 nm. Luminescence emission was recorded as a function of time after the pulse and filters were used to block the excitation light from entering the photomultiplier. Markey *et al* [13] used the 514 nm line from an argon ion laser to study pulsed luminescence from aluminum oxide (α-$Al_2O_3 : C$), a luminescence dosimeter. Pulse widths of 10–100 ms were used and luminescence was recorded for 0.5 s after the end of the pulse. This work was further extended to other wavelengths of stimulating light by McKeever *et al* [8]. Clark *et al* [10] discussed the development of a laser based pulsing system (5 ns width) with stimulation wavelength of 850 nm and gave some examples of luminescence time–resolved spectra from feldspars. Bulur and Göksu [9] reported luminescence from α-$Al_2O_3 : C$ using pulsed 565 nm green light emitting diodes. Pulse widths of 1 s were used and luminescence was recorded for 4 s after the end of the pulse. Clark and Bailiff [11] using the previous system [10] reported further investigations concerning the dependence of feldspar time–resolved spectra on the wavelength of the

luminescence detected.

For this thesis, a pulsed light emitting diode system capable of producing time–resolved spectra was developed. The system was used to pulse light emitting diodes with pulse widths ranging from 25 ns (FWHM) up to 30 μs. Preliminary tests concerned the study of luminescence time–resolved spectra from feldspar. This was followed by detailed measurements from quartz which is the main focus of this thesis.

1.4 Aims of the thesis

The aims of this thesis are to demonstrate that studies of pulsed optical stimulation of luminescence from feldspar and quartz for half life analysis are possible using a light emitting diode based pulsing system. Properties of half lives then provide new knowledge that may aid in understanding the physical processes responsible for the emission of optically stimulated luminescence from quartz. This knowledge is derived from the nature of half lives abstracted from luminescence time–resolved spectra recorded under various experimental conditions.

1.4.1 Synopsis of the thesis

Chapter 1 discusses the theoretical aspects of luminescence in general and continuous and pulsed optical stimulation in particular. Chapter 2 will review some models that explain the emission of optically stimulated luminescence. Chapter 3 will describe experimental apparatus used for measurements reported in this thesis followed in chapter 4 by a discussion of the experimental techniques used. In chapter 5 will be presented results of preliminary measurements that were done prior to the more detailed work reported in later

chapters. The development, testing and implementation of the light emitting diode based pulsing system is also discussed in chapters 3, 4 and 5. Chapter 6 will present results of half life measurements from quartz that were made using green and blue light emitting diodes for stimulation of luminescence. This will be followed by a discussion of experimental results in chapter 7 and overall conclusions of the research in chapter 8.

Chapter 2

Luminescence Models

The theory of luminescence emission and its applications has been discussed in many texts e.g [14, 15, 16, 17] and reviewed in many articles e.g [18]. A model that leads to emission of luminescence is illustrated in Fig. 2.1 using a simple energy band diagram of one electron trap and one luminescence centre [16]. Ionizing radiation from natural or laboratory sources enables electrons to be transferred from the valence band to an electron trap T, at an energy E below the conduction band. The charges can then be excited from the trap to the recombination centre via the conduction band. If the transition from the conduction band to the recombination centre is radiative, luminescence is emitted. If excitation from the trap to the conduction band is achieved by heating, the process is called thermoluminescence. If light is used, the process is called optically stimulated luminescence (or photoluminescence).

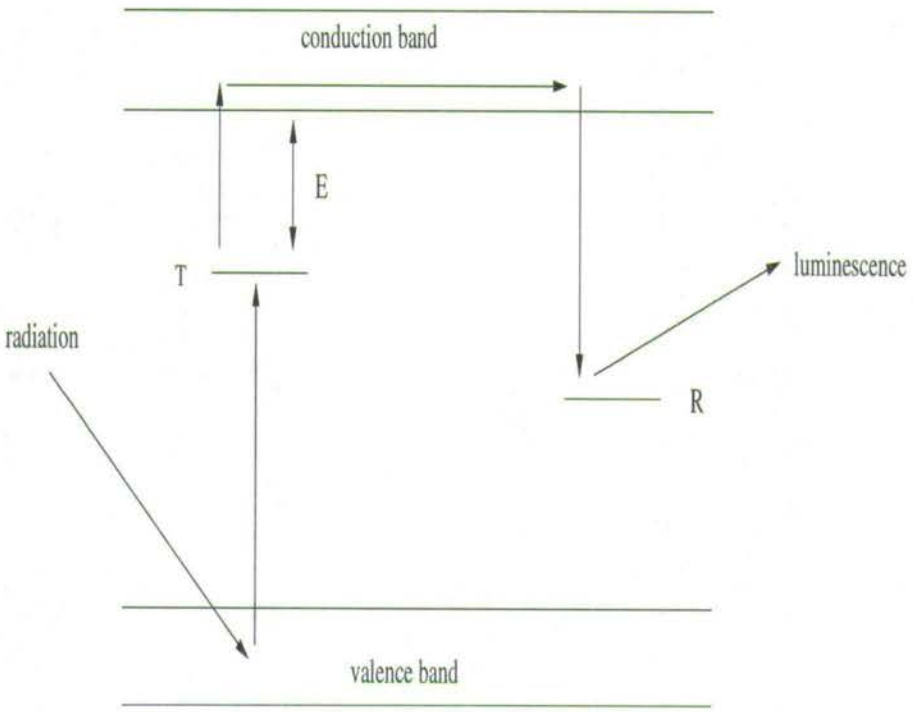

Figure 2.1 An energy band diagram to describe the process of luminescence emission. Ionizing radiation can transfer electrons to an electron trap T, at an energy E below the conduction band. The electrons can then be thermally or optically excited to the conduction band. Luminescence is emitted in the transition from the conduction band to the recombination centre, R.

2.1 Continuous optical stimulation of luminescence

The method of optical stimulation of luminescence for dating applications introduced by Huntley *et al* [1], is variously referred to as Continuous or Continuous wave optical stimulation of luminescence [7]. In this technique, light of a particular wavelength is continuously shone on a sample to stimulate luminescence. If the emitted luminescence is monitored as a function of time, the luminescence is observed to decrease as a function of time. An example of the fall of luminescence with time is shown in Fig. 2.2 from a sample of quartz, the mineral studied in this thesis. The decrease of luminescence with time indicates the emptying of traps [16, 18]. By comparison, in thermoluminescence the emptying of traps appears as a series of temperature–resolved emission peaks.

Studies concerning the nature and identity of traps involved in the emission of luminescence from quartz suggest that some traps responsible for thermoluminescence are also involved in optically stimulated luminescence [19, 21, 20, 22]. Smith *et al* [19] proposed that charges responsible for the emission of optically stimulated luminescence originate from the same trap that is responsible for the thermoluminescence that appears at $325^{o}C$. Later, Smith and Rhodes [20] and Spooner [21] reported that optical stimulation moves charges from the $325^{o}C$ thermoluminescence trap to the conduction band from where part of the charge recombines with luminescence centres to produce optically stimulated luminescence, and that some of the charge gets re-trapped at other defects in the lattice. Bailey *et al* [23] also recently studied the characteristics of the decrease of luminescence with time of optical stimulation and suggested the possibility of

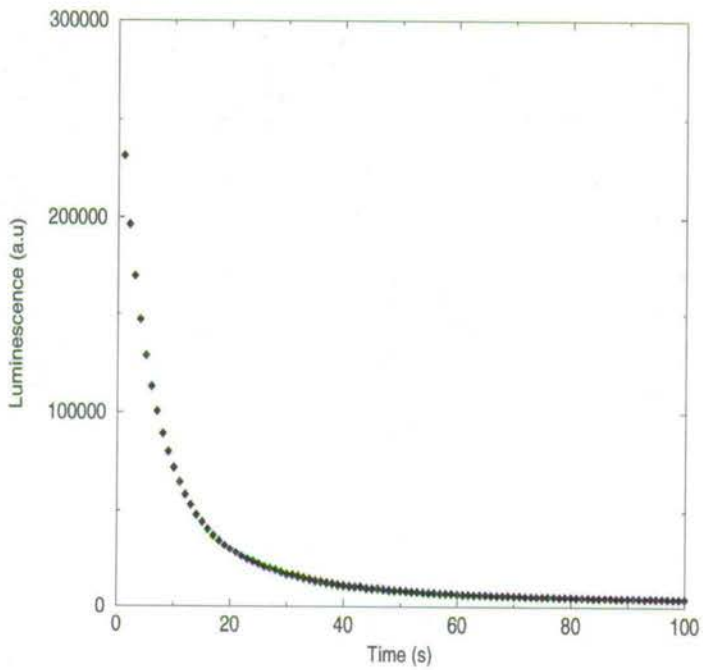

Figure 2.2 An example of the time dependence of luminescence emission from quartz.

an intermediate trap between the $325^{o}C$ thermoluminescence trap and luminescent recombination centre. The previous studies [19, 20, 21, 23] were all done using optical stimulation by the 514.5 nm wavelength from an Ar ion laser. Murray and Wintle [24] who used green light filtered from a halogen lamp concluded that shallow traps below about $150^{o}C$ do not contribute a large fraction of the OSL signal by direct stimulation.

An alternative suggestion for the emission of optically stimulated luminescence was proposed by Huntley *et al* [25] from their study of natural quartz, that optically stimulated luminescence in quartz is due to a range of traps and not only the $325^{o}C$ thermoluminescence trap. McKeever and

Chen [18] have discussed possible models to explain the emission of optically stimulated luminescence. In the simplest of these, one electron trap with a trapped electron concentration n interacts with one luminescence centre where recombination follows. Then if m and n_c denote, respectively, the concentration of holes, and electrons in the conduction band, and if f is the rate at which light stimulates electrons into the conduction band, one writes

$$\frac{dn_c}{dt} = -\frac{dn}{dt} + \frac{dm}{dt}$$

since for charge neutrality,

$$n_c + n = m.$$

Further, assuming negligible re-trapping and that

$$\frac{dn_c}{dt} << \frac{dn}{dt}, \frac{dm}{dt}$$

and also that $n_c << n, m$ then the intensity of emitted luminescence I_{lum} is given by

$$I_{lum} = -\frac{dn}{dt} = nf$$

the solution of which is

$$I_{lum} = I_o e^{-tf}$$

where I_o is the initial luminescence intensity at time = 0.

This simple equation can be extended to include possibilities of charge getting re–trapped, competition for charge by other optically (and thermally) inactive traps and also by recombination centres some of which are non–radiative.

One empirical source of evidence for charge re–trapping is the so called photo-transferred thermoluminescence e.g [20, 22, 26]. The phenomenon is

that once low temperature thermoluminescence peaks are removed by heating the sample to a temperature above the position of the peak, the peak re-appears following optical stimulation of the sample. An example is shown in Fig. 2.3 of photo–transferred thermoluminescence following stimulation by green light (525 nm) of a quartz sample, one of the samples studied in this thesis. It is believed that charge is transferred from deep traps by light to shallow traps. In quartz, the photo-transferred peak near $110°C$ is one example of this [16, 20, 22, 26].

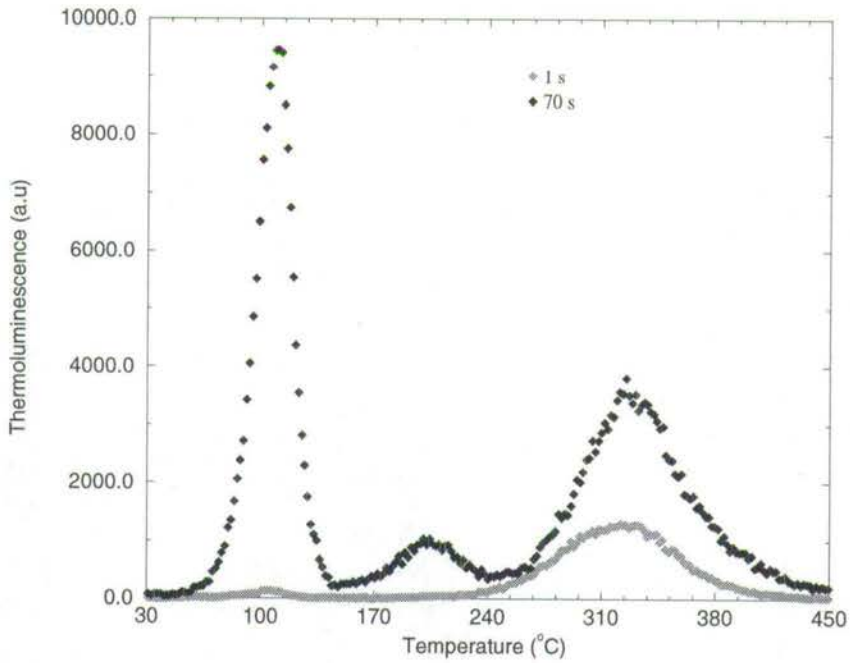

Figure 2.3 An example of photo–transferred thermoluminescence at $110°C$ and $200°C$ in a sample of quartz due to optical exposure of 1 and 70 s respectively. The intensity values from the two graphs are not normalised so that all photo–transferred peaks should clearly be distinguished.

Since the influence of other factors such as charge getting re–trapped cannot be safely ignored , the need is recognized for a model that matches more realistically experimental results. One example is an energy band diagram that takes into account the participation of charge re–trapping as proposed by Murray and Wintle [24] and shown in Fig. 2.4. For this model, it was deduced from experimental data that while most of the measured optically stimulated luminescence can be associated with the OSL trap, some of the charge released from the OSL trap which gets re–trapped can be stimulated optically. Further, it was concluded that a proportion of the charge in shallow traps eventually return to the OSL trap.

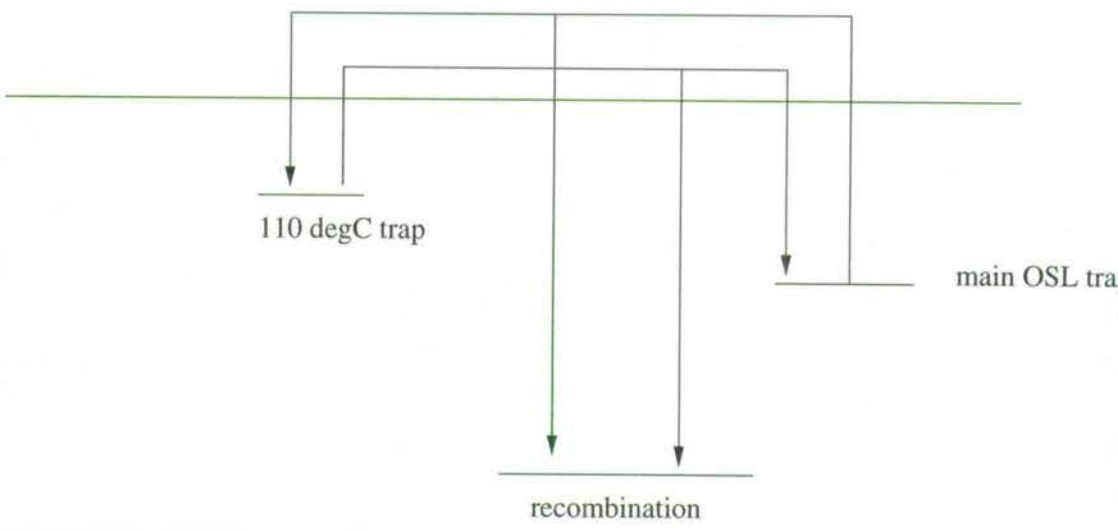

Figure 2.4 An energy band diagram to explain the process of luminescence emission. Luminescence can occur as a result of direct recombination of charge from the OSL trap via the conduction band. Some of the charge released from the OSL trap that gets re–trapped in the $110°C$ trap also contributes to the measured luminescence signal.

2.2 Pulsed optical stimulation of luminescence

The measurement aim in pulsed optical stimulation of luminescence is to separate in time luminescence stimulating light and the luminescence. It is then possible to record luminescence time–resolved spectra from which luminescence half lives can be abstracted e.g [10, 11]. This may provide more information on the charge transitions involved in the emission of luminescence.

Pulsed optical stimulation of luminescence from minerals of interest for dating applications has concentrated on mechanisms of luminescence in feldspars [10, 11, 12]. The work reported in this thesis, however, is concerned with features of luminescence resulting from pulsed optical stimulation of quartz. A measurement system was developed for these applications and was used for the experiments [27]. Since previous studies of pulsed stimulation of luminescence have been devoted to feldspars, the number of references on pulsed optically stimulated luminescence from quartz is, as yet, meager e.g [27, 28, 29].

It has been suggested that features of pulsed stimulation may be understood in terms of a trapped electron population [27]:

Consider a very simple model for optically stimulated luminescence. An electron trap with an initial electron population A is stimulated with a probability of stimulation per unit time of s and there is a probability λ per unit time that a stimulated electron will produce luminescence. If the number of stimulated electrons at time t is $N(t)$, then during stimulation,

$$dN(t) = sAd(t) - \lambda N(t)dt$$

so that

$$N(t) = \frac{sA}{\lambda}(1 - e^{-\lambda t}).$$

The time dependence of luminescence emission during stimulation will be given by

$$\lambda N(t) = sA(1 - e^{-\lambda t}).$$

an exponential rise from the start of stimulation at $t = 0$. At the end of the stimulating pulse ($t = t_1$) the number of stimulated electrons will be $N(t_1)$ which will thereafter ($t > t_1$) decay exponentially as will the luminescence

$$\lambda N(t) = \lambda N(t_1)\,(e^{-\lambda(t-t_1)}).$$

Since the half life τ associated with luminescence decay is related to the decay constant λ by $ln2 = \lambda\tau_{1/2}$, half life values may be worked out from time–resolved spectra.

In practice, this model may be modified by the presence of multiple traps and other mechanisms such as charge re–trapping.

2.3 Physical processes of luminescence

2.3.1 Role of defects

The basic assumption for the occurrence of luminescence as illustrated in Fig. 2.1 is the existence of two types of defect sites in the crystal. One type of defect acts as the charge trap, and the other as a radiative recombination site. The range of defects that are relevant to the discussion of luminescence is wide and includes point defects, vacancies and substitutional impurities [14, 17].

The presence of imperfections and impurities interrupts the periodicity of the crystalline structure. Electrons (or holes) can move into the defect

centres and thus attain energies which are forbidden in the perfect crystal [14, 30]. The energies associated with defects are localised energy levels. It is usual e.g [14, 17] to consider the electron trapping state (or trap) to be close to the conduction band and hole trapping state (or recombination centre) to be close to the valence band. In this model, the electron may be released from the trap in many ways, for example thermally or optically, and hence recombine with the luminescence centre producing emitted photons (or luminescence).

2.3.2 Configurational coordinate diagrams

An alternative method of describing the recombination process is by use of configurational coordinate diagrams. The configurational coordinate is the displacement of the atoms in the neighbourhood of the defect [14]. This is illustrated in Fig. 2.5 and is now summarised.

An electron in a ground state can absorb energy e.g from radiation, and make the transition AB to the excited state. In order to reach the minimum of the excited state, the electron loses an amount of energy E_1 (as heat). The electron can then make a radiative transition CD back to the ground state. Again in order to reach the original minimum of the ground state, the electron loses an amount of energy E_2. Thus the emitted energy E is less than the absorbed energy by an amount $E_1 + E_2$. In the the transition CE, an electron can absorb a thermal energy ΔE and make a transition to the ground state without the emission of luminescence. Non–radiative transitions are relevant for discussion of thermal quenching as done later in section 7.5.

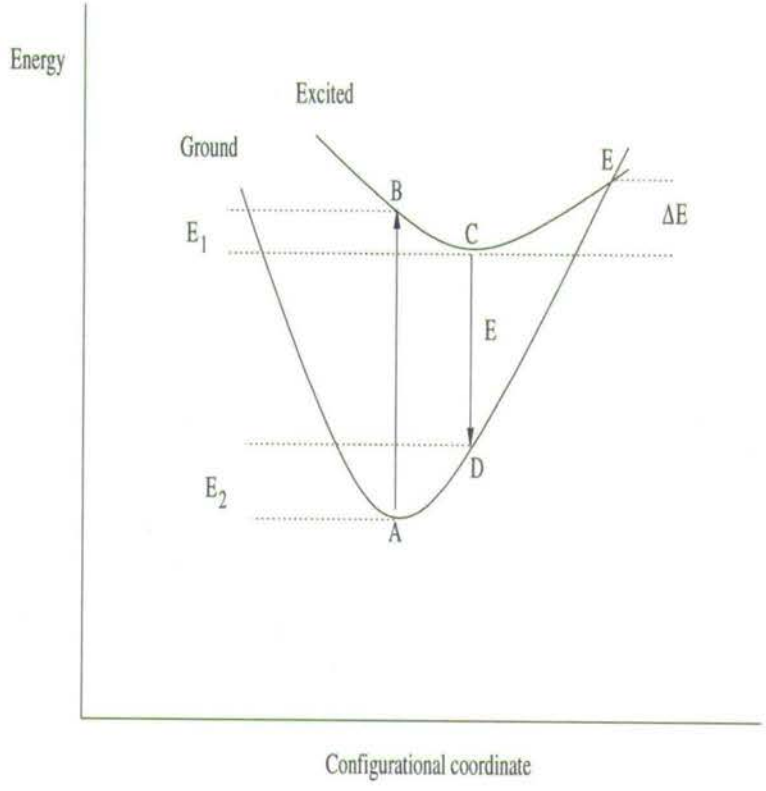

Figure 2.5 An example of the variation of the electron energy with configurational coordinate for excited and ground states in an insulator or semiconductor.

2.3.3 Kinetics of recombination processes

The basic kinetics of optically stimulated luminescence were described in section 2.1 for continuous optical stimulation and in section 2.2 for pulsed optical stimulation.

Using simplifying assumptions concerning concentration of electrons in traps, and in the conduction band as done in section 2.1, and if the probability of thermal release of electrons from traps is $S\exp(-E/kT)$, it follows [17] that the simplest (first–order) kinetics for thermoluminescence is

$$I = nSe^{-E/kT}$$

[31] where I is the intensity of thermoluminescence, n is the number of trapped electrons, and S is the frequency factor related to the number of times an electron attempts to escape from a trap. Normally $S \geq D_\nu$ where $10^{12} \leq D_\nu \leq 10^{14}$ where D_ν is the Debye lattice vibration frequency [14]. In practise, the intensity changes with either time or temperature producing a glow peak. Thus T may be replaced by a heating rate function. By introducing modifications in the assumptions e.g high re–trapping, it is possible to generate formulas for other orders of kinetics and such models have been discussed by many authors e.g [14, 17, 31].

Kinetic analysis of the emitted luminescence is useful for extracting parameters that describe the luminescence process such as trap depth (activation energy), lifetime of charge in trap, lifetime of the luminescence etc.

2.3.4 Computation of kinetic parameters

Trapped charge lifetime

Measurement of optically stimulated luminescence or thermoluminescence is possible because the trapped charge resides in the trap for a finite time τ_l given by

$$\tau_l = S^{-1}e^{-E/kT}$$

[14] which can readily be computed as values of S and E at temperature T can be measured experimentally.

Activation energy

In cases where the probability of thermal release of electrons from traps is $S\exp(-E/kT)$ such as in first or general order models of thermoluminescence, the intensity (up to about 10 - 15% of the maximum intensity) is approximately proportional to $\exp(-E/kT)$. Thus a plot of ln (I) against 1/T is linear with a slope -E/k from which the the activation energy E can be evaluated.

Other methods for computing E depend on the complexity of the thermoluminescence peak and include formulas of E as a function of measurable parameters such as heating rate, or analysis of the whole peak by computer programs. Many of these methods are discussed in standard luminescence texts e.g [17].

For optically stimulated luminescence, the vital parameter is the wavelength of excitation as in general it is expected that electron de–trapping can be achieved if the excitation energy is greater than the trap depth. One exception is feldspar where use of infrared light (E 1.4 eV) results in luminescence although the trap depth is larger, 2.5 eV [2]. For this material, a two step process was proposed in which the optical excitation moves electrons to a higher energy state from where the final transition to the conduction band is achieved by thermal activation.

The optimum wavelength (and so energy) for excitation in samples is determined empirically because in many samples such as quartz and feldspar, the luminescence can be excited by a range of wavelengths. The relevant excitation energies for quartz and feldspar are discussed in sections 4.6.1 and 4.6.2 respectively.

Chapter 3

Instrumentation

Experiments reported in this thesis were carried out using different measurement systems. The main measurement apparatus used was the pulsed light emitting diode system since the main aim of this research, studying the nature of luminescence half lives in quartz and feldspar, required recording of luminescence time–resolved spectra. The development, testing and application of the pulsed light emitting diode system is reported. Other systems used were the automatic 40-sample system, two single sample systems for optically stimulated luminescence and the thermoluminescence apparatus. The thermoluminescence apparatus was used to measure photo-transferred thermoluminescence from quartz following optically stimulated luminescence measurements using green or blue light. The development and use of the latter systems has been reported before elsewhere (for example [4] [32], [33], [34]).

3.1 Thermoluminescence apparatus

The thermoluminescence apparatus was constructed for measurement of glow curves for dating applications. The basic design of the apparatus was described by Galloway [32] but the apparatus has been modified and improved since that report. The apparatus was used to record photo-transferred thermoluminescence (PTTL) as an additional aid to help understand the observed characteristics of optically stimulated luminescence from quartz. Recently, Mckeever and Chen [18] discussed models for the PTTL process which occurs when light transfers charge from deep to shallow traps. The relationship between optically stimulated luminescence and photo–transferred thermoluminescence in quartz has also been discussed by Wintle and Murray [22].

The design of the apparatus follows standard layout of thermoluminescence apparatus for measurement of glow curves as discussed for example, by McKeever [14]. The apparatus consists of a sample chamber with all seals made by O–rings, a sample heater housed within the chamber, heater–temperature control circuitry, a light detection system made up of a 9635QA photomultiplier and associated electronics for detection of luminescence. In this study, thermoluminescence glow-curves were measured in a nitrogen atmosphere, the chamber having initially been evacuated down to 10^{-1} torr or better.

3.1.1 The heater–temperature control system

A block diagram of the temperature control and luminescence detection and recording assembly is shown in Fig. 3.1.

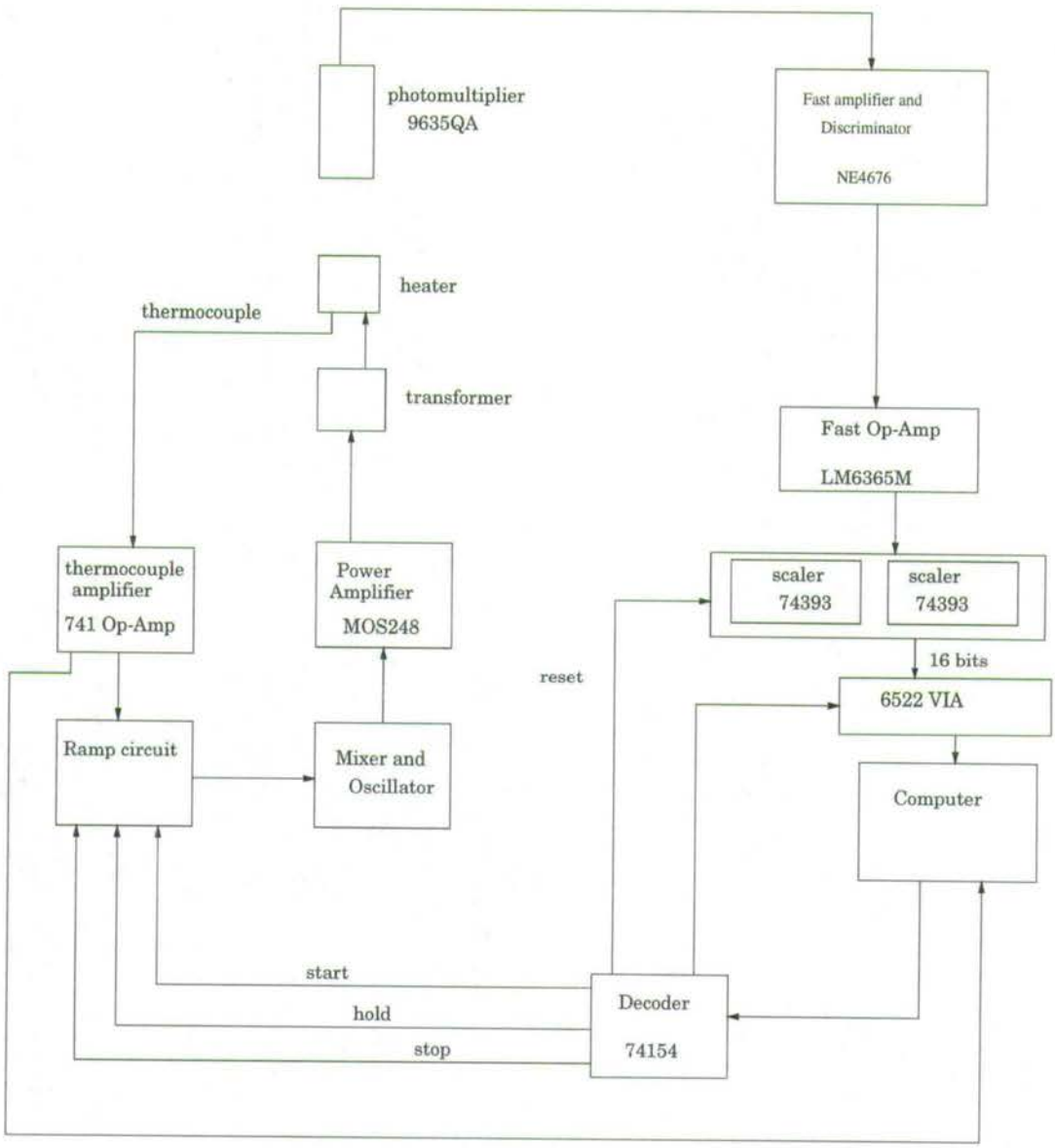

Figure 3.1 A block diagram of the heater control circuitry and luminescence detection assembly for the thermoluminescence apparatus.

The temperature controlling electronics is labelled 'Ramp circuit' and 'Mixer and Oscillator'. This control system is used to raise the temperature of the heater from room temperature, typically 20 °C up to about 500 °C at a linear heating rate of 5 °C s^{-1}. The heater is a piece of nichrome 10 mm square, 0.125 mm thick. The temperature of the heater strip is monitored by a K–type thin wire thermocouple welded underneath the heater strip. A linear rise of temperature with respect to time is achieved by feedback control. This is done by comparing the EMF from the thermocouple with a linearly increasing ramp voltage using a modified version of the circuit described by Mills *et al* [35]. The difference signal modulates the amplitude of a 40 kHz oscillation which is then amplified by a 120 W audio-amplifier before being fed into a transformer to power the heater. The heater, bent into an inverted U shape, is mounted on the knife edges of a pair of copper blocks connected to the secondary winding of the transformer.

3.1.2 Luminescence detection

A vertically mounted photomultiplier, 9635QA, is used for detection of thermoluminescence from a sample in position on the heater. The filter combination BG39, UG11 and HA3 is put in front of the photomultiplier. The BG39 and UG11 are used to pass thermoluminescence to the photomultiplier and the heat absorbing HA3 is used to protect filters and the photomultiplier from excessive heat from the sample heater. The combination of BG39 and UG11 filters has a transmission window between roughly 300–450 nm, a region that coincides with typical quartz thermoluminescence [36]. The BG39 filter has high attenuation in the infrared region of the spectrum and acts to suppress measurement of unwanted blackbody radiation through the UG11 which has an additional transmission window in the infrared range. Once

detected, luminescence pulses are fed into an NE4676 fast amplifier and discriminator unit, then recorded by the computer after passage through a fast operational amplifier (LM6365M) and two binary scaler chips (2N74393).

If necessary, the photomultiplier can be removed and replaced by a shielded Sr^{90} beta source for irradiating a sample. The design of the shielded beta source assembly was described by Liritzis and Galloway [37]. The beta source carrier is moved by a motor down onto the top of the sample chamber. The beta source is stored at the centre of a cylindrical shield, comprising an outer layer of lead 16 mm thick, an aluminium layer 23 mm thick and a core of perspex. The source is mounted on a wheel to provide easy rotation from the storage position to the exposure position. The dose rate of the beta source is about 110 mGy s^{-1}. The design of the shielding for the beta source is common to all measurement systems used in this study.

3.2 The Automatic 40-sample system

A detailed description of the automatic 40-sample system was given by Galloway [33]. The main features of the system whose operation is fully automated, are a 40–sample carrier on a turn table of 200 mm radius, a retractile sample heater, a beta source, and a luminescence detection assembly.

3.2.1 The 40-sample carrier

The turn table, with cut-out slots for 40 samples is used to move samples to various ports of the disc shaped sample chamber. The table is rotated by a synchronous motor (250 rpm at 50 Hz) with a gear–box to reduce the rate of rotation to 1 rpm. The table position is detected by reflective optical sensors comprising infrared emitting diodes and photo–transistor mounted on the top

plate of the sample chamber. The angular position of each sample is indicated by a short radial line machined onto the turn table surface which is blackened and so can be detected by an optical sensor as the table rotates. The positions are found with reference to 'position 1' which is indicated also by a second sensor. Any other required position is found by counting the number of lines which pass under the optical sensor as the table rotates, the motor being switched off when the desired position is reached. The table was designed to suffer no more than ± 0.1 mm vertical movement [33]. This ensures that for all samples, the vertical distance from the beta source when under dosing, or from the photomultiplier during measurement of luminescence, is identical.

3.2.2 The sample heater

The design of the heater assembly described earlier in section 3.1.1 was developed for use in the automatic 40–sample system to allow the heater to move up vertically through one of the cut-outs on the turn table and lift the sample off the sample bay when heating is required [33]. Samples need to be lifted off the table to prevent conduction of heat away from the sample disc. The heater assembly is mounted on the bottom plate of the sample chamber. A precisely machined slide mechanism and cam wheel drive achieves the required vertical motion of the heater (Fig. 3.2). Optical sensors on the lift mechanism indicate whether the heater is up, having lifted the sample, or down at the park position. A feedback control circuitry is used to check that the temperature of the heater is at or lower than 30 °C before heating of sample starts or at 30 °C for measurement of luminescence. The same control circuitry is also used to hold the heater at a desired temperature for a fixed duration e.g when preheating a sample prior to stimulation of luminescence.

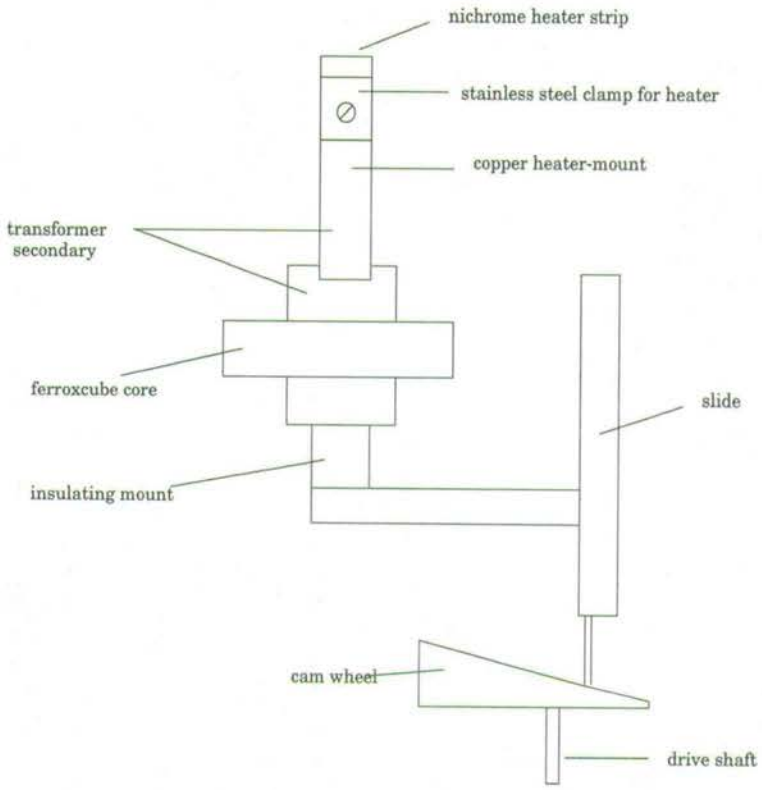

Figure 3.2 A diagram of the slide mechanism and cam wheel drive used for vertical movements of the heater.

3.2.3 Beta source

A controlled beta radiation dose can be provided to a sample in position on the turn table cut-out by a shielded beta source mounted on the top plate. The design of the beta-source carrier is similar to the one on the thermoluminescence apparatus. To aid control by computer, an external disc on the drive shaft is used to indicate to optical sensors the position of the source. The dose rate onto a mono–layer of quartz grains on a 0.2 mm thick stainless steel disc used with this system is 270 mGy s^{-1} when in the dosing position. An extra layer of lead is interposed between the beta source and the photomultiplier port. This is to reduce scintillations in the filters which tend to increase the background counting rate. The scintillations are probably a result of *bremsstrahlung* radiation related to scattering of beta particles from the radiation source in the shielding [37].

3.2.4 Luminescence detection

Luminescence can be stimulated optically from a sample once it is moved in position directly below a set of light emitting diodes. The port fits a light emitting diode holder described by Galloway [33], a design which has since been adopted for use on all apparatus for measurement of optically stimulated luminescence in the laboratory. 16 light emitting diodes are mounted in a Dural block equidistant from each other and inclined at the same angle from the horizontal axis [3]. Stimulated luminescence is 'seen' by the photomultiplier through the middle of the ring of light emitting diodes. To change wavelength of stimulation it is only necessary to fit the holder with the desired light emitting diodes. For the results reported here, continuously operated green light emitting diodes (NSPG-500, peak wavelength 525

nm) and blue light emitting diodes (NSPB-500, peak wavelength 475 nm) as well as pulsed blue LEDs (NSPB–500) were used on this system. Additional specifications for these LEDs according to the manufacturer are: maximum DC forward current of 30 mA, maximum pulse current of 100 mA, luminous intensity of 6 cd for the green LEDs and 2 cd for the blue LEDs, and an angular spread of 15°. Under continuous operation, the light emitting diodes are switched on by the computer and are operated in parallel from a constant current supply shown in Fig. 3.3.

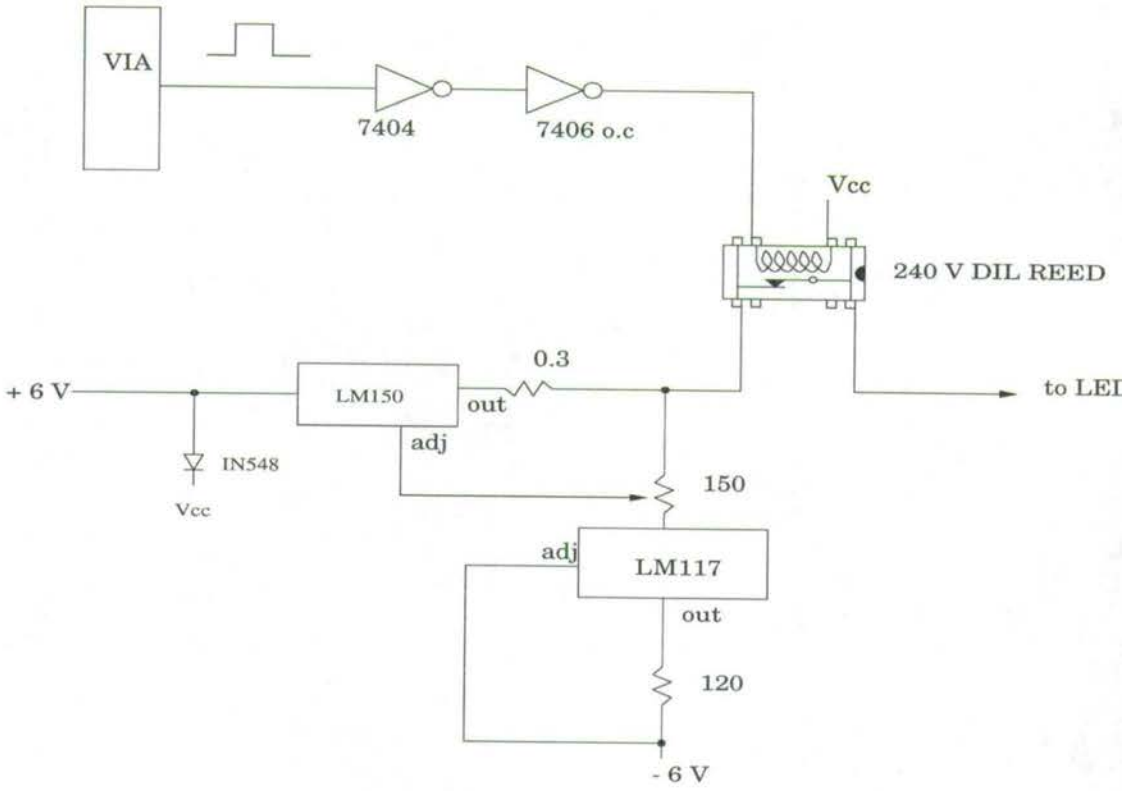

Figure 3.3 A schematic diagram of the constant current source that operates the light emitting diodes under continuous operation.

Luminescence is detected by an EMI 9635QA photomultiplier. The luminescence recording system is similar to that shown in Fig. 3.1 with pulses from the photomultiplier passing through an amplifier (ORTEC 474) and discriminator (ORTEC 463). In order to optimise the luminescence signal to background ratio, the filters DUG11 and HA3 are placed in front of the photomultiplier and a GG475 filter in front of each green light emitting diode and a GG420 filter in front of each blue light emitting diode. Both the GG475 and GG420 filters prevent emission from the diode appearing in the band used to detect the luminescence. The DUG11 filter was found most efficient for the dual purpose of passing quartz luminescence to the photomultiplier and suppressing scattered green light from the diode. Quartz has an optically–stimulated–luminescence emission band in the region 360–420 nm [38]. The HA3 heat absorbing filter was included to protect the filters and photomultiplier from excessive heat because the photomultiplier and heater share the same port where samples are sometimes heated prior to stimulation of luminescence. This choice of filters is based on tests done on the system by Galloway *et al* [34].

Green light is efficient at stimulating luminescence from quartz. Studies by for example, Spooner *et al* [39], Bøtter-Jensen *et al* [40] showed that shorter wavelengths were more efficient at stimulating luminescence from quartz than longer wavelengths. Thus typical wavelengths used for stimulating luminescence from quartz include the 514 nm from an argon ion laser, or light filtered from incandescent halogen or xenon lamps (for example [41]). Use of green light at 565 nm from diodes was demonstrated by Galloway [4] with subsequent improvements reported by use of 525 nm wavelength [34]. Use of blue light emitting diodes is relatively new and offers an alternative high intensity light source for stimulation of luminescence from quartz [5, 6].

3.3 System control

A block diagram of the control arrangement for the automatic 40–sample system is shown in Fig. 3.4. The interfacing and other circuitry were developed from those used on the thermoluminescence system. The basic luminescence detection circuitry is similar with pulses detected by the photomultiplier being fed through an ORTEC 474 fast amplifier, discriminator (ORTEC 463), and an integrated circuit fast operational amplifier (LM6365M) to binary scalers (2N74393).

The luminescence detection circuitry is interfaced to the controlling computer by a 1 MHz bus. The computer is used to input or output an 8–bit or 4–bit code. The 4–bit code is input to a decoder (74154). The output signals from the decoder are used to reset the 16–bit scaler, to identify the 6522 VIA used to transfer the scaler contents to the 1 MHz bus, and to identify the VIA used to control the mechanical movements in the system. The 16 bits from the scaler are transferred by the VIA to the computer as two sequential 8–bit words. The second VIA accepts signals from optical sensors which indicate the positions of the heater, beta source, and turn-table. This VIA also sends signals to operate the constant current power supply to switch on the light emitting diodes, and control signals that move the beta source, turn–table and heater.

Computer programs in BASIC are used to control the operation of the system. A typical sequence of measurements on a sample might be to dose the sample, preheat it for a given time, stimulate and then measure the luminescence. To achieve this, separate procedures will recognise 8–bit signals from optical sensors and move the table to the dosing position, rotate open the beta source and keep it in the dosing position for the duration entered in the program then rotate it back to the closed position, then move the ta-

ble to the measuring position where the heater lifts the sample off the table, heating it for a preset time and moving back onto position when it has cooled down to a preset temperature, usually $30°C$. After this the light emitting diodes would be switched on for stimulation of luminescence.

A simple measurement of the number of luminescence photons counted in a given time is printed out as soon as the measurement is made. Measurements such as the time dependence of luminescence, running into tens up to thousands of seconds, are stored in 250 time channels for subsequent analysis.

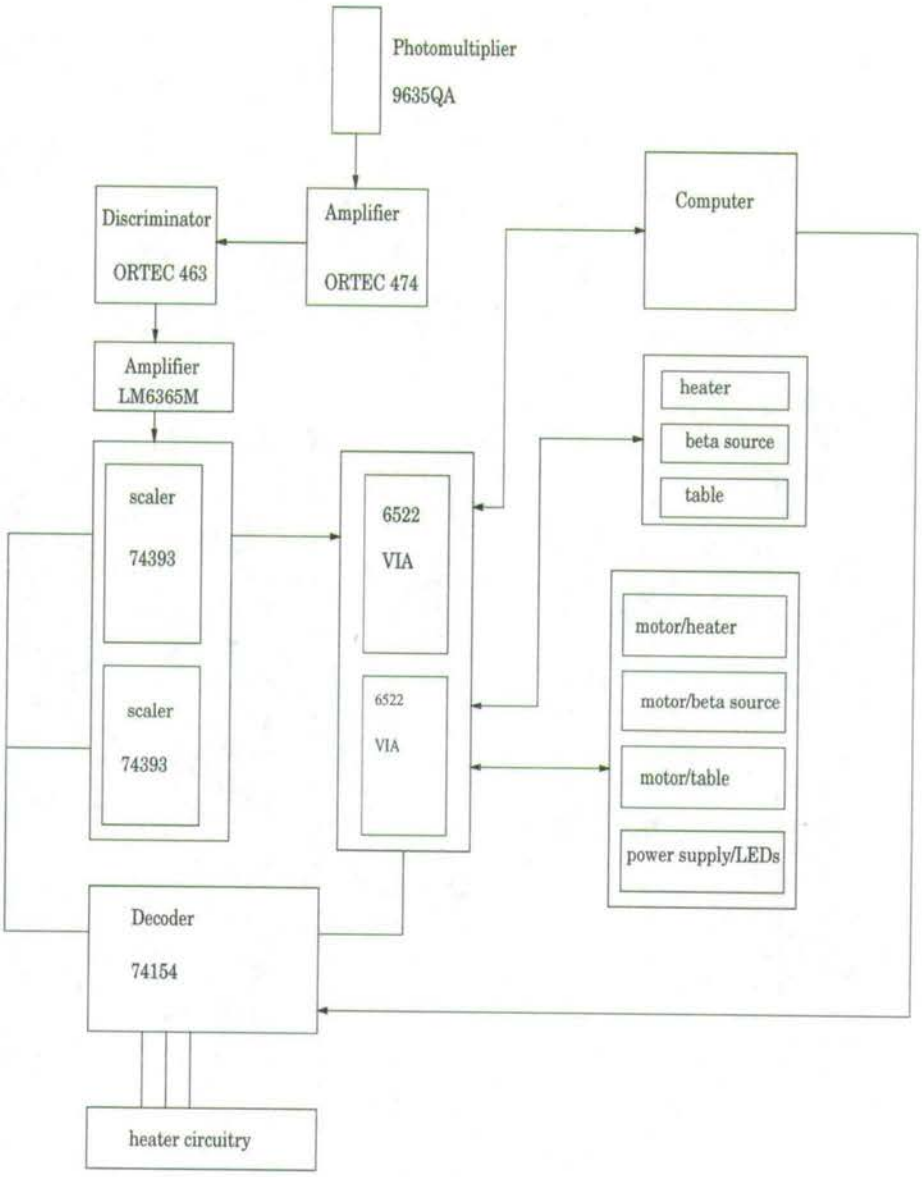

Figure 3.4 A block diagram of the control system for the automatic system showing heater circuitry, luminescence detection system and interface arrangements.

3.4 Single aliquot semi-automatic systems

Two systems, each designed for use with a single sample were used. One measurement system was configured for use with green light emitting diodes and the other with infrared light emitting diodes. The green LED system was used for measurements on quartz and feldspar and the infrared LED system was used for stimulation of luminescence from feldspar. The systems were also used for beta dosing and preheating of samples that were used on the Pulsing systems described later in section 3.5. Because most aspects of the two systems are similar (heater, system control, etc.), the discussion in this section applies to both of them unless specific differences are pointed out.

The box–shaped sample chamber has three ports; a sample loading port in the centre, a shielded beta-source (dose rate 150 mGy s^1) similar in construction to the one on the automatic 40–sample system, and at the other end a port for a light emitting diode holder on top of which is a vertically mounted photomultiplier. To prevent *bremsstrahlung* causing scintillations in the filters in front of the photomultiplier, a likely cause of high background, a cylindrical lead shield at the luminescence measuring port surrounds the filters and photomultiplier cathode. A computer program controls the heating and movement of sample holder, sample dosing, and the operation of the constant current power supply to the light emitting diodes.

3.4.1 Sample heater

The sample heater was designed for use with one sample, usually in powder form, on a stainless steel or aluminium disc. In this study stainless steel discs about 12 mm diameter and 0.2 mm thick were used.

The sample heater is a 25 mm square piece of nichrome heated indirectly

by an element consisting of a mica former on which are wound 4 turns of flat nichrome wire. The conduction of heat from the element to heater is made through a 25 mm square piece of mica which also serves to electrically insulate the nichrome heater plate from the element. The heater assembly is mounted on a carriage which can be moved by a drive belt along two parallel guide rods to either the dosing position or under the photomultiplier for measurement of luminescence. Optical sensors denote the arrival of the carriage at any of dosing, heating or measurement positions.

The temperature controlling circuitry is shown in Fig. 3.5. A 1.5 A, 9 V a.c signal is used for resistive heating of the element. The temperature of the heater plate is sensed by a K-type thermocouple fixed underneath the heater plate. The thermocouple is connected to an integrated circuit thermocouple amplifier, an AD595 which is used to provide feedback control over the required temperature range by switching on and off the 9 V a.c supply to the heating element. With this circuitry, the heater temperature can be held constant about any desired temperature for a fixed duration. The heater is connected to the 9 V a.c supply via a pair of rails running the length of the sample chamber underneath the rods. The rails are insulated under the dosing position to exclude the possibility of a sample being heated while in the dosing position.

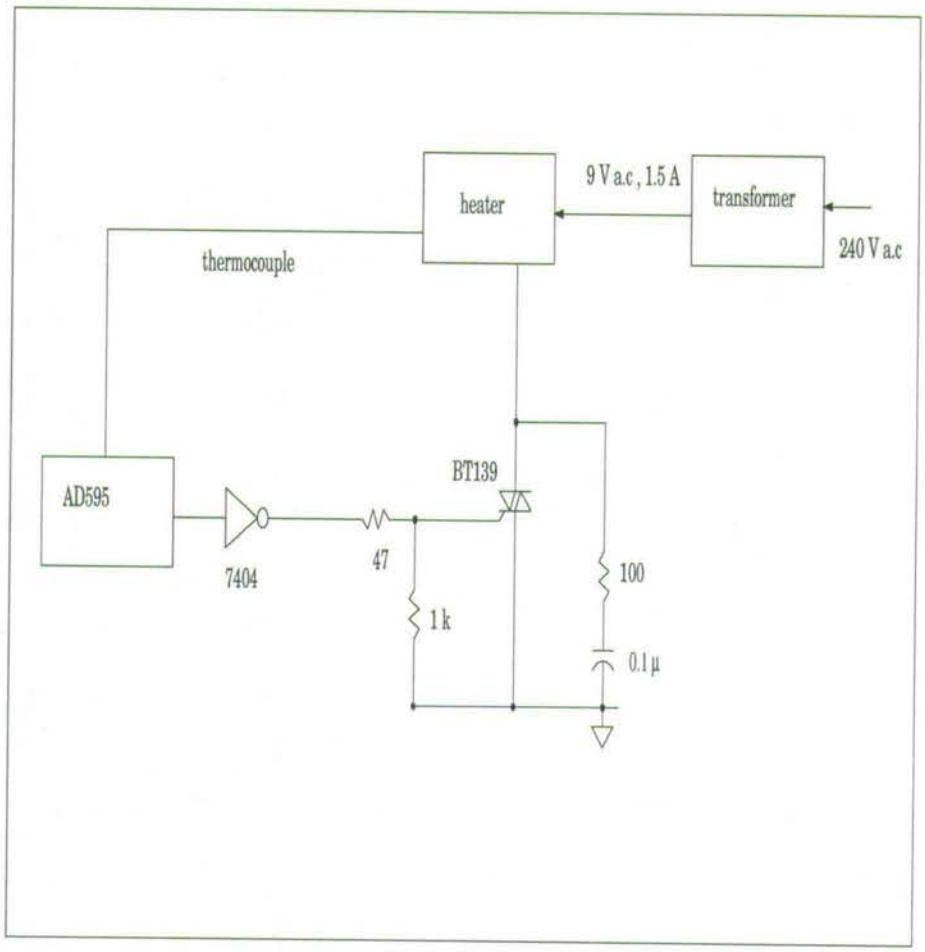

Figure 3.5 The circuitry that controls the heating on the single sample systems. Heating is accomplished by use of a 1.5 A, 9 V a.c signal.

3.4.2 Luminescence stimulation and detection

The green LED system uses 525 nm green light emitting diodes (Nichia type NSPG-500) for stimulation of luminescence. Each of the diodes has a 3 mm thick GG475 long pass filter in front to reduce the effect of scattered stimulating light on the photomultiplier, a 9635QA. The filters DUG11 and HA3 are put in front of the photomultiplier.

The infrared LED system has two sets of light emitting diodes for use in stimulating luminescence from feldspars, the TEMPT 484 with peak emission at 880 nm and the TSUS5402 with peak emission at 950 nm. The TEMPT 484 set was found to be about 10 times better than the TSUS5402 at stimulating luminescence from feldspars. An EMI 9635QA photomultiplier was used to detect luminescence through filters BG39 and 5–58. The combination of the BG39 and 5–58 provides a transmission window in the range between roughly 300–450 nm. This range is suitable for measurement of optically stimulated luminescence from feldspar which appears in the band 380–420 nm [7].

The selection of the 880 nm wavelength for stimulation of luminescence follows the work of Hütt *et al* [2] who showed the existence of a stimulation peak in the infrared range. Subsequent work by Bailiff [42] and Bailiff and Barnett [43] showed the stimulation peak at room temperature to be at 854 nm. Thus for feldspar stimulation, light sources close to 854 nm are preferred [38].

Computer programs are used to control the operation of the systems such as dosing, heating, and measurement of luminescence. Control circuitry for detection and recording of luminescence including the constant current supply for the light emitting diodes are similar to those used in the 40–sample automatic system.

3.5 The Pulsed light emitting diode system

A pulsed light emitting diode system for stimulation of luminescence was developed. The system was used to record luminescence time–resolved spectra from quartz and feldspar. The time–resolved spectra were used to study the characteristics of luminescence half life values in quartz and feldspar. This section reports the development of the light emitting diode pulsing system.

3.5.1 Design considerations

Three approaches to measure pulsed luminescence have been used before, two using lasers and the other using light emitting diodes, and their features can be compared with the new system to be described below. Markey *et al* [13] and Mckeever *et al* [8] described a method in which the laser itself was not pulsed but electronically controlled shutters used to periodically intercept the laser beam to an aluminum oxide sample and in this way stimulate luminescence from the sample by light pulses. A set of narrow band filters were used to pass luminescence to the photomultiplier. With this arrangement pulse widths of 10 – 100 ms and longer were achieved and luminescence with lifetimes in the range 35 – 5000 ms could be detected. The use of laser pulses is exemplified by Clark *et al* (1997) and Clark and Bailiff (1998) who used 880 nm pulsed laser stimulation and filters in front of the photomultiplier to define the luminescence detection band and to reduce the effect of scattered stimulating laser light. The pulsed laser systems, with faster switching speeds of the order of 5 ns, were able to detect luminescence lifetimes down to 5 ns. Bulur and Göksu (1997) used a circuit in which a 555 IC timer was used to trigger a current source and produce 1 s width pulses from light emitting diodes. A filter was placed in front of the photomultiplier to select

the wavelength of luminescence which was recorded for 4 s after the end of the pulse.

For this work, the luminescence stimulating light sources selected were the Nichia 525 nm green LEDs (type NSPG 500) and 470 nm blue LEDs (type NSPB 500).

The circuitry developed for pulsing the light emitting diodes is shown in Fig. 3.6. For clarity, the circuit has been subdivided into three sections, the 'normal' pulsing circuit in (a), the 'short pulse' circuit in (b) and the light emitting diode drive circuitry in (c). The light emitting diodes in Fig. 3.6 (c) are pulsed by signals from either of the circuits in Fig 3.6 (a) or (b) which use an integrated circuit multivibrator, a 2N74221, as source of input pulses. The multivibrator output pulse width and duty cycle are defined by the external RC timing components on the 2N74221. The pulse width T_w can be estimated as

$$T_w = kR_xC_x$$

where k $\approx$ ln 2 [44].

The circuit of Fig. 3.6 (a) was used to produce pulse widths in the range 3 – 30 μs. Most measurements were made with this arrangement hence the label 'normal'. The measurements reported here were all made with a repetition rate of 11 kHz.

For the short pulse width option (Fig. 3.6 b), the output signal from the multivibrator was fed into a dual input 2N7408 AND gate whose output was then used to drive the 16 light emitting diodes. The width of the pulse fed to drive the LEDs is determined by the propagation delay through the 2N7404 gates. The minimum usable pulse obtained with Fig. 3.6 (b) was 25 ns (FWHM).

In the drive circuit, Fig. 3.6 (c), each of the 16 light emitting diodes is operated independently. This makes it possible to pulse a specific number of diodes, for example, fewer than 16, in order to reduce the overall light intensity. The light emitting diodes are forward biased for the duration of the pulse and reverse biased otherwise. The logic LOW level transition used then turns the diodes on. Since with pulsing, currents higher than levels normal in continuous operation are possible, integrated circuit open collector/inverter/buffers, 2N7406, were selected to interface to the light emitting diodes. Using all 16 LEDs, each pulsed at 70 mA for 11 μs duration at a repetition rate of 11 kHz, the mean light intensity at the sample was measured as 1 mW cm^{-2} using a calibrated PIN diode (Ealing Electro-Optics).

During routine measurement, the light emitting diodes were not pulsed continuously but only under program control. The program initiated a signal from an interface which enabled the multivibrator pulse to be fed to the light emitting diodes for the duration of the measurement. This ensured that there was no sample bleaching, no matter how insignificant, during times when luminescence was not being measured.

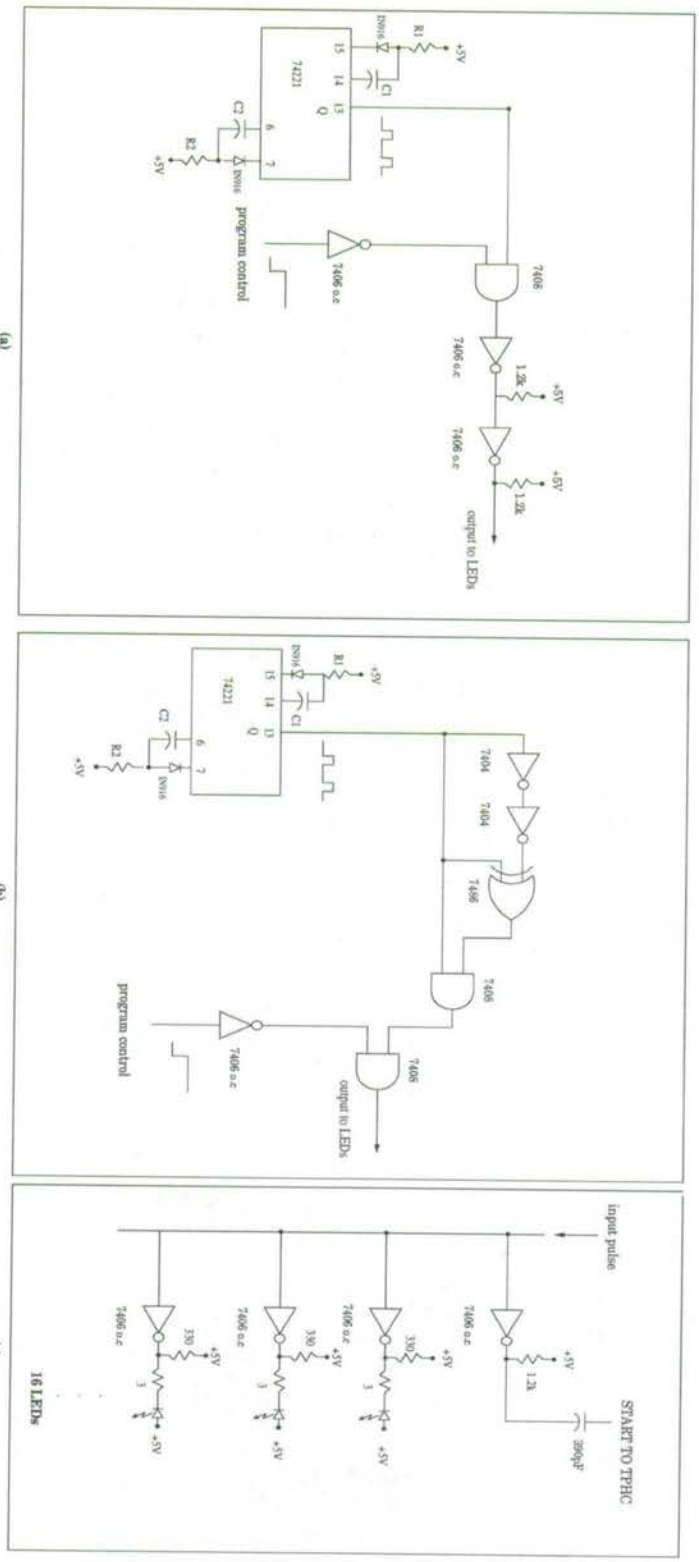

Figure 3.6 The circuitry that pulses the 16 light emitting diodes using the 2N74221 as source of signal. The diodes are pulsed under program control.

3.5.2 Luminescence detection

A block diagram of the luminescence stimulation and detection assembly used is shown in Fig. 3.7. The luminescence is detected by the photomultiplier, an EMI 9635QA with filters BG39 and UG11 in front. An ORTEC model 467 Time to Pulse Height Convertor (TPHC) determines the time interval between stimulation and detection of a luminescence photon. Measurement of the time interval is initiated by the arrival of a START pulse from the pulsing circuitry shown in Fig. 3.6 (c). Detection of a luminescence photon by the photomultiplier results in a signal being sent to the STOP input of the TPHC which then produces an analog output with amplitude proportional to the measured time. The amplitude of these analog pulses from TPHC are measured by the 256 channel Analog to Digital Convertor (Laben 8213) and fed, in digital form, to the computer to generate a graph of pulsed luminescence against time, the luminescence time–resolved spectrum. In order to emphasize chosen areas of the time–resolved spectrum, the dynamic range on the TPHC can be altered or alternatively, the arrival of either the STOP or START signal deliberately delayed.

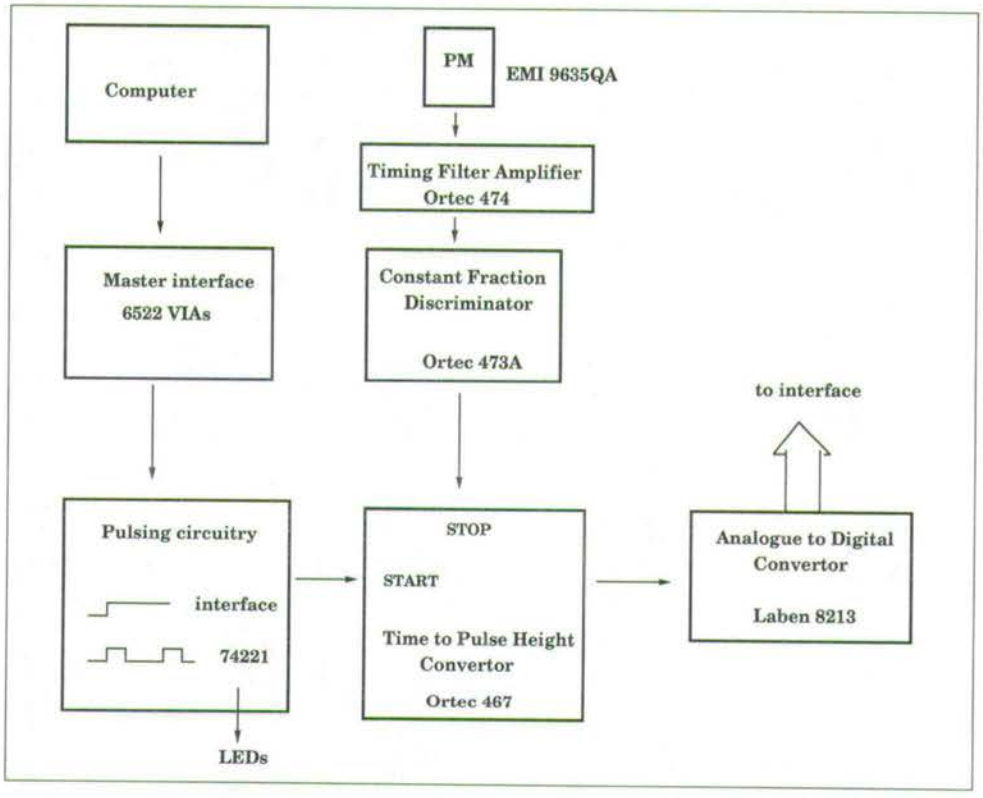

Figure 3.7. A schematic diagram of the pulsing system showing the pulsing circuitry, and the arrangement for detection and recording of luminescence time–resolved spectra.

3.5.3 The Time to Pulse Height Convertor

The ORTEC 467 Time to Pulse Height Convertor (TPHC) was configured for use in the Pulsing system in order to make measurements of luminescence time–resolved spectra possible.

The TPHC generates a rectangular output pulse whose peak amplitude is linearly proportional to the time interval between a START and STOP input pair. The analog output pulse is available at the TPHC output. This enables time–to–amplitude conversion to be used for analysing the time relationships between stimulation and emission of luminescence. Luminescence time–resolved spectra are displayed with a time range equal to the selected dynamic range on the TPHC.

The principle of operation of the TPHC (ORTEC 467 in particular) is that a START–to–STOP time to pulse height conversion is done only after a valid START input (threshold voltage -250 mV) has been accepted within the selected time range. The START input is then disabled during this 'busy' interval. When a valid STOP pulse (threshold voltage -250 mV) is accepted, this indicates that a time interval has been measured and its analog equivalent can be read at the TPHC output.

For the ORTEC 467 Time to Pulse Height Convertor, the START signal was fed in from the Pulsing circuitry and the STOP signal from an ORTEC model 473A discriminator. The acceptance of a START signal is necessary to initiate a response in the Time to Pulse Height Convertor.

In order to calibrate the time axis and hence determine the resolution of the dynamic range selected, a light emitting diode pulse was initiated with only neutral density filters in front of the photomultiplier and the system was operated to obtain a time–resolved spectrum. A delay, Δt, was then introduced to either the START or STOP pulse. This was done by simply

using a calibrated delay cable to connect between TPHC and the Pulsing circuitry or between TPHC and the discriminator. When the system was operated again, the time–resolved spectrum shifted by a time Δt from its original position. An example of this is shown in Fig. 3.8. Since the dynamic range of the time–resolved spectrum was known beforehand, the resolution of the time axis could be calculated.

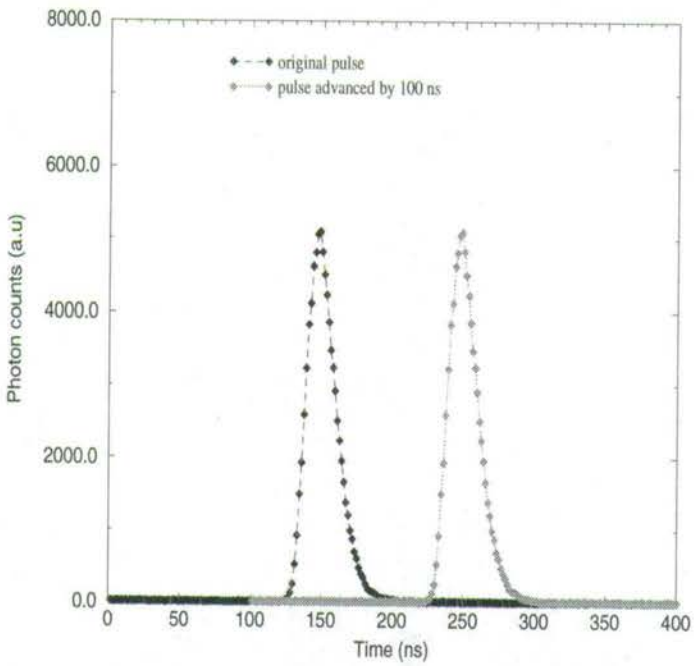

Figure 3.8. A light emitting diode pulse shifted from its position by the introduction of a 100 ns delay to the STOP signal.

Chapter 4

Experimental techniques

This chapter discusses experimental techniques that were used to obtain data for this thesis. A discussion of measurement conditions for recording luminescence time–resolved spectra (section 4) is followed by a description of methods not exclusive to pulsed optical stimulation. These are methods concerning sample preparation, preheating and multiple as well as single aliquot techniques. An account of wavelengths used for stimulation and detection of luminescence from quartz and feldspar is then given with the aim of putting into context the choice of stimulation wavelengths and luminescence detection filters used in the work reported in this thesis.

4.1 Measurement of luminescence time–resolved spectra

4.1.1 Measurement conditions

The electronic system described in section 3.5 requires that no more than one photon be detected per light pulse. The TPHC will react to the first STOP

pulse to arrive after a START pulse. If more than one STOP pulse arrives after a START pulse, the time information associated with the second (and later) pulses will be lost and the time–resolved spectrum will be distorted, with later times being falsely low in recorded counts. Thus for undistorted time-spectra, the STOP pulse rate should be less than the START pulse rate i.e luminescence–photon counting rate should be less than the light pulse rate. The dependence of the distortion on the STOP pulse rate was investigated experimentally. Continuously lit light emitting diodes were used to stimulate luminescence from a previously dosed and preheated quartz sample. Luminescence pulses detected thus provided a source of random STOP pulses. The rate of START pulses from the pulsing circuitry of Fig. 3.6 was kept constant at 11 kHz. Fig. 4.1 shows examples of time–resolved spectra recorded with STOP pulses arriving in a random manner.

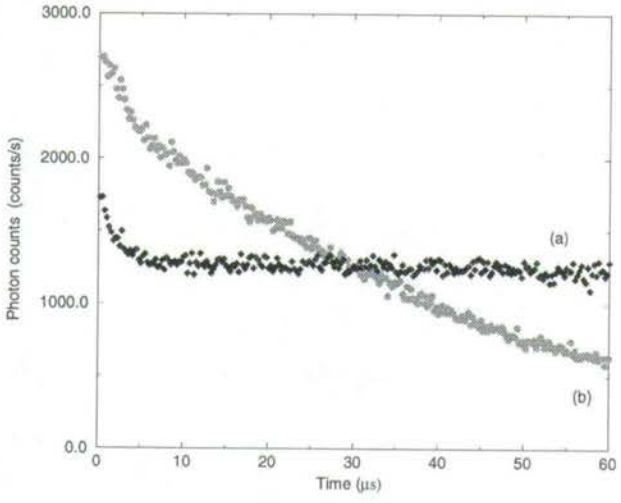

Figure 4.1 Time–resolved spectra recorded with different counting rates (a) $10^3 s^{-1}$ (b) 2 x $10^4 s^{-1}$. Luminescence was stimulated using continuously lit LEDs to generate random STOP pulses. The START pulse frequency was 11 kHz.

Since there is no time correlation between START and STOP pulses, the resulting time–resolved spectrum should show equal numbers at all times (apart from statistical scatter) as in Fig. 4.1 a (the overshoot in the first few channels is a feature of the measurement electronics; these channels are not included in subsequent analysis for half life). At high counting rates there is distortion of the time–resolved spectrum due to multiple STOP pulses following each START pulse as is shown in Fig. 4 (b). Time–resolved spectra with an inherent distortion can lead to apparent but spurious half life values.

4.2 Assessment of counting rates

In order to establish 'safe' levels of counting rates for measurement of time–resolved spectra, the set–up shown in Fig. 3.7 was used with the rate of STOP pulses measured simultaneously by the scalar counter and by the TPHC. The number of STOP pulses measured by the TPHC in a given time was determined by integrating the measured time–resolved spectrum over the entire 256 channels. The rate of STOP pulses over time was changed by simply measuring time–resolved spectra repeatedly from a sample. As the sample got bleached, the rate of STOP pulses got less but the rate of START pulses was kept constant at about 11 kHz throughout the measurement. Counting rates recorded by the scalar and rates determined from time–resolved spectra are compared in Fig. 4.2 for stimulation using green LEDs. In the absence of any dead–time in the TPHC, these counts would be equal. However, because there is a finite dead–time in the TPHC, the counts integrated from time–resolved spectra are lower than counts recorded by the scalar. The non–linearity from about 8000 counts s^{-1} (y-axis) occurs because the second and later STOP pulses are being missed by the TPHC. Time–resolved spec-

tra in this region would be extremely distorted as counts would be registered only in the first 2 or 3 channels of the ADC. Half lives calculated from such time–resolved spectra are considered spurious.

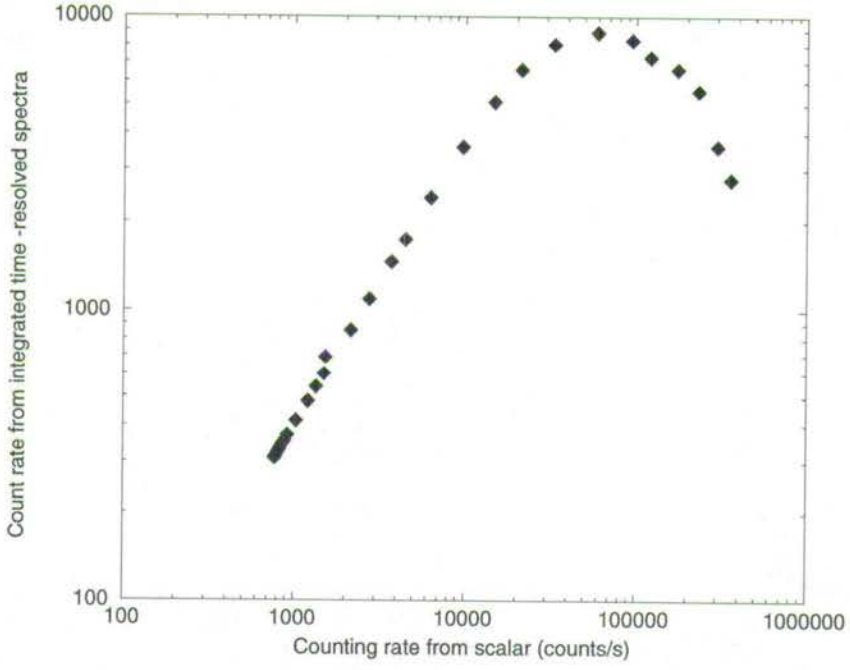

Figure 4.2 A comparison of counting rates recorded by a scalar counter and counting rates determined from time–resolved spectra.

A 'safe' working region will therefore be where the count rates integrated from time–resolved spectra are linearly proportional to count rates from the scalar. The region selected for use in this work was that at less than 5000 counts s^{-1} (y-axis).

A similar experiment was done using continuously operated blue LEDs with the expectation that since both green and blue LEDs initiate STOP

pulses that are detected by the same system, the counting rates measured should be similar. The results are shown in Fig. 4.3 and as expected the 2 graphs overlap.

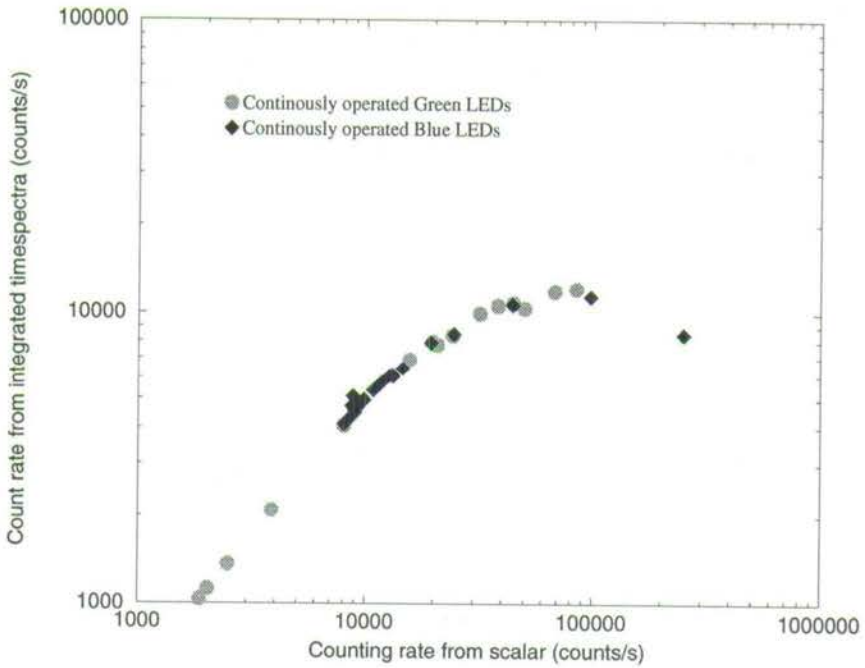

Figure 4.3 A comparison of counting rates when stimulation of luminescence was done using either green or blue light emitting diodes.

Both sets of light emitting diodes were operated at a current of 30 mA/LED. Another experiment was done to check that the form of the graph did not change with LED current. Fig. 4.4 compares data obtained with a current of 10 mA/LED and with 30 mA/LED. As the graph shows, the form of the graph and so the working region did not change with a change of current.

The significance of this was that values measured at different LED intensity could be compared directly.

Time–resolved spectra generated with random STOP pulses were further analysed for spurious half life (i.e half life values associated with unacceptably high counting rates according to the criteria discussed in section 4.2) and these are plotted against the corresponding counting rates in Fig. 4.5. When measuring a half life, the counting rates were to be chosen so that the possible spurious half life of Fig. 4.5 was much longer than the half life being measured. In all cases where counting rates were not a problem, half lives were evaluated by fitting data with single exponential functions. Multiple component fits had been tried but did not present any improvement over single exponential fitting and so were not used any further.

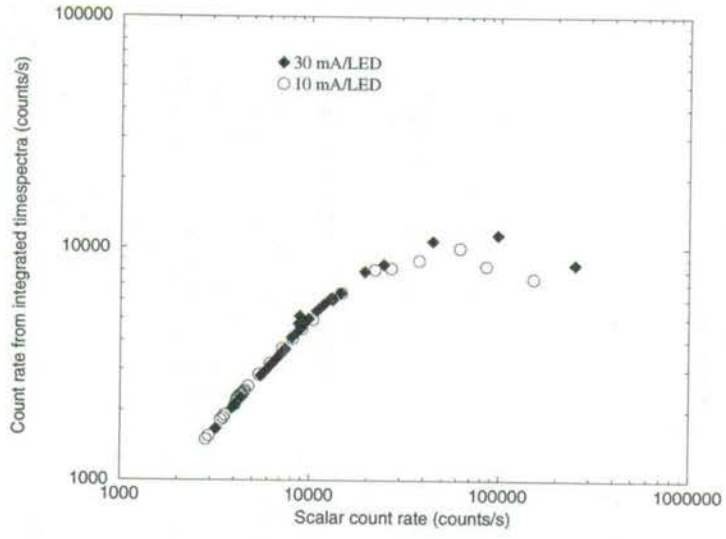

Figure 4.4 A comparison of counting rates when light emitting diodes when operated with either 10 or 30 mA/LED.

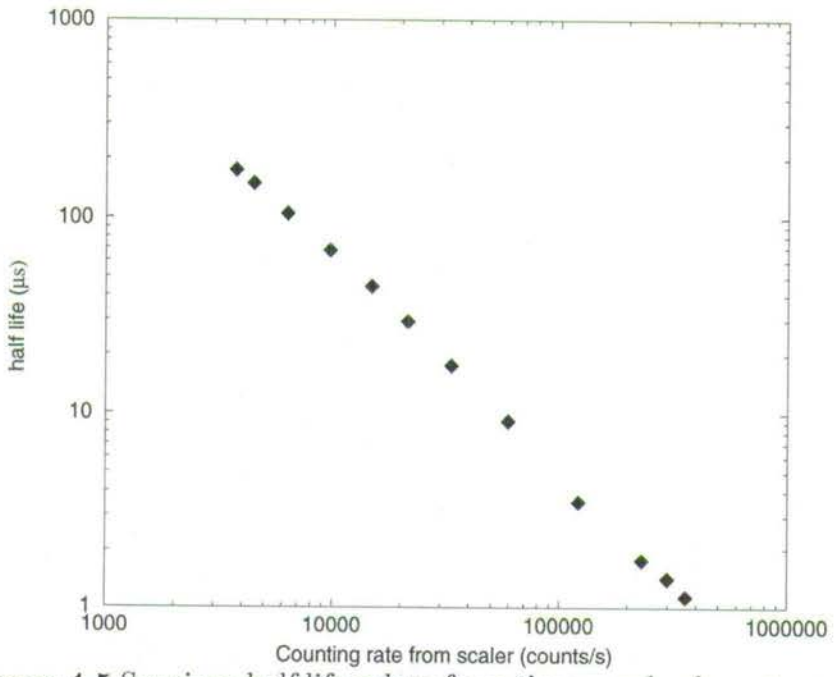

Figure 4.5 Spurious half life values from time–resolved spectra generated with random STOP pulses plotted against the corresponding counting rates. The START pulse frequency was about 11 kHz.

4.3 General techniques

4.3.1 Sample preparation

Samples of quartz and feldspar were used in this study. Quartz samples were prepared from 'acid washed' sand (90 – 500 μm grain size) from BDH Ltd and used either as coarse sand, 90 – 500 μm grain size, or sieved to 90 – 125 μm grains. Any remanent luminescence in the coarse sand was removed

by heating at $500^{o}C$ for 2 minutes and from the (90 – 500 μm) grains by exposure to daylight for 4 weeks.

The 90 – 125 μm quartz grains were deposited by sedimentation in a water column onto 1 cm^2 circular stainless steel discs. Samples were prepared together to achieve identical mass, typically about 10 mg per disc. Samples of feldspar, microcline and orthoclase, were also prepared onto discs by sedimentation and bleached by daylight for 4 weeks or more.

All samples were used without any further chemical treatment. The purity of the quartz from feldspar contamination was checked using an infrared stimulation test in which a time–independent count consisting of scattered stimulating light and photomultiplier noise was compared to a count measured after the sample had been given a beta dose and preheated. The latter was found to be only slightly larger than the first count indicating a negligible amount of feldspar in the quartz sample. This test is based on the fact that infrared stimulation is effective with feldspar but not with quartz [45, 46].

4.4 Preheating

The general aim of preheating a sample after laboratory irradiation prior to measurement of optically stimulated luminescence is to simulate the conditions applicable to a natural OSL signal. There are several ways in which this is achieved. Following laboratory irradiation of a sample, some charges are retained in shallow traps unlike in the case of natural irradiation where charges in shallow traps are removed at ambient temperatures during geological time–scales [47]. Preheating a sample after dosing clears shallow traps of such charges. Preheating is also used to complete the indirect transfer of charge from shallow traps to traps responsible for OSL. During natural

irradiation, some charges in shallow traps will thermally decay to traps responsible for OSL. An appropriate preheat protocol will enable an equivalent charge transfer to occur following laboratory irradiation [48, 49].

One technique for selecting an appropriate preheating procedure is to make a series of measurements on naturally (N) and laboratory irradiated (β) samples using increasing preheat temperature or duration of preheat until a plateau of $N/(N+\beta)$ is obtained. Rhodes [48] used this procedure on quartz for preheating at temperatures between $160°C$ and $280°C$ for 5 minutes. The ratio of $N/(N+\beta)$ was reported to have been steady at temperatures of $220°C$ and above. The same technique was used by Li [50] to suggest that feldspar could appropriately be preheated at $220°C$ for 10 minutes or at $160°C$ for 5 hours. Other preheat procedures for quartz include preheating at $160°C$ for 16 hours [53] , at $220°C$ for 1 minute [51], at $150°C$ for 48 hours [52] and at $280°C$ for 10 s [54]. However only the procedures $220°C$ for 5 minutes and $160°C$ for 16 hours have been used extensively in OSL studies. Stokes [55] made an intercomparison of the two methods and reported no significant differences between them.

In this study feldspars were preheated at $220°C$ for either 10 minutes or 1 minute between dosing and stimulation of luminescence. Quartz samples were preheated at $220°C$ for 5 minutes except in experiments aimed at investigating the effect of preheat procedure on half life in which case additional preheat routines were used.

4.5 Measurement of growth curves

One of the preliminary experiments was concerned with examining the relationship of luminescence intensity to added beta dose. Data for graphs of

luminescence intensity against dose, growth curves, were determined using two methods, the multiple aliquot method and the single aliquot method. The methods as used are described in sections 4.5.1 and 4.5.2.

4.5.1 Multiple aliquot additive dose method

This method was used only with feldspar samples. For each value of dose, up to 10 samples were used. Typically, 8 dose values were used requiring a total of up to 80 samples for one growth curve. Values of dose (in Gy) used were: 0, 7.5, 15, 30, 60, 90, 120, and 150 Gy. Every datum point on a growth curve was an average of several points with the experimental uncertainty represented by the standard deviation in the average.

Measurements were made in four cycles. In cycle 1, the background count (background 1) from a sample was recorded and later subtracted from subsequent counts. The background count was the sum of photomultiplier noise and scattered stimulating light. In cycle 2, each sample was given a beta dose and preheated at $220°C$ for 10 minutes before luminescence (count 2) was recorded at $30°C$ under infrared or green LED stimulation. Because of inevitable differences in the amount of sample on each disc, it was necessary to normalise every set of counts. Thus the sample was given a second beta dose and preheated again (cycle 3). The amount of the second dose was the difference between the maximum dose (150 Gy) and the dose given in cycle 1. For example, if the first dose given was 30 Gy, then the second dose would be 120 Gy. The sample was then bleached for 15 minutes using an 11 W double tube Philips fluorescent lamp (type PL-S). The aim of this was to reduce to negligible levels any OSL signals remaining from the preceding cycle in which the sample had been given a beta dose and preheated. A background signal (background 2) was then measured before each sample was given a 150

Gy beta dose and preheated before stimulation of luminescence (count 4) . This ensured that each sample had received the same total beta dose and had been preheated for the same number of times. The normalised count corresponding to a given beta dose was calculated as:

$$Count = (Count\,2 - background\,1)\,x\,Normalization\,number$$

where count 2 was measured in cycle 2, and count 4 corresponds to the reading after bleaching by the fluorescent lamp. The normalization number was calculated as (count 4 - background 2) divided by an arbitrarily chosen reference number. The same reference number was used to calculate all normalization numbers.

4.5.2 Single aliquot additive dose method

In the single aliquot method as described by Duller [56], two samples are used. One sample is used for generating an additive dose growth curve. The sample is given a series of beta doses and preheated after each dose before stimulation of luminescence. The preheating after each dose removes more trapped electrons than does the optical stimulation. It is therefore necessary to correct counts for loss of signal due to preheating.

The correction was done by dosing a sample and repeatedly preheating it without adding any further dose. The signal monitored at every stimulation indicated the signal remaining after that preheat. Each correction curve data point was then used to correct a corresponding data point on the growth curve. There are several advantages that this method has over the multiple aliqout method, for instance, the fact that the equivalent dose using this method can be determined with a high precision. The single aliquot method also does not require normalization of counts for differences in sample mass.

4.6 Stimulation wavelength

This section is concerned with the wavelengths used to stimulate luminescence from quartz and feldspar. The aim is to put into context the choice of stimulation wavelengths used in this study.

4.6.1 Quartz

The first OSL experiments on quartz were made using the 514.5 nm line from an argon ion laser [1]. Subsequent studies made with a view to understanding further properties of quartz OSL, for instance, studies of Godfrey–Smith *et al* [57] where 615–684 nm light from a tunable dye laser was used suggested that shorter wavelengths might be more efficient at stimulating luminescence from quartz. This was confirmed by other separate measurements [40, 58]). It has been argued that the main effect of decreasing the stimulation wavelength is to increase the electron de–trapping probability and thus increase the OSL production rate [38].

Bøtter-Jensen and Duller [41] designed a filtered lamp system for stimulation of luminescence. The output region of the lamp was reported as 420–560 nm although recently Wintle and Murray [22] concluded that the lamp behaves as a stimulation source with an effective wavelength of 468 nm.

Use of green LEDs for stimulation of luminescence was reported by Galloway [4] who used a set of 565 nm green LEDs to stimulate luminescence from quartz and feldspars. Subsequently, Galloway *et al* [34] reported an improvement over this system in terms of a better signal to background ratio and the yield of luminescence detected by using green LEDs with peak emission at 525 nm.

Use of blue LEDs for stimulation of luminescence from quartz has been

reported by Hong and Galloway [5] and by Bøtter-Jensen *et al* [6]. Hong and Galloway [5] observed that the precision with which equivalent dose values could be determined was much improved when stimulation of luminescence was done using blue rather than with green LEDs.

In summary, wavelengths in the visible part of the spectrum have been used successfully to stimulate luminescence from quartz. In this study, stimulation of luminescence from quartz was done using 525 nm and 470 nm LEDs both from Nichia Chemical Industries and 565 nm green LEDs type TLMP 7513 manufactured by III-IV.

4.6.2 Feldspar

Stimulation of luminescence from feldspars was also demonstrated by Huntley *et al* [1]. Subsequently, Huntley *et al* [59] used 514.5 and 633 nm laser lines to stimulate luminescence from feldspar with detection set at wavelengths less than 500 and 550 nm respectively. In a more detailed study, Jungner and Huntley [60] used a set of narrow pass detection filters and concluded that the dominant wavelength of emission for plagioclase feldspars is at 400 nm.

Stimulation techniques not involving the use of lasers required filtration of required wavelengths from a lamp as done by Bøtter-Jensen and Duller [41] or by use of a monochromator [2]. The significance of the work of Hütt *et al* [2] was that it demonstrated that feldspars could be stimulated by infrared light. The main stimulation band was identified to be typically around 850 nm [42] although the presence of secondary stimulation peaks near 775 nm has also been reported [61].

In this study stimulation of luminescence from feldspar was done using TEMT 484 LEDs whose peak emission is at 880 nm and TSUS5402 LEDs

which have maximum emission at 950 nm.

4.7 Luminescence emission wavelength

This section presents some details regarding wavelengths at which luminescence is emitted from quartz and feldspars. Emission wavelengths provide information on defects in the lattice which act as recombination centres and hence physical processes that lead to luminescence emission. Knowledge of emission wavelengths is also valuable in aiding proper choice of luminescence detection filters.

4.7.1 Quartz OSL

The first OSL signals from quartz were detected through a filter stack which had peak transmission at 400 nm [1]. Information concerning the wavelength of emission of quartz OSL was later augmented by Huntley *et al* [59] who used colour glass filters which revealed an emission peak at 320 nm. An alternative stimulation wavelength of 647 nm revealed a single wide band 300 – 550 nm centred at 365 nm [62]. It is generally accepted, at least as far as choice of detection filters illustrates, that with stimulation using visible wavelengths, quartz luminescence emission is over the 300 – 500 nm region. As an example, Bøtter-Jensen and Duller [41] used a U-340 detection filter while Galloway *et al* [34] used a DUG–11 filter to measure luminescence from quartz. Both filters have a transmission window in the region 300 – 400 nm.

Detection filters used in this study for quartz have been discussed in section 3.2.4 . In general, filter combinations were selected to allow detection of luminescence in the region 300 – 450 nm. Filters GG475 and GG420 were put in front of each green and blue LED respectively in order to attenuate

the low wavelength end of the LED emission spectrum which extends into the region used to detect the luminescence. The complete filter stack was chosen to optimise the level of OSL signal detected while suppressing the scattered stimulating light.

4.7.2 Quartz thermoluminescence spectra

The thermoluminescence measured from many types of quartz between about 20 and 500°C usually exhibits peaks at about 375, 325 and 110°C [38]. These TL peaks have been linked to emission at various wavelengths.

Spectral studies by Scholefield *et al* [63] showed that the 375°C peak has maximum emission at 480 nm, while the 325°C peak has an emission peak at 380 nm. The peak at about 110°C also has maximum emission at 380 nm. The 110°C peak can be induced by laboratory irradiation as well as by the photo-transfer effect [38].

In this study, photoransferred thermoluminescence resulting from green or blue LED stimulation was measured from quartz.

4.7.3 Feldspar

Some information regarding the OSL emission spectra in feldspar has been discussed in section 4.6.2. The first emission spectra from feldspar were also obtained using stimulation at 514.5 nm [1] and 633 nm [59] with the luminescence being recorded at wavelengths shorter than 500 nm and 550 nm respectively. Jungner and Huntley [60] demonstrated that feldspar OSL is most prominent at 400 nm although the full range of emission covers 300 – 550 nm. Further measurements [62] using infrared LEDs (775 – 980 nm) indicated main emission peaks at 410 nm for K feldspars and at 570 nm for plagioclase feldspars. Krbetschek *et al* [64] reported emission bands at 330,

410 and 560 nm for K-rich feldspar extracted from a sediment for stimulation using infrared light.

In general, the evidence is that the emission from feldspar is dominated by emission bands in the wavelength region 300 – 560 nm. This makes it convenient to use infrared stimulation (typically 850 – 880 nm) because stimulation and emission wavelengths are well separated. In this study, green light stimulated luminescence from feldspar was measured through a DUG11 filter and infrared light stimulated luminescence through a combination of 5–58 and BG–39 filters whose transmission window covers the region 300 – 700 nm.

Chapter 5

Preliminary Measurements

This chapter presents results of preliminary experiments conducted in setting up the system for pulsed optical stimulation of luminescence. These experiments formed the basis for more detailed investigations of time–resolved spectra and luminescence half lives from quartz. This chapter also includes reports of peripheral experiments made on aspects relevant to luminescence dating. These experiments were made on samples of feldspar and quartz with the aim of getting acquainted with the OSL equipment used in the laboratory.

5.1 Continuous optical stimulation

As part of familiarisation with OSL equipment, three experiments were conducted. The purposes of these experiments were to compare the increase of luminescence as a function of dose (the luminescence growth curve) determined using single and multi aliquot methods, to assess the influence of radiation dose on the single aliquot correction curve, and to check the influence of the duration of preheating on the single aliquot correction curve.

The single and multiple aliquot methods for generating luminescence growth curves have been discussed in section 4.5.

The measurements were made on a Norwegian microcline used in previous studies by Galloway [4, 46, 65, 66, 67] and a Norwegian orthoclase [66, 67], as well as on samples of heated quartz. The quartz, whose preparation was discussed in section 4.3, had also been used in other previous investigations [4, 34, 66].

Luminescence was stimulated from samples of quartz and feldspar using 525 nm green LEDs (Nichia NSPG–500), 565 nm green LEDs (III–V TLMP7513), 470 nm blue LEDs (Nichia NSPB–500) and except for quartz, infrared LEDs (TSUS5402 with peak emission at 950 nm, and TEMPT 484 with peak emission at 880 nm).

5.1.1 Comparison of single and multi aliquot methods using infrared stimulation

This experiment was made to compare the form of luminescence growth curves in microcline and orthoclase as determined using the single and multiple aliquot methods. The luminescence was measured as a function of dose for the doses 7.5, 15, 30, 60, 90, 120 and 150 Gy. The value of luminescence at any dose in the multi aliquot method was calculated as an average of 10 measurements. In the single aliquot method, correction for loss of signal due to repeated heating and optical stimulation was done using the method proposed by Duller [56]. Following each beta dose, each sample was preheated at $200^{o}C$ for 10 minutes before stimulation of luminescence at $30^{o}C$ for 1 s using the 950 nm infrared LEDs (type TSUS5402).

The luminescence measured as a function of dose using the multi aliquot method is shown in Fig. 5.1 for microcline feldspar. The luminescence is

observed to increase linearly as a function of dose. There is a small count against zero dose i.e a positive intercept on the counts axis. This observation of a small count against zero dose had previously been attributed to the combined effects of photomultiplier noise, scatter from stimulating light and a small recuperated signal [68].

Four single aliquot measurements were made and corrected [56] in order to compare with the the multi aliquot response of luminescence to dose in microcline feldspar. A comparison of the growth curves is shown in Fig. 5.2 (for one of the single aliquots) where the form of the increase in luminescence appears similar in both cases. A quantitative comparison of the growth curves was made by examining the ratios of the single aliquot counts/s to multiple aliquot counts/s for each beta dose. The basis for this method is that if the luminescence readings at corresponding doses are similar for the single and multiple aliquot methods, the ratio of the single aliquot counts/s to multiple aliquot counts/s should be a constant independent of dose [69]. Fig. 5.3 shows, for one of the single samples, a plot of the ratio of single to multiple aliquot counts against beta dose. A least squares fit to the data suggests a slight increase in the ratio against beta dose. However, given the size of the error bars, such an increase is not statistically significant. Thus the luminescence growth curves determined using the two methods are similar.

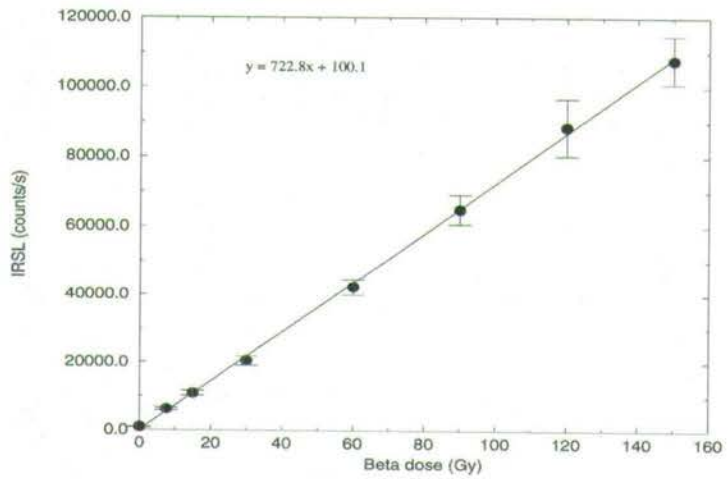

Figure 5.1 The luminescence growth curve from microcline measured using the multiple aliquot method.

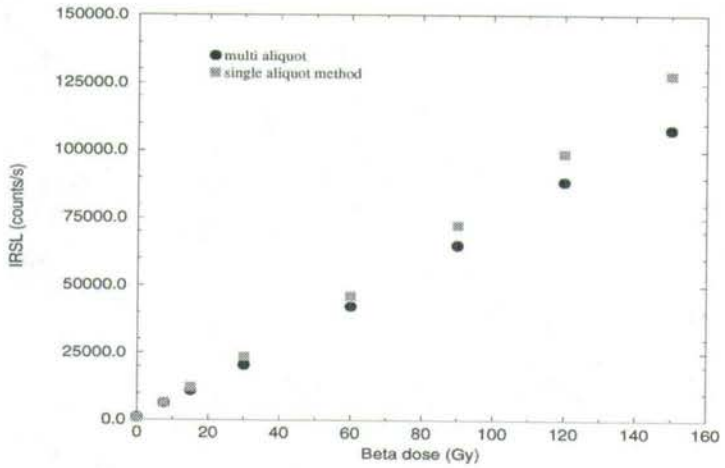

Figure 5.2 A comparison of luminescence growth curves in microcline determined by the single and multi aliquot methods. The error bars for points corresponding to the same dose would overlap and are omitted for clarity.

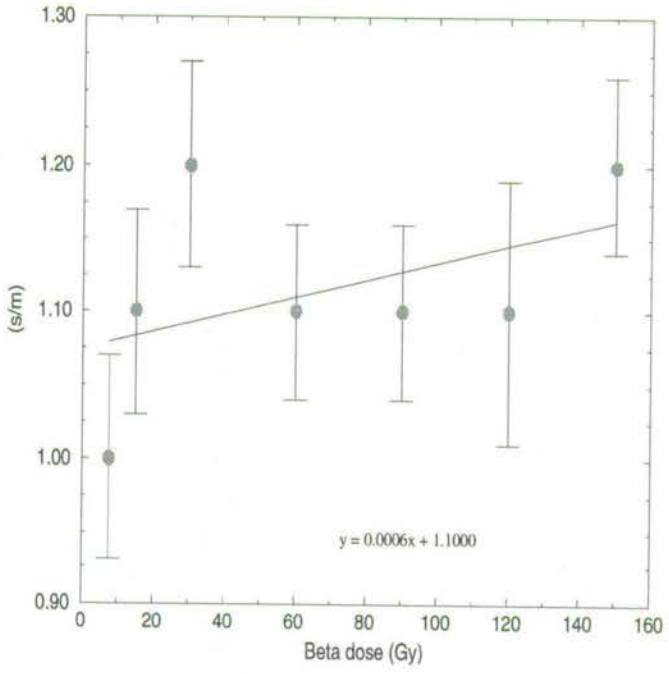

Figure 5.3 The ratio of single to multiple aliquots counts/s at equal beta doses for microcline feldspar stimulated by infrared (950 nm) LEDs.

5.1.2 Comparison of single and multi aliquot methods using green light stimulation

The growth curve of luminescence stimulated by 525 nm green LEDs (Nichia NSPG–500) in microcline using the multi aliquot method is shown in Fig. 5.4. The luminescence response as a function of dose appears to be linear. In this case a least squares fit to the data gives a negative intercept. However, the size of the uncertainties to the fit show a consistency with an expected

small value of luminescence at zero dose. One important difference between growth curves in Fig. 5.4 and Fig. 5.1 is the better precision in values of luminescence at each dose in Fig. 5.4 as denoted by the size of the error bars.

For comparison, five single aliquot measurements of growth curves were made an example of which is shown in Fig. 5.5. In this example, it appears that the luminescence increase with dose determined by the single aliquot method is also linear. In this example, the intercept is negative as the size of the uncertainty in the fit shows. There is the possibility therefore that the increase of green light stimulated luminescence with dose at small doses might be supralinear (also [68]).

The form of the luminescence growth curves in microcline as determined using the single and multiple aliquot methods are compared in Fig. 5.6 where the ratios of the single to multiple aliquot luminescence counts/s are plotted against added beta dose. It can be observed that the ratio of counts/s against beta dose is essentially constant as also illustrated by the least squares fit to the data. In comparison with the ratios determined using infrared stimulation shown in Fig. 5.3, it is apparent that there is better agreement between single and multiple aliquot method in Fig. 5.6. It is notable that this better agreement between the methods occurs in this case where the precision in multi aliquot counts/s was better than for the infrared (950 nm) stimulation.

This experiment showed a good agreement in luminescence as a function of dose using the multiple and single aliquot methods. The advantage of using the single aliquot method as pointed out previously [56] became apparent. For example, the improved precision in values of luminescence corresponding to each dose since only one sample is used and no normalisation is required for sample mass variations.

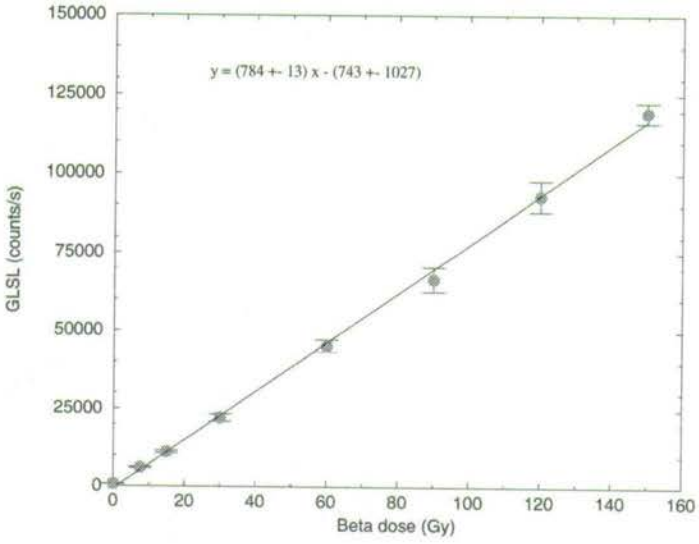

Figure 5.4 A luminescence growth curve from microcline measured using the multiple aliquot method.

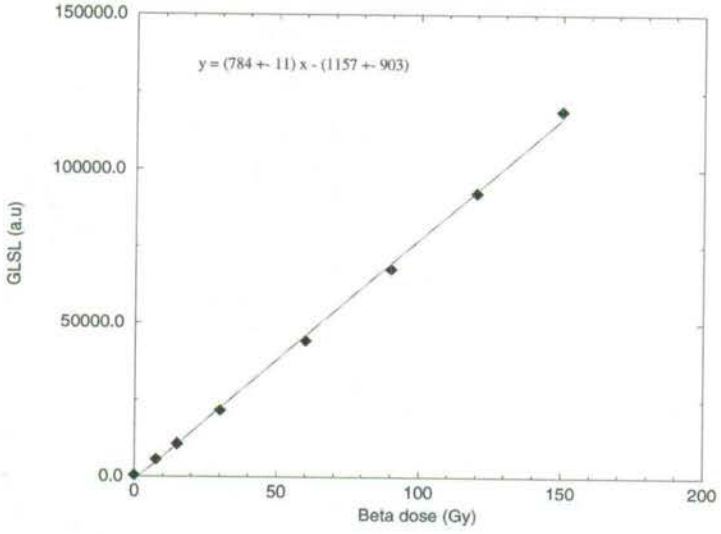

Figure 5.5 A luminescence growth curve from microcline measured using the single aliquot method.

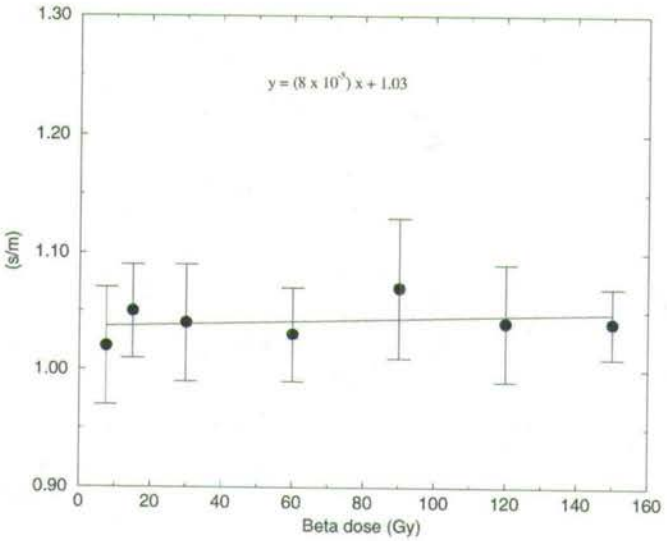

Figure 5.6 The ratio of single to multiple aliquots counts/s at equal beta doses for microcline feldspar. Luminescence was stimulated using green LEDs.

5.2 Dose dependence of the single aliquot correction method

The aim in this set of short experiments was to investigate whether the decay of luminescence induced by a beta dose decayed during successive preheating in a way which depended on the size of the beta dose used. The resulting plot of luminescence against number of preheats (the correction curve) is necessary for correcting single aliquot data for loss of signal due to repeated preheating and optical stimulation.

5.2.1 Infrared light stimulation of feldspar

The decay of luminescence due to repeated preheating and optical stimulation was investigated using for stimulation, 950 nm LEDs (type TSUS 5402) and 880 nm LEDs (TEMPT 484).

In one experiment, separate samples of orthoclase were dosed up to 30, 150 and 600 Gy and preheated at $200°C$ for 10 minutes before every 1 s stimulation of luminescence at $30°C$ by the 950 nm infrared LEDs (type TSUS 5402). Fig. 5.7 compares the correction curves for the three samples.

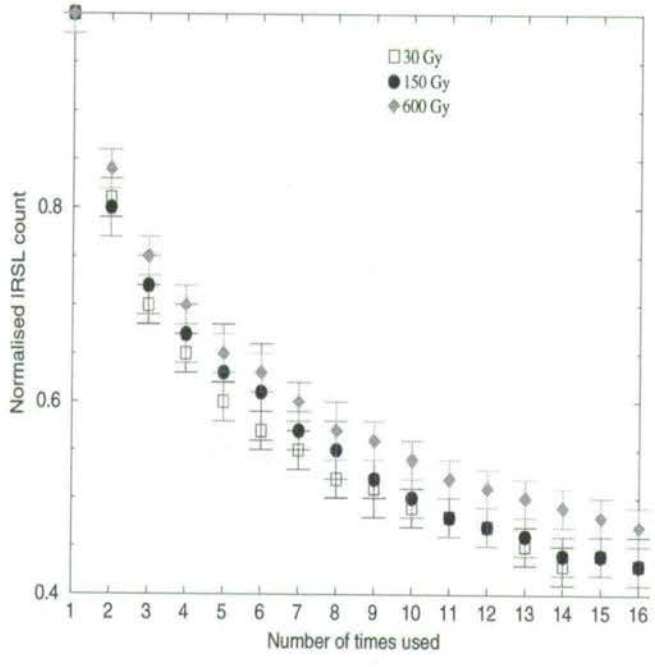

Figure 5.7 A comparison of the single aliquot correction curves from orthoclase dosed to 30, 150, and 600 Gy.

In this set of results, the shape of the luminescence correction curve does not appear to be influenced by the size of the initial dose. However, a comparison of the curves corresponding to 30 and 600 Gy, doses differing by a factor of 20, shows the luminescence from the sample with the higher dose to be decreasing at a slightly slower rate.

In the second experiment, luminescence correction curves were generated from samples of microcline. Samples were dosed to 1.5, 15 and 75 Gy and preheated at $220°C$ for either 10 minutes or 1 minute before every 0.1 s stimulation at $30°C$. Luminescence was stimulated using TEMPT 484 LEDs which have an emission maximum at 880 nm. The rate of decay was compared directly using the slope of a least squares fit of the form suggested by Galloway for feldspars [65]:

$$f(n) = 1 - a \ln n$$

where f(n) is the fraction of luminescence remaining, n is the number of measurements on the sample and the parameter a depends on duration of preheating, preheating temperature, duration of optical stimulation and mineralogy of the feldspar. Fig. 5.8 compares for beta doses 1.5, 15 and 75 Gy, the influence of dose on the correction curves. It can be seen that the rate of decay as represented by the slope to the linear fit, is essentially independent of the size of beta irradiation used at both preheats.

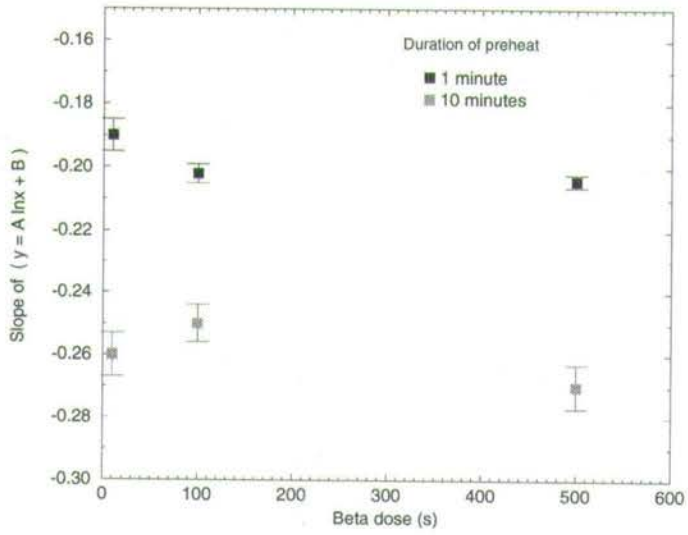

Figure 5.8 A comparison of the effect of dose on the correction curve for microcline with preheating at $220°C$ for either 10 minutes or 1 minute.

5.2.2 Green light stimulation of feldspar

The influence of dose on the correction curve for microcline was also investigated using green light stimulation. In this case, samples of microcline were dosed up to 15, 75, 300 and 600 Gy and preheated at $200°C$ for 10 minutes before every 1 s measurement of luminescence at $30°C$. Fig. 5.9 compares the correction factors from each of the four samples. It can be observed that the value of beta dose given to the sample appears not to influence significantly the way the luminescence decays with successive preheating.

The general conclusion from this set of experiments was that the single aliquot correction curve is essentially independent of the size of dose that the sample is given prior to measurement of the correction data. Further,

experimental data showed the correction curve to be independent of dose regardless of type of feldspar used (microcline or orthoclase), the preheating method (either $200°C$ or $220°C$ for 10 minutes or $220°C$ for 1 minute) and the wavelength used to stimulate the luminescence (520 nm, 880 nm or 950 nm). These results are in agreement with previous tests on potassium feldspar under infrared stimulation [56] where it was concluded that there was no significant difference in the way the beta induced luminescence signals decayed due to repeated preheating.

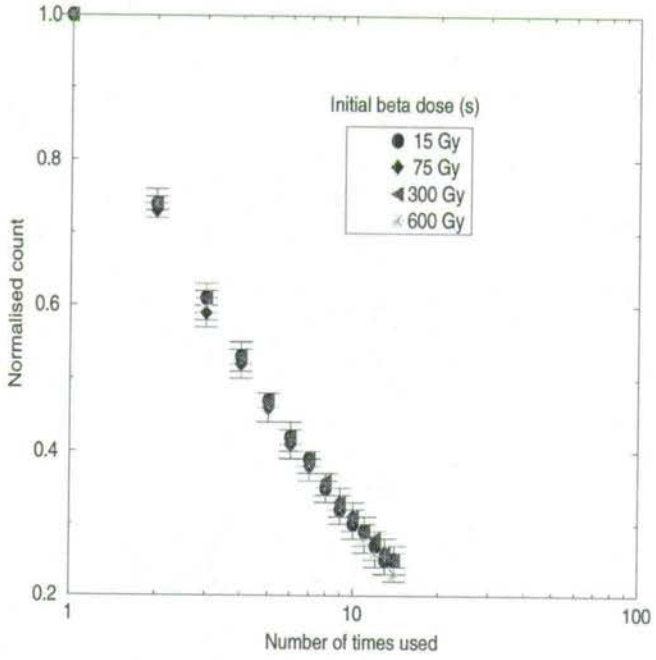

Figure 5.9 A comparison of single aliquot correction curves in microcline under green light stimulation.

5.2.3 Blue light stimulation of quartz

The influence of beta dose on the rate of decay of luminescence was also investigated for quartz heated prior to dosing. In this case, samples were dosed up to 2, 3.5, 14 and 28 Gy. Preheating was done at $220°C$ for either 5 minutes or 1 minute before every 0.1 s measurement of luminescence at $30°C$. Luminescence was stimulated using blue LEDs, Nichia type NSPB–500 with a peak emission at 470 nm.

The decay data was well fitted by a modified version of the feldspar correction [5, 65], namely

$$ln\, l = An + C$$

where l is the luminescence remaining, n the number of times the sample is heated and A and C are fitting parameters. Using the values of the slope from curves corresponding to various beta doses, the effect of dose on the correction curve could be examined. Fig. 5.10 compares the effect of dose on the decay of luminescence from quartz under successive heating and optical stimulation. Apart from statistical scatter, the similarity in values of the slope show that the rate of decay of luminescence is independent of the value of initial dose. It is also evident that the duration of preheating influences the rate of decay. This is illustrated in a more conventional manner in Fig. 5.11 where decay curves are compared of samples given the same dose but preheated for either 1 minute or 5 minutes at each preheating stage. It is evident in Fig. 5.11 that the longer preheating depletes signal faster than the shorter preheating.

The general conclusion from the experiment is that the single aliquot correction curve in heated quartz (the type used) under stimulation by blue light is not influenced by how much the sample has been dosed to.

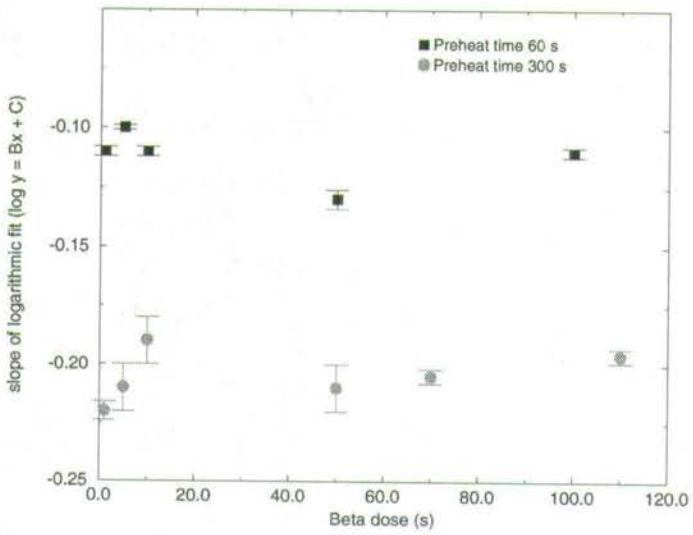

Figure 5.10 A comparison of the effect of dose on the correction curve for heated quartz with preheating at $220°C$ for either 5 minutes or 1 minute.

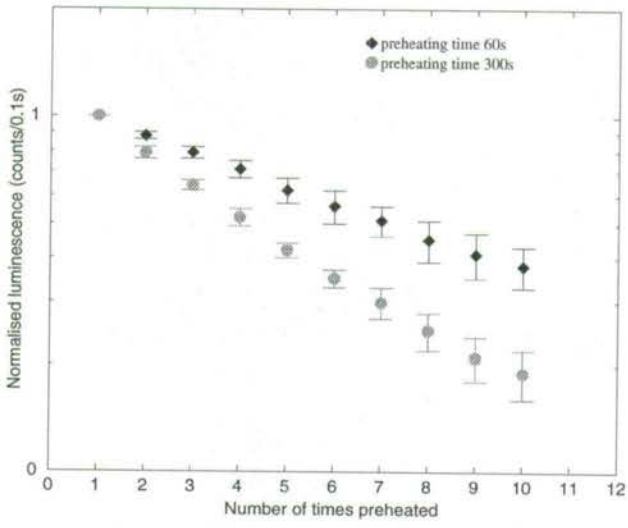

Figure 5.11 A comparison of the decay of luminescence in quartz given the same dose but preheated repeatedly at $220°C$ for either 1 minute or 5 minutes.

5.3 Pulsed optical stimulation of luminescence

This section reports initial measurements made to test the performance of the pulsing system. The section also includes experimental data concerning time dependence of luminescence.

5.3.1 Preparatory measurements

Initial measurements of pulsed optical stimulation were concerned with optimising the performance of the pulsing system. Experiments were conducted to optimise the light emitting diode intensity, rise and fall times and to achieve well defined time–resolved spectra of the light emitting diodes. Subsequent measurements were concerned with determining luminescence half lives from quartz. The first measurements, however, were made on feldspar in order to obtain half life data to compare against other published data as a way of assessing the performance of the system. These experiments also proved useful in choice of dynamic ranges for use when measuring half lives from feldspar and quartz.

Measurements of time–resolved spectra were made using samples of Norwegian microcline and orthoclase described earlier in section 4.3. Fig. 5.12 compares a green light emitting diode emission time–resolved spectrum and the stimulated luminescence time–resolved spectrum from microcline feldspar. The light emitting diode time–resolved spectrum was recorded with only neutral density filters in front of the photomultiplier (EMI type 9635QA, rise time 10 ns). In Fig. 5.12 the counting rate scales have been arbitrarily adjusted for ease of comparison of shapes. Subsequent luminescence measurements were made with the Schott BG39 and UG11 filters in front of the photomultiplier.

It can be seen in Fig. 5.12 that there is a slight delay between the diode rise time and the resultant luminescence signal. Consequently, maximum luminescence emission was observed to occur about 14 ns later than the peak of the stimulating pulse. This test showed that the luminescence from microcline consists of fast half life components of the order of 20 ns as well as slower components of the order of tens of μs and that to study properties of these half life components would require use of appropriate dynamic ranges.

As a follow up, the same pulse width and duty cycle settings were used to search for evidence of luminescence emission from quartz. However with the set–up that was suitable for feldspar, no luminescence decay from quartz could be detected. As an example, Fig. 5.13 compares a signal before and after a beta dose measured from a sample of quartz using a pulse width of 1 μs and displayed over a dynamic range of 4 μs. In this set–up, no luminescence decay is apparent. However, the fact that a signal larger than the background could be obtained signified that an appropriate pulse width and dynamic range were necessary to observe the decay of pulsed luminescence emission from quartz.

Fig. 5.14 compares time–resolved spectra from samples of quartz and feldspar. In this case an 8 μs luminescence stimulating pulse and a 32 μs dynamic range were used. The comparison shows that there are no half life components in the ns scale from quartz and emphasizes that this fast half life component is dominant in pulsed luminescence from feldspar. Also, both samples show luminescence half life components of the order of tens of μs.

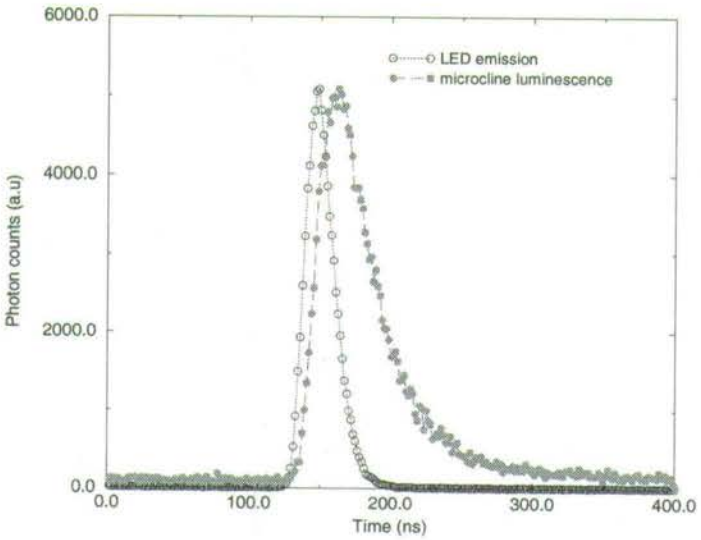

Figure 5.12 A comparison of a green light emitting diode emission time–resolved spectrum and a stimulated luminescence time–resolved spectrum from microcline.

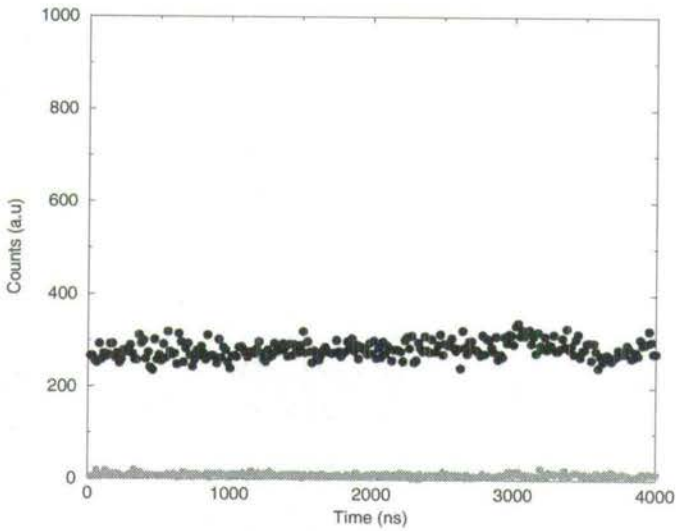

Figure 5.13 A comparison of signals measured from quartz before and after a beta dose using a 1 μs pulse and a 4 μs dynamic range.

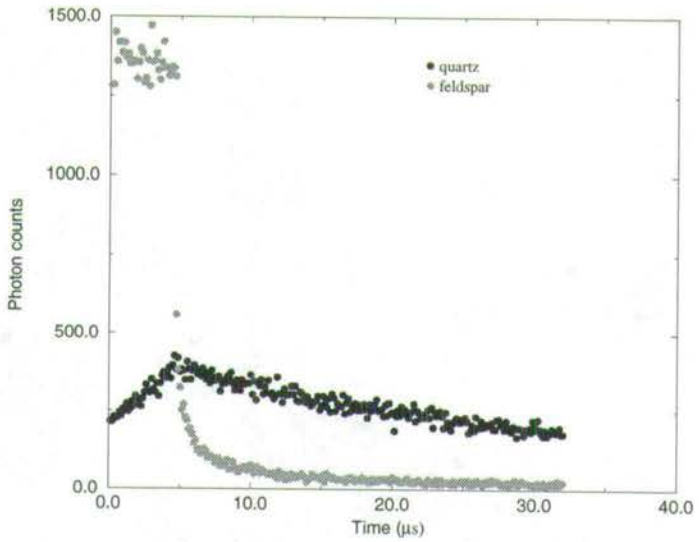

Figure 5.14 A comparison of time–resolved spectra measured from quartz and feldspar using an 8 μs pulse and 32 μs dynamic range.

5.3.2 Time dependence of luminescence from feldspar

The time–dependent decrease of luminescence from a sample under continual stimulation was also used as a test of performance of the pulsing system.

The effectiveness of the pulsing system in bleaching luminescence from microcline and orthoclase feldspar samples was compared against DC operated LEDs. The test compared the time taken to bleach luminescence from a dosed sample to half the initial maximum. The DC operated LEDs, which were run at a current of 30 mA per LED, were blue LEDs (Nichia NSPB–500, 470 nm), green LEDs (Nichia NSPG–500, 520 nm; III–V TLMP7513, 565 nm), and Infrared LEDs (TSUS5402, 950 nm; TEMPT 484, 880 nm).

Fig. 5.15 compares the time to reduce luminescence to 50% of its initial value as measured by the different sets of 16 LEDs. Of particular interest is the comparison between the pulsed and DC operated green LEDs which

shows a factor of 2.5 difference in bleaching the luminescence. The DC operated green LEDs took about 100 s to reduce luminescence to half maximum in comparison with the pulsed LEDs which took about 250 s. Given that the approximate 10% duty cycle present in pulsing arrangement means the LEDs are on for only 10% of the time, it would be expected that the time for the pulsed LEDs would be 10 times as long as that for DC operated LEDs i.e 1000 s. Since the DC operated LEDs were run at 30 mA/LED in comparison with about 70 mA/LED for the pulsed LEDs, the estimated time for the pulsed LEDs should then come down to 500 s. The experimentally obtained time of 250 s is consistent with this calculation given the possibility of differences in LEDs, one possible source of non–uniformity in LED brightness.

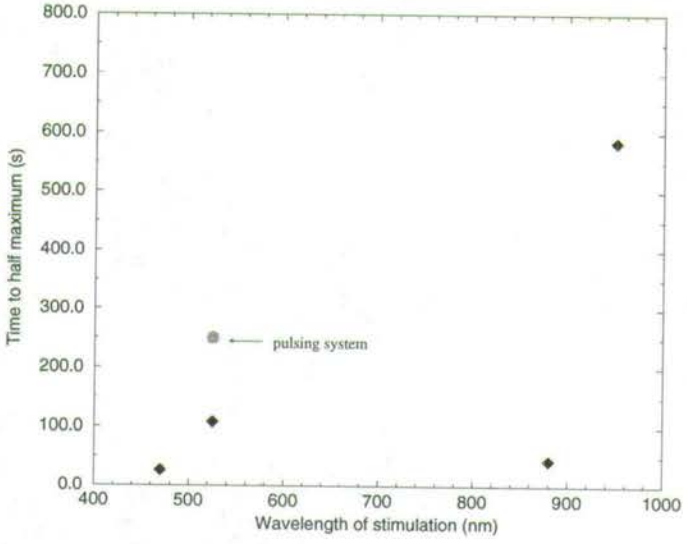

Figure 5.15 A comparison of bleaching times measured from dosed samples of microcline using green LEDs (520 nm, 560 nm), blue LEDs (470 nm), and infrared LEDs (880 nm, 950 nm).

5.3.3 Time dependence of luminescence from quartz

The properties of the decrease of luminescence with time, the decay curve, was studied in samples of quartz. The information from this study was relevant in relation to the study of the time dependence of luminescence half lives from quartz. In principle, time–resolved spectra can be measured from a sample immediately after dosing and preheating or after bleaching to reduce the amount of luminescence. Thus in each case the properties of luminescence half lives can be related to a decay curve measured in similar conditions.

The fall of luminescence with time that results from continuous stimulation of luminescence from quartz as shown earlier in Fig. 2.2 can usually be described by a sum of three exponentials e.g [20, 23]with the third component (the slow component) being characterised by a very slow decay rate. It has been suggested that mechanisms of luminescence emission at long stimulation times could be indicative of effects such as electron re–trapping or the release of charge from multiple traps each with a distinct probability of stimulation [18, 23].

Although each of the three exponential components may not necessarily be associated with a separable physical mechanism, the method provides a convenient representation of the shape of the decay curve. Samples of quartz used in this study exhibited the slow component. An example is shown in Fig. 5.16. Although the luminescence has decayed to less than 1 % of the initial maximum, the rate of decay is evidently slow and the decay curve has not converged to the background level.

The relative intensities of the exponential components extracted from a decay curve are shown in Fig. 5.17 where the ratio of each component to the sum of the three components is plotted against the time of exposure to stimulating light. As Fig. 5.17 shows, in the initial transient, nearly 75% of the measured luminescence is due to the fast component with the slow component contributing 10%. As stimulation progresses, the fast component declines to an insignificant percentage of the total sum while the medium component increases in importance from about 20 to 40% of the sum in the first 30 s and progressively declines thereafter. It is notable that the fast component is important only in the initial 30 s or so. In contrast, the contribution of the slow component evolves from a minimum of about 10 to 50% of the total in the first 50 s and by 150 s the measured luminescence

predominantly consists of the slow component. Although in Fig. 5.17 the abscissa is presented in hundreds of seconds, the slow component can still be measured after hundreds of thousands of seconds as similar measurements showed.

5.4 Measurements of luminescence half life

This section presents preliminary measurements of half life values from samples of feldspar. This sample was studied first before detailed measurements were made using quartz.

During the luminescence–stimulating light pulse the time–dependence of the luminescence is influenced by both the shape of the light pulse and the luminescence half life, whereas after the end of the light pulse only the luminescence half life is relevant. Consequently, half lives were determined only from the part of the time–resolved spectrum following the end of the stimulating light pulse.

Although in luminescence studies the use of mean lifetime is usual to denote decay times, e.g [10, 11, 24, 25] in this thesis use of half life was adopted as is customary in nuclear physics. One advantage in this was the convenience of inspecting half lives directly from time–resolved spectra.

Fig. 5.18 shows a luminescence time–resolved spectrum obtained with a stimulation pulse width of 4.4 μs and displayed over a dynamic range of 32 μs. In the plot, time–resolved spectra are shifted from zero so that the origin in the graph does not correspond to the switching on of the LEDs. The region up to 4 μs which appears essentially flat consists primarily of luminescence from feldspar during the light pulse. Because the build-up of luminescence reaches a maximum after a time of the order of 100 ns, the shape in this

region is dominated by the longer (4μs) and flatter light emitting diode pulse. Following the pulse is the decay of stimulated luminescence. In this example, values of half life calculated were 180 $\pm$ 1 ns and 12 $\pm$ 2 μs.

Table 1 compares luminescence half lives from feldspars found in this study with those from other works for luminescence detection in the wavelength region 300 – 400 nm. Values of luminescence half lives found in this study were in the range 23 ns – 15 μs for orthoclase and 24 ns – 12 μs for microcline, values covering a similar range. Luminescence half life values of the order of 20 ns and 200 ns found in this study (e.g 23 $\pm$ 1 ns, 220 $\pm$ 1 ns) are in good agreement with values reported by Clark *et al* [10] and Clark and Bailiff [11] (e.g 22.5 $\pm$ 0.1 ns, 195 $\pm$ 3 ns). In these preparatory measurements, however, the longest value of half life found was about 15 μs, and no half life values around 3 μs were measured. In comparison, although Clark *et al* [10] and Clark and Bailiff [11] reported luminescence half life values of the order of 15 μs, they noted that this long component made a small contribution (typically less than 2 %) to the total measured signal. In general, differences in values of half lives in this work and in the works shown in table 1 could be attributed to differences in sample mineralogy, stimulation wavelength, and possibly the wavelength of luminescence detected.

The information gained in making measurements of half life from feldspar and evidence of possible pulsed luminescence emission from quartz as described in section 5.3.1 were the basis for more detailed investigations concerning luminescence half lives in quartz.

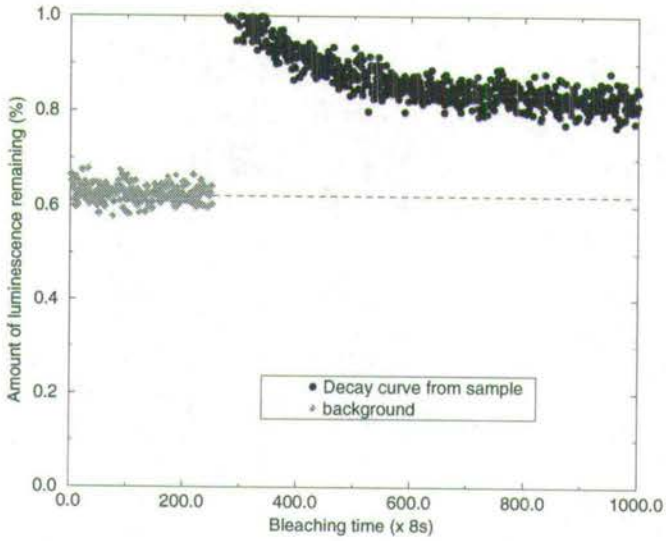

Figure 5.16 The luminescence decay curve from quartz after 1000 s of stimulation compared to the background level.

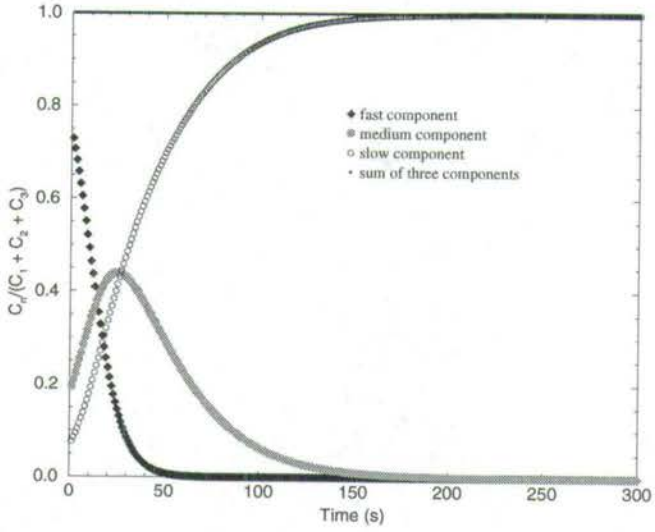

Figure 5.17 Components of a decay curve.

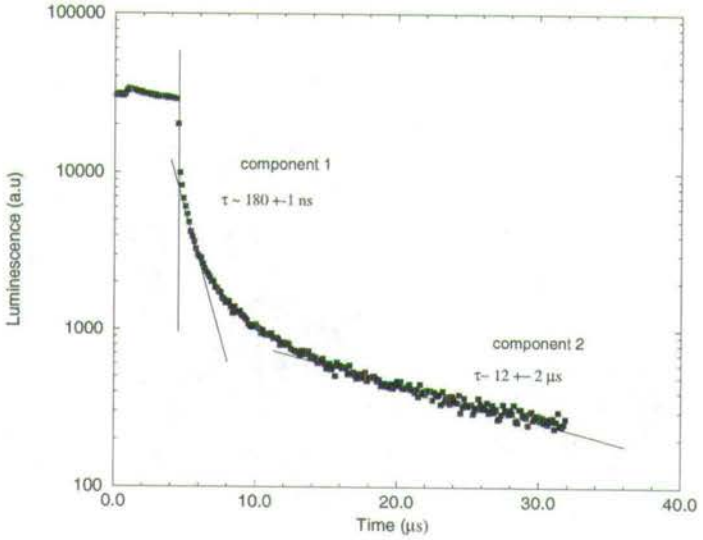

Figure 5.18 A luminescence time–resolved spectrum from microcline stimulated at 525 nm. The pulse width used was 4.4 μs and luminescence was recorded over a dynamic range of 32 μs. The sample was given a beta dose and preheated at $220^{o}C$ for 10 minutes prior to recording of the time–resolved spectrum. The lifetime of the fast component (180 ± 1 ns) had been determined separately using a measurement similar to that described in Fig. 5.12.

stimulation wavelength (nm)	Pulse width (ns)	Dynamic range (μs)	Detection band (nm)	Sample	Half life (ns)	Reference
470 (LASER)	10	320	280 - 380	alkali feldspars	exact values not specified	Sanderson and Clark (1994)
850 (LASER)	5	40	280 - 380	orthoclase	19.4 +- 3.0, 23.6 +- 0.7, 266 +- 4, 2700 +- 200**	Clark *et al* (1997)
850 (LASER)	5	40	300 - 550	orthoclase	13.2 +- 0.3, 17.7 +- 0.3, 22.5 +- 0.1, 23.9 +- 0.1, 195.4 +- 2.8, 297.3 +- 0.7, 3167 +- 20.8**	Clark and Bailiff (1998)
525 (LED)	50, 4400	32	330 - 380	orthoclase	23 +- 1, 220 +- 1, 15000 +- 1000	This work
525 (LED)	50, 4400	32	330 - 380	microcline	24 +- 1, 180 +- 1, 8000 +- 1000, 12000 +- 2000	This work

**Values quoted here are those that were reported to have contributed >30 % of measured signal. Original data has been converted to half life by multiplying by 0.693.

Chapter 6

Measurements of luminescence half life

This chapter presents results of measurements of half life and intensity of the luminescence stimulated from quartz by pulsed green- and blue-light emitting diodes. Results concerning stimulation by pulsed green LEDs are reported in section 6.1 and results for pulsed blue LED stimulation in section 6.2.

6.1 Green light stimulation

Section 6.1.1 presents results of investigations conducted on time dependent measurements of luminescence half life at room temperature. Section 6.1.2 is on the effect of radiation dose on luminescence half life. Section 6.1.3 is concerned with the influence of preheating on luminescence half life. Sections 6.1.4 and 6.1.5 report temperature related characteristics of luminescence half life. Section 6.1.4 concentrates on measurements at specific temperatures while sections 6.1.5 reports results from dynamic temperature experiments. Features of luminescence half life and luminescence intensity in the slow

component are reported in section 6.1.6.

6.1.1 Time dependent measurements of half life at room temperature

It was observed during initial measurements of time–resolved spectra from quartz that values of half life calculated from time–resolved spectra differed depending on whether or not the sample had been heated prior to dosing. Heating was one of the methods used to remove remanent luminescence from samples, the other was to expose samples to daylight for 4 weeks or more. The experiment on time–dependent characteristics of half life was therefore conducted to investigate how the values of half life from the two types of quartz (heated or daylight bleached) would be affected by continuous optical stimulation. The method used was to repeatedly record time–resolved spectra from a sample and in effect observe the change of half life with stimulation time.

The results reported in this section are for measurements made at room temperature, typically $20 \pm 2^{o}C$. All samples in this experiment were given a beta dose of 150 Gy and preheated at $220^{o}C$ for 5 minutes before measurement of time–resolved spectra. The dose was chosen to enable measurements of time resolved spectra with high enough counts to enhance the accuracy in the calculated half life values, and to have measurements cover a long stimulation time.

The green LEDs used for stimulation of luminescence were operated with a pulse width of 11 μs, a period of 90 μs, a duty cycle of about 12.4% and a repetition rate of 11 kHz. Time–resolved spectra were recorded over a dynamic range of 64 μs using different counting times. Each counting time was corrected for the duty cycle to give the LED–on–time or the total time

of exposure to luminescence–stimulating light. The first few measurements following dosing and preheating could be made with counting times as short as 1 s without loss of accuracy (i.e with little scatter of experimental data points) in the recorded time–resolved spectra. However, at long stimulation times, with the luminescence intensity gradually decreasing, longer counting times became necessary in order that half lives calculated from time–resolved spectra could be reliable.

In order to evaluate half lives, the time–resolved luminescence after the pulse, L, were fitted by single exponential functions of the form

$$L = Ae^{-\lambda t} + R$$

where A is a constant related to the maximum intensity of luminescence, R is a constant related to the background signal, λ is the decay constant of the luminescence and t is time.

The commercial software package *Fig. P* was used for curve fitting. In the program, initial estimates for the parameters A and λ had to be supplied. A known and constant value for R was also supplied as the background signal was measured first in every case. The program then iteratively improved on then estimates (using the Marquardt minimization routine) until the estimates converged to a final set of values of A and λ. The final values were displayed in a statistical report which included the associated standard errors, t ratios, and confidence intervals. Thus a 'best fit' could be recognized and assessed quantitatively. Since the half life τ associated with luminescence decay is related to the decay constant λ by $ln2 = \lambda\tau_{1/2}$ half life values could be evaluated.

Fig. 6.1 shows examples of luminescence time–resolved spectra recorded from samples of heated quartz (Fig. 6.1 a) and from quartz bleached by exposure to daylight (Fig. 6.1 b). A background signal is shown in each

case for comparison. Both samples were dosed up to 150 Gy and preheated at $220^{o}C$ prior to measurement of luminescence time resolved spectra. The luminescence builds up during the light pulse and the signal at any time during this time consists of a monotonically increasing luminescence signal and a small constant scatter from the light emitting diodes. It can be seen for the example in Fig. 6.1 (a) that the background signal after the stimulating pulse (the region used for half life calculations) is usually a negligible component of the total luminescence signal. In this example, a mean of 5 for the background compares with a maximum count of 4555 and a minimum count of 731 for the luminescence. For daylight bleached quartz, the relatively lower level of luminescence signal leads to a larger scatter in the data points. The time–resolved spectrum for the less sensitive daylight bleached quartz [16] has an intensity at the beginning of decay that is well below the maximum of the luminescence build–up signal plus scattered light.

Fig. 6.2 shows the relationship of half life with cumulative time of luminescence stimulation in heated and daylight bleached quartz. In this example, the samples were also given a beta dose of 150 Gy to record measurements over relatively long times. It can be seen that in heated quartz, half life values display a 'growth curve' characteristic, increasing from about 20 μs to a constant value of about 26 μs. In daylight bleached quartz, continual stimulation of luminescence did not affect half life values which remained constant at around 24 μs throughout the measurement period. In general, both types of quartz show that a constant value of half life is reached after extended stimulation. For samples studied in this experiment, the limiting values were 26.8 ± 0.4 μs and 24.2 ± 0.4 μs for heated and daylight bleached quartz respectively. Thus both limiting values and stimulation–time related characteristics of half life with time in the samples are different suggesting

that theses factors are affected by the method used to bleach the samples prior to dosing.

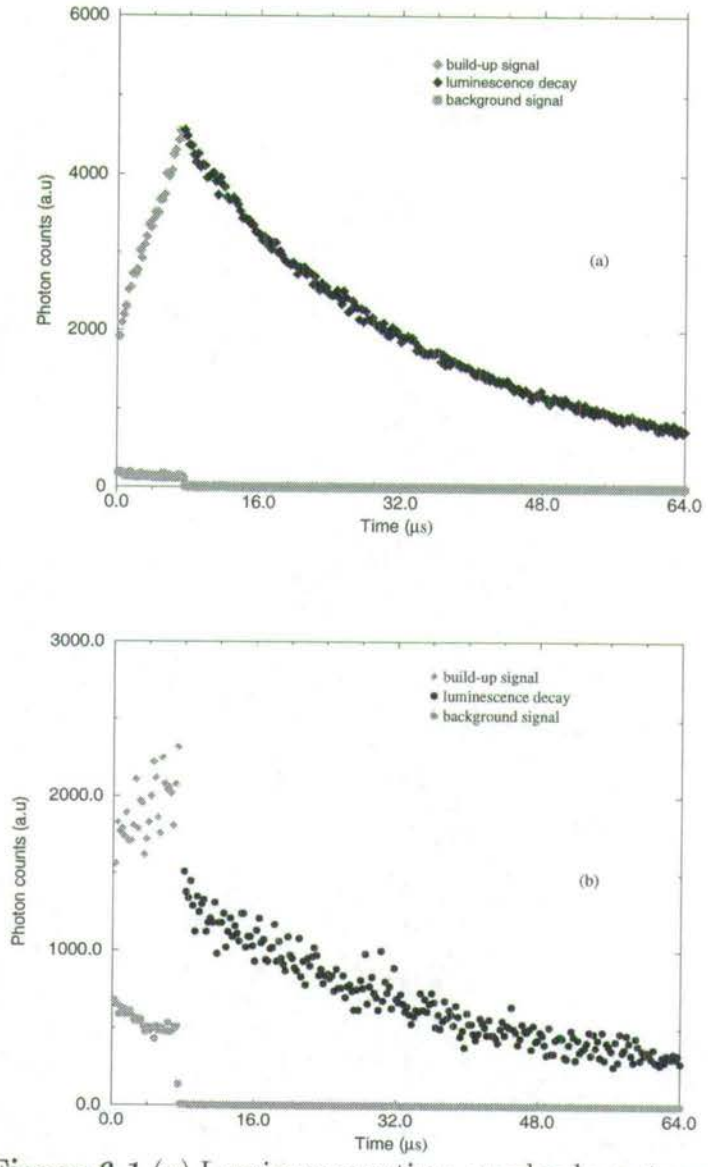

Figure 6.1 (a) Luminescence time–resolved spectrum from heated quartz and in (b) daylight bleached quartz. The pulse width used was 11 μs and luminescence was recorded over a dynamic range of 64 μs. Background measurements are shown for comparison.

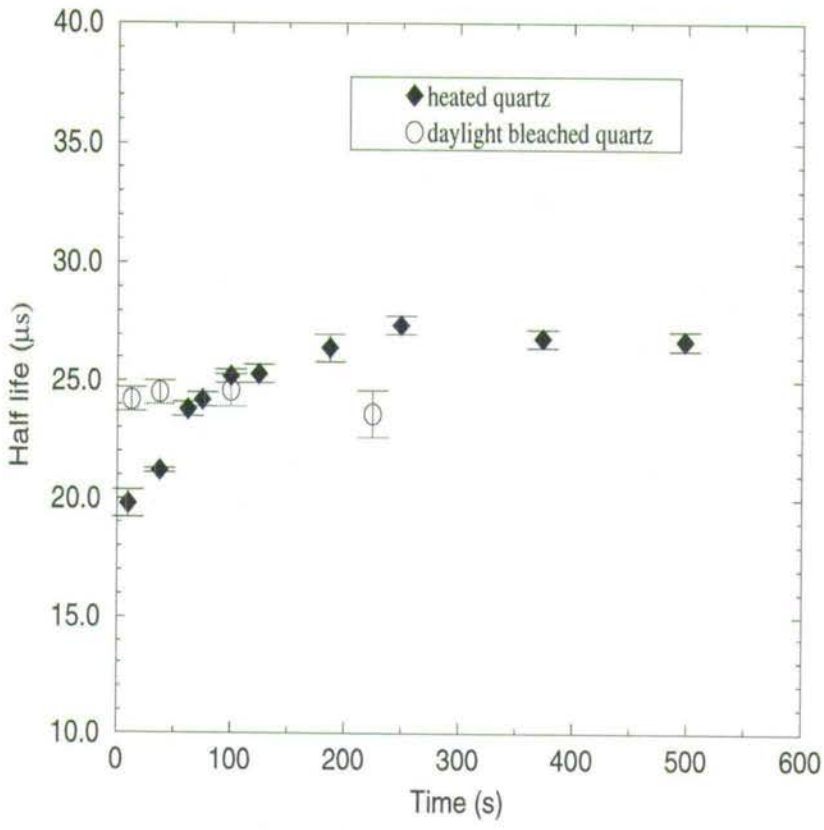

Figure 6.2 A plot of half life as a function of time for measurements made on heated and daylight bleached quartz. All samples were given a beta dose of 150 Gy and preheated at $220°C$ for 5 minutes.

6.1.2 The effect of radiation dose on luminescence half life

The relationship of half life and stimulation time was investigated over a wider dose range for daylight bleached quartz owing to its limited sensitivity to luminescence stimulation and for values less than 150 Gy for heated quartz. Stimulation of luminescence from heated quartz following doses larger than 150 Gy was not done to avoid high counting rates which lead to false half lives as discussed in section 4.1.

Separate heated quartz samples were each given a beta dose of 1.5, 15 and 150 Gy and preheated at $220°C$ for 5 minutes before recording of time resolved spectra for half life analysis. Daylight bleached samples were given doses of 150 Gy and 1500 Gy.

Fig. 6.3 compares the change of half life values with stimulation time for samples of heated quartz given beta doses of 1.5, 15 and 150 Gy. In all three samples, the half life increase with time to a constant value. Inspite of the large difference in dose, the difference between final values in all cases is no more than 10%. Even the difference in minimum (initial) values is only 10% i.e 22 μs for the 1.5 Gy sample and about 20 μs for samples dosed with 15 and 150 Gy beta dose. The good agreement between half life values associated with the 15 and 150 Gy samples suggests that over this dose range, the change of half life with time is independent of dose. The general observation from this set of samples is that larger values of dose are associated with smaller initial values of half life while the final values seem to be independent of dose in the dose range of 1.5 to 150 Gy.

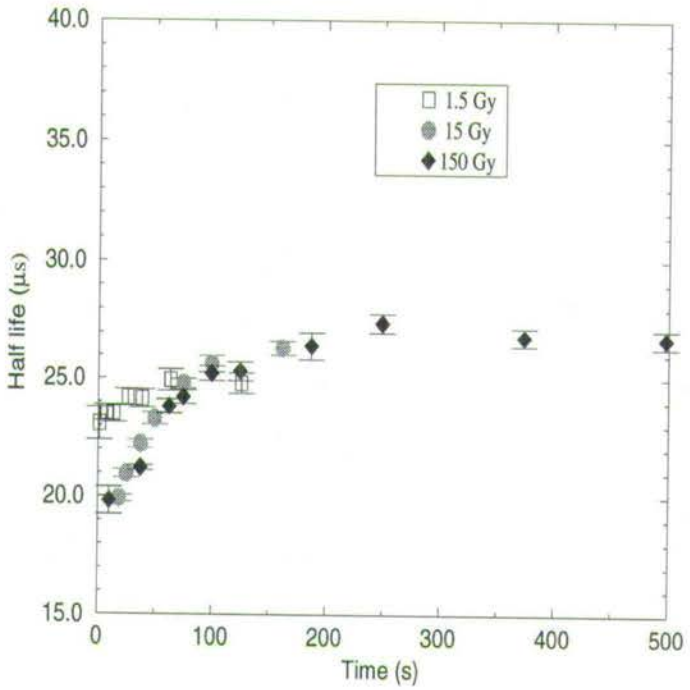

Figure 6.3 Change of half life with time for a heated quartz sample given beta doses of 1.5, 15 and 150 Gy.

Fig. 6.4 compares half life values for samples of daylight bleached quartz given beta doses of 150 and 1500 Gy with values of half life from a sample of heated quartz given a dose of 150 Gy. It can be seen that the one order of magnitude increase in dose, did not lead to a significant change in the half life values as function of time in daylight bleached quartz. Unlike in the heated quartz, the values of half life are evidently independent of dose at about 24 μs. Fig. 6.5 summarises the dose-dependent characteristics of the initial and average final values of half life from samples of heated and bleached quartz studied.

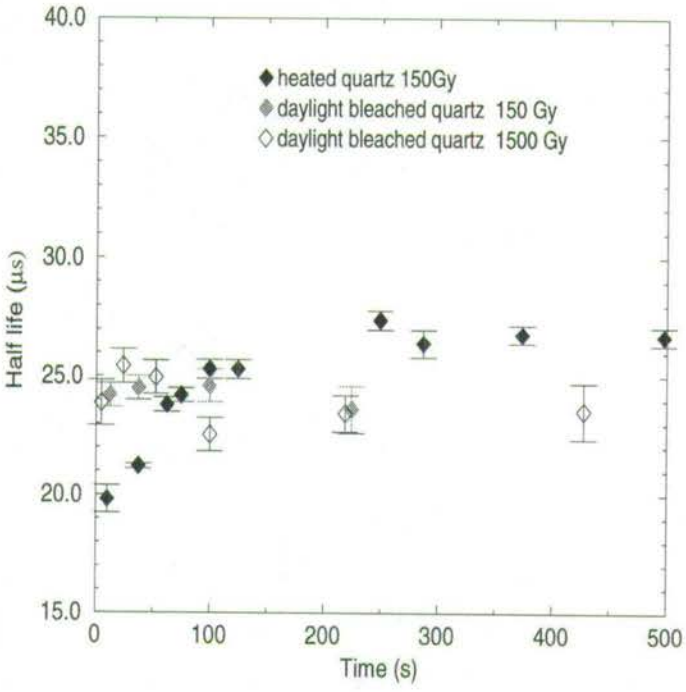

Figure 6.4 A comparison of half life values in daylight bleached quartz and heated quartz over the beta dose range 150 – 1500 Gy.

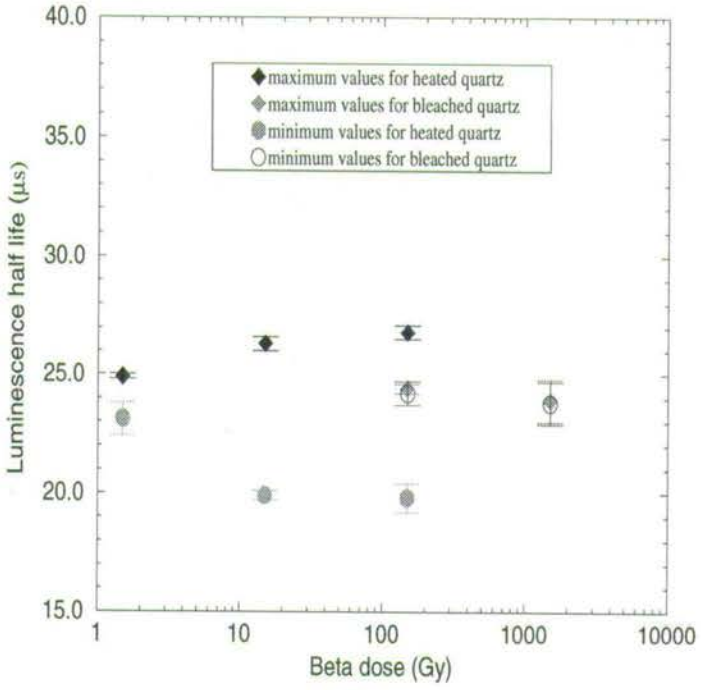

Figure 6.5 A comparison of initial and maximum half life values in daylight bleached and heated quartz over the beta dose range 150 – 1500 Gy.

6.1.3 Influence of preheating procedure on half life

The aim of this experiment was to investigate the effect of preheating on luminescence half life in quartz. Samples were heated at $220°C$ for 5 minutes, 20 minutes, and 1 hour and also at $280°C$ for 10s after beta irradiation for 150 Gy, but before measurement of luminescence time resolved spectra. The duration of preheating used in this experiment were chosen purely for convenience and heating for more than 1 hour was not attempted.

Fig. 6.6 shows graphs of half life against time for samples of heated quartz preheated for 5 minutes, 20 minutes and 1 hour at $220°C$ and at $280°C$ for

10 s. It is evident that all samples preheated for less than 1 hour show half lives increasing with time. Samples preheated for 5 and 20 minutes have an initial half life value of about 20 μs and the half life values increase with stimulation time to reach 26.7 $\pm$ 0.4 μs and 24.6 $\pm$ 0.7 μs respectively. In the sample preheated for 1 hour, the half life value is constant at about 24 μs. The similarity in the general shape of graphs for samples preheated for 5 and 20 minutes suggest that the two methods may be equivalent. In the sample preheated at $280°C$ for 10 s, half life values increase from about 22 μs to about 26 μs, a value not very different from those for samples preheated for 5 or 20 minutes. A consequence of preheating for one hour is the removal of features present in samples treated with alternative preheat protocols, namely, half life values shorter than 24 μs including the initial increase of half life with time, and final values of half life of the order of 26 μs.

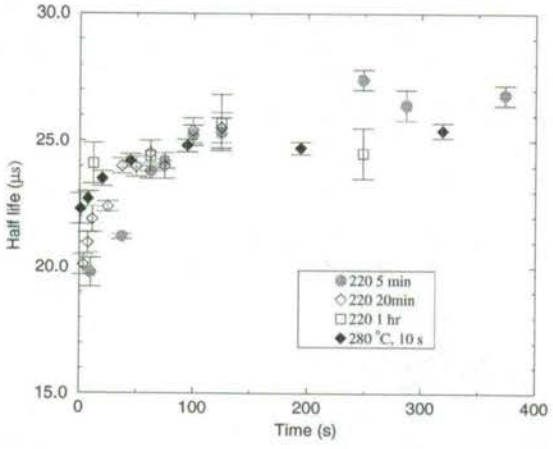

Figure 6.6 Influence of preheating method on half life in heated quartz.

6.1.4 Time–dependent measurements of half life at higher temperatures

The time–dependent characteristics of half life for quartz under pulsed green light stimulation were also investigated at 80 and 150°C in addition to measurements made at 20°C. Before each measurement of a time–resolved spectrum, an allowance of 2 minutes was made for samples to come up to temperature.

Heated quartz

Fig. 6.7 compares the change of half life with time of optical bleaching at 20, 80 and 150°C in heated quartz. The trend in all three cases is that half life values increase with time of optical stimulation. The change in half life may conveniently be described in terms of the initial and final values. Values of half life, both initial and final are observed to be temperature–dependent. For instance, while the maximum half life values measured at 20°C and 80°C are of similar order i.e 26.1 $\pm$ 0.9 μs and 24.0 $\pm$ 0.3 μs, at 150°C the value has dropped to 17.2 $\pm$ 0.2 μs. The initial values also decrease with temperature i.e 19.9 $\pm$ 0.6 μs, 17.5 $\pm$ 0.2 μs, 11.8 $\pm$ 0.1 μs at 20, 80 and 150°C in that order.

Daylight bleached quartz

The time dependence of half life at 20, 80 and 150°C for daylight bleached quartz is shown in Fig. 6.8. In this case, half life values remain constant with time at the three temperatures. At 20 and 80°C, values of half life are similar and constant at about 24 μs.

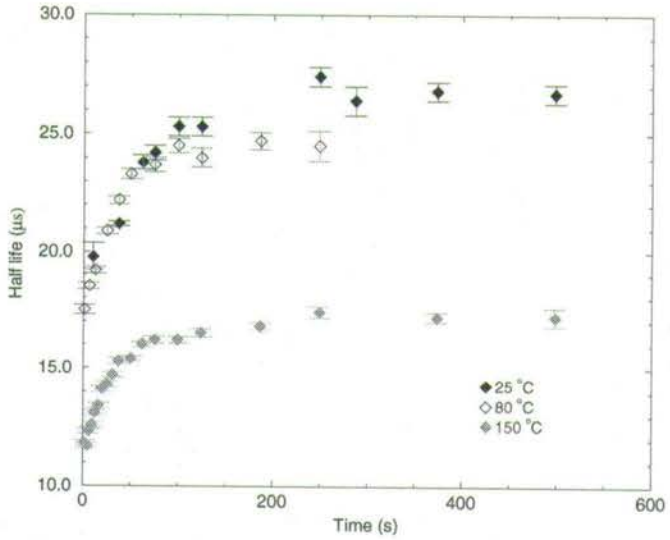

Figure 6.7 Change of half life with time at 20, 80 and 150°C for a sample of heated quartz.

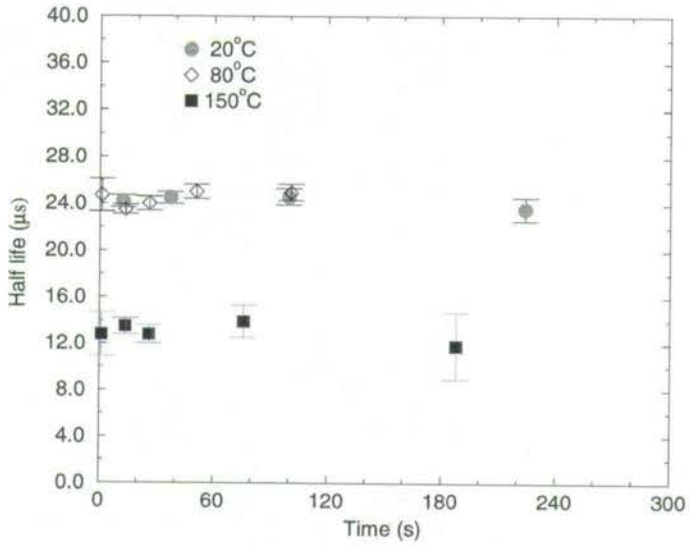

Figure 6.8 Change of half life with time at 20, 80 and 150°C for a sample of daylight bleached quartz.

At the higher temperature of $150°C$ the half life value decreases to about 13 μs. In general, the shortest half life is associated with the highest temperature. A complete indication of the influence of each temperature of measurement on half life can be obtained by making a measurement at the temperature. However, when values of the initial and final half life values are plotted as shown in Fig. 6.9, the evidence is that values of half life in heated quartz decrease monotonically with temperature unlike in daylight bleached quartz where all values are constant with time at 20, 80 and $150°C$.

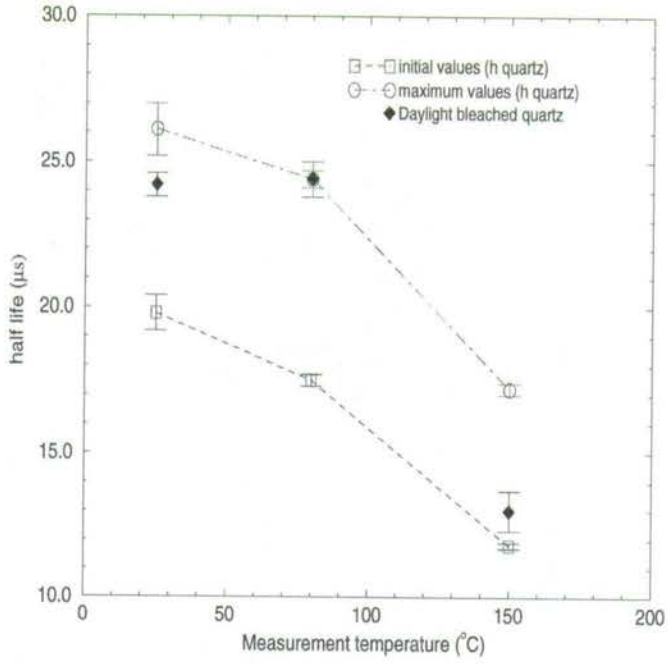

Figure 6.9 A comparison of initial and maximum half life values from heated and daylight bleached quartz at 20, 80 and $150°C$.

6.1.5 Temperature–dependent measurements of half life at long stimulation times

In order to identify and separate features due to optical stimulation from those due solely to temperature, time resolved spectra were recorded at temperatures from 20 to 200°C using a short, 1 s exposure at each temperature. For heated quartz, the temperature was increased from 20 to 100°C in 10°C intervals and then in 20°C intervals from 100 to 200°C. For daylight bleached quartz the temperature was increased from 20 to 200°C in 20°C steps. For each sample there was an allowance of 240 s between measurements for the sample to come up to temperature. Samples were given a dose of 150 Gy so that luminescence would last the entire temperature range and that time–resolved spectra recorded would have large enough counts to enhance the accuracy of the half lives calculated. Before any measurement, the sample was given a long bleach to remove the initial high intensity signals.

Heated quartz

Fig. 6.10 shows the variation of half life with temperature for a sample of heated quartz. It is apparent from this plot that half lives decrease with temperature. The decrease is monotonic and proceeds at an even faster rate above 125°C. This indicates a strong temperature influence beyond 125°C. This data is consistent with observations reported in Fig. 6.9 in which half life values decreased with temperature. The value of half life at 20°C was measured as 20.1 $\pm$ 0.3 μs and at 125°C as 16.7 $\pm$ 0.2 μs. This is a decrease of about 17% over 105°C. In comparison, the value of 5.1 $\pm$ 0.1 μs at 200°C represents a decrease of nearly 70% over a temperature range of 75°C i.e 125 to 200°C.

To investigate whether values of half life associated with particular temperatures could be reproduced, the measurement temperature on the same sample was varied. To do this, one sample was used with the temperature only being varied. A sequence of measurements were made as shown in Fig. 6.11. Here recording of time resolved spectra from 20 to $200^{o}C$ was followed by two measurements at $20^{o}C$ and two measurements at $200^{o}C$. It can be seen that in each case the half life value of the right order was reproduced. From a value of 5.1 $\pm$ 0.1 μs at $200^{o}C$, the half life value with the temperature reduced to $20^{o}C$ is 23.3 $\pm$ 0.1 μs which can be compared with the value, 20.1 $\pm$ 0.3 μs, the first value in the sequence. When the temperature is again increased to $200^{o}C$, the half life value measured was 5.5 $\pm$ 0.2 μs in good agreement with 5.1 $\pm$ 0.1 μs, the last value in the 20 – $200^{o}C$ cycle. The slight increase in half life between the first and repeat half life values can be ascribed to the small inherent change of half life with time in the slow component region as discussed in section 6.1.1. The experimental results demonstrated that half life values at specific temperatures could be reproduced and hence are uniquely related to temperature.

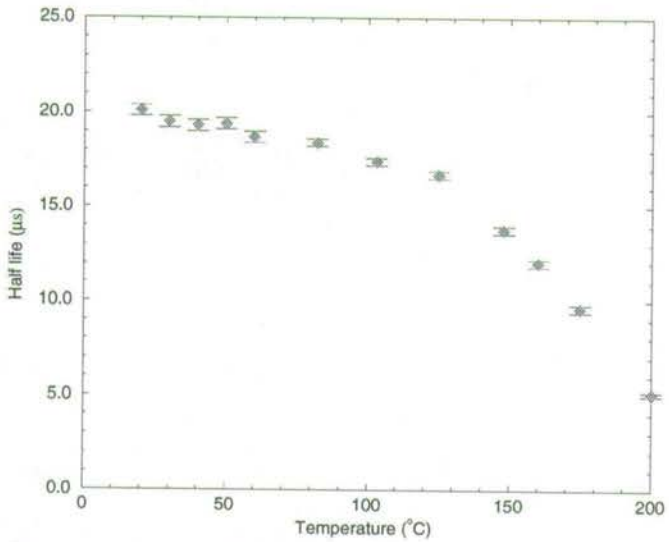

Figure 6.10 Change of half life with temperature in heated quartz. Measurements were made from 20 to 100^oC in 10^oC intervals and from 100 to 200^oC in 10^oC intervals.

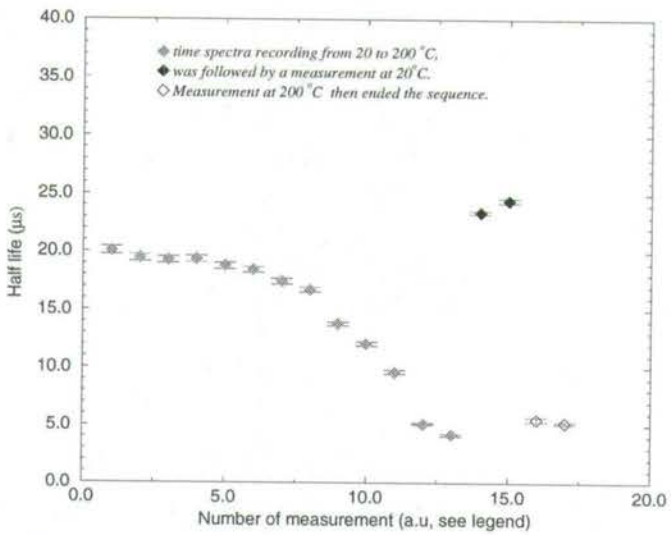

Figure 6.11 Sequence of measurements to illustrate that half lives are uniquely related to temperature.

Daylight bleached quartz

A dynamic temperature investigation of half life in daylight bleached quartz produced the variation of half life values with stimulation time as shown in Fig. 6.12. The values appear to stay constant at about 24 μs from 20^{o}C up to about 80^{o}C and decrease from then on. In this sample, the shortest half life value is about 15 μs at about 175^{o}C and the longest value is about 24 μs. These values are in good agreement with the data shown in Fig. 6.8 for measurements at fixed temperature where values were about 13 μs and 24 μs at 80 and 150^{o}C respectively. No value is plotted for 200^{o}C owing to low intensity of luminescence, but qualitatively, the shape of time–resolved spectra did not indicate any marked change in half life. There are noticeable differences in profiles of half life as a function of temperature for daylight bleached and heated quartz. For instance, although in both materials, half lives decrease with temperature, this does not occur monotonically in daylight bleached quartz. The rate of decrease of half life in the region of rapid decrease also differs. For example, in the daylight bleached sample the rate of decay is about 0.5% per ^{o}C (i.e 125 to 175^{o}C) compared to 0.9% per ^{o}C (i.e 125 to 175^{o}C) in heated quartz.

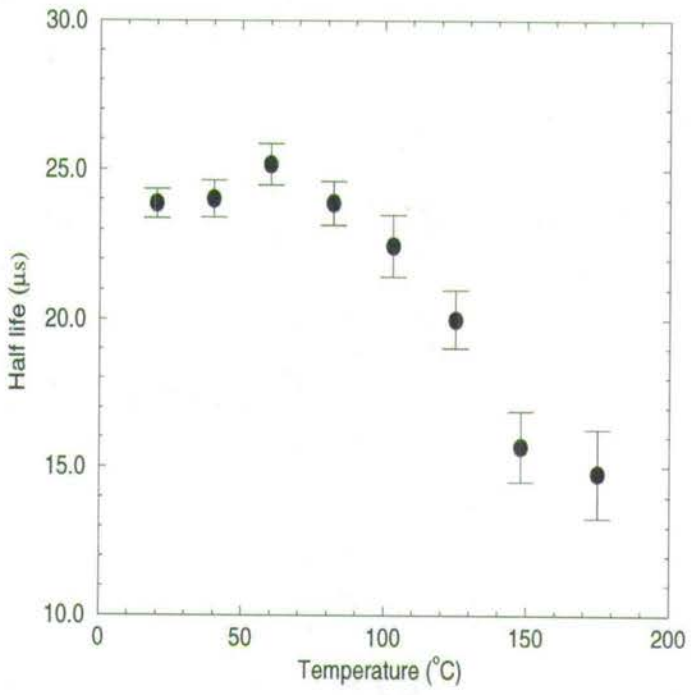

Figure 6.12 Dependence of half life on temperature in daylight bleached quartz. Measurements were made from 20 to 200^oC.

6.1.6 The effect of temperature on luminescence intensity at long stimulation times

In this set of experiments,the temperature–dependent properties of luminescence intensity were investigated at long stimulation times in heated quartz. Samples were given beta doses of 1.5, 15 and 150 Gy prior to heating at $220^{o}C$ for 5 minutes. The fast decaying parts of the decay curve were then removed by optically bleaching the samples. Sample 1 (150 Gy) was bleached down to 0.8% of the initial intensity while sample 2 (15 Gy) and sample 3 (1.5 Gy) were each bleached down to 4 and 8% of the maximum intensity respectively. One other sample given a beta dose of 150 Gy and preheated at $220^{o}C$ for 5 minutes was left unbleached.

Fig. 6.13 illustrates for sample 1 (150 Gy, 0.8%), the level of bleaching in comparison with the background signal. Experimental measurements on the effect of temperature on luminescence intensity were commenced after the sample had been bleached for 1000 s. Two sequences of measurements, each going from 20 to $200^{o}C$, were made. At each temperature, a time resolved spectrum was recorded at a counting time of 50 s. An allowance of 240 s was made between measurements for the sample to come up to temperature. The value of luminescence intensity at each temperature was obtained by integrating the time resolved spectrum.

The luminescence intensity measured as a function of temperature is shown in Fig. 6.14. This shows the intensity increasing with temperature to a maximum and then falling off as the temperature is further increased. The increase is slow at first, specifically between 20 and $40^{o}C$, and is more rapid thereafter. In this measurement, the intensity peak occurs at $148^{o}C$, with the intensity increasing by as much as 70% between 20 and $148^{o}C$.

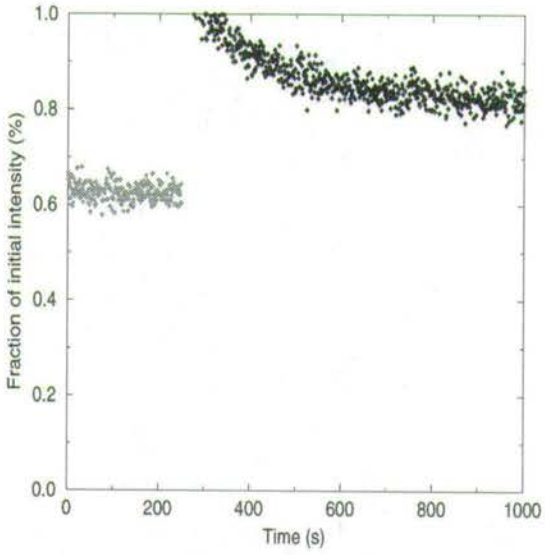

Figure 6.13 The decay curve at the beginning of the heating cycles in comparison to the background signal for sample 1.

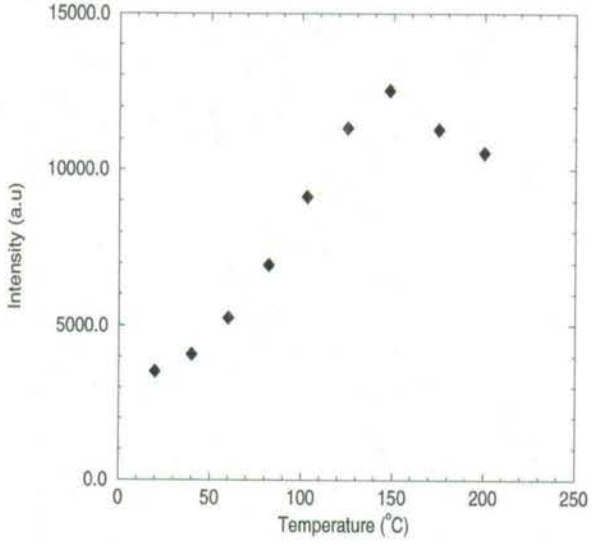

Figure 6.14 The change of luminescence intensity with temperature.

This is a significant increase and shows a notable influence of temperature in a region of low luminescence intensity. After this run, the sample was cooled down to $20°C$ after which the experiment was repeated. Fig. 6.15 compares the intensity–temperature graphs for the first and repeat experiments. The luminescence values have been normalised to the overall maximum value. It can be seen that the broad features of the two graphs are similar. For instance, the slow initial increase of intensity with temperature between 20 and $40°C$ and the occurrence of the peak intensity at about $148°C$.

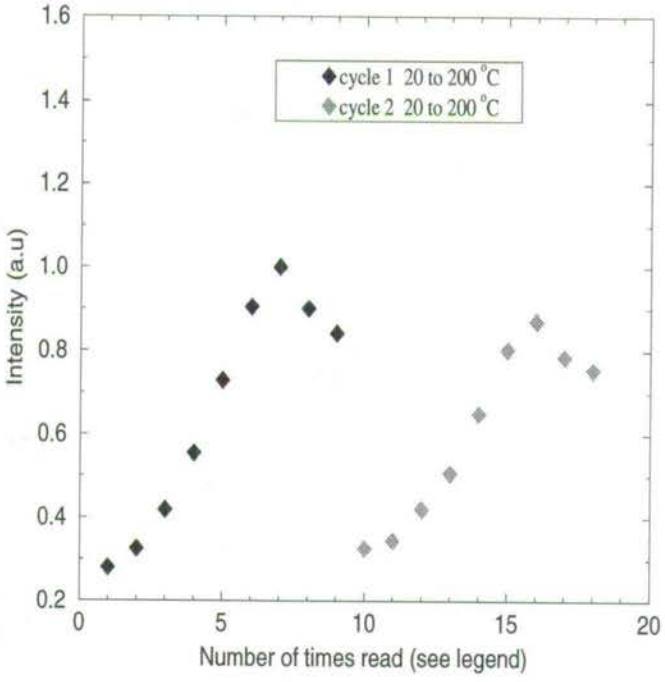

Figure 6.15 A comparison of intensity changes in cycles 1 and 2.

An assessment was made on how the rate of decay of luminescence was affected by introduction of the two 20 – 200°C heating cycles. Comparison of the data points at 200°C in cycle 1 (10528) with that at the same temperature in cycle 2 (9433) separated in time by 900 s shows a luminescence depletion rate of 0.01% s^{-1}, despite the intensity changes in between. The depletion rate expected in the presence of light only without heating was estimated from the decay curve measured on the same sample prior to the heating experiments. The rate was calculated from the values of luminescence intensity after 800 s (1928) and after 1000 s (1881) to be about 0.01% s^{-1}. Evidently, the intervening temperatures changes did not alter the rate of change of luminescence in the slow component region.

The change of luminescence intensity due to light exposure only and that due to simultaneous optical exposure and heating are compared for sample 1 (0.8%) in Fig. 6.16, for sample 2 (4%) in Fig. 6.17 and for sample 3 (8%) in Fig. 6.18. The significance of these bleaching levels are that the effect of temperature alone can then be assessed for sample 1 which is well into the slow component and for samples 2 and 3 which are bleaching down to the slow component. For purposes of definition in this study, the slow component is regarded as luminescence levels below 1 % of the initial maximum intensity of the luminescence.

Since for sample 1, there is hardly any change brought about by optical bleaching, the change in luminescence intensity is due to increase in temperature. It is also evident that the luminescence intensity at all temperatures above 20°C is always greater than that at 20°C.

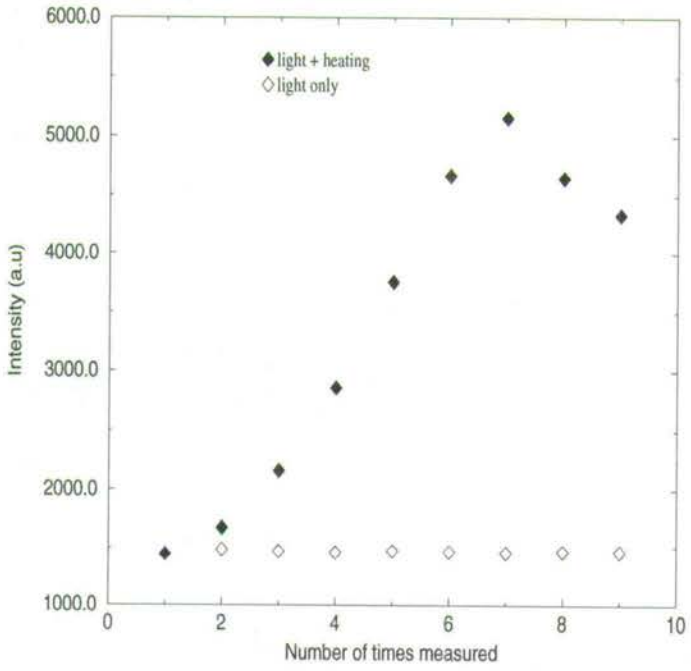

Figure 6.16 Change of intensity with temperature for sample bleached to less than 1% of the maximum intensity.

Samples 2 and 3 had, in comparison with sample 1, an appreciable amount of luminescence at the beginning of concurrent heating and optical stimulation of luminescence. Unlike sample 1, however, the decay of luminescence caused by optical stimulation alone is not negligible as can be appreciated from Fig. 6.17 and Fig. 6.18. Therefore, the measured change of luminescence intensity due to simultaneous heating and optical stimulation underestimates the increase in luminescence intensity due to increase in temperature. The measured luminescence is thus corrected for luminescence lost due to optical stimulation alone.

It can be observed in all three graphs (Fig. 6.16, Fig. 6.17, and Fig.6.18) that the increase in luminescence intensity at temperatures above room temperature is quite significant. Thus the amount of luminescence that can be ascribed to increase in temperature is greater than that lost due to light only. Broadly, the three graphs all show the luminescence to go through a peak as a function of temperature in the temperature range 20 – 200^{o}C.

The increase of luminescence intensity with temperature in quartz at elevated temperatures over that measurable at room temperature has been the subject of many investigations and is well recognized e.g [21, 24, 46, 70]. Of particular interest however is that the form of graphs of luminescence intensity as a function of temperature reported by Spooner [21] using green light (514 nm from a laser) are broadly similar to curves reported here. A possible interpretation of the shape of these graphs based on notions of thermal assistance and thermal quenching [21, 24] is discussed later in Chapter 7.

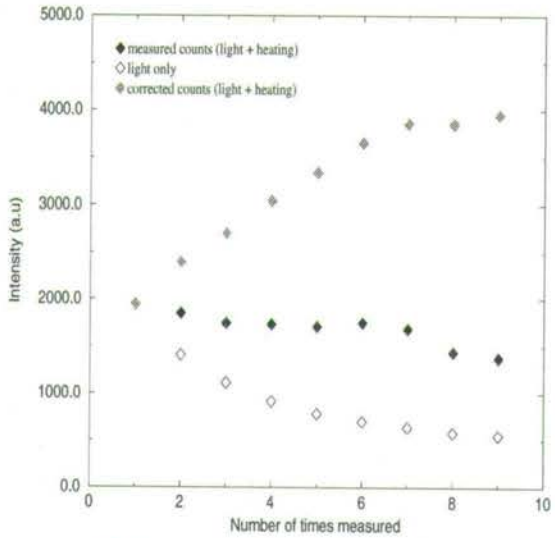

Figure 6.17 Change of luminescence intensity with temperature in sample 2 compared to that from a sample subjected to optical bleaching only. different levels.

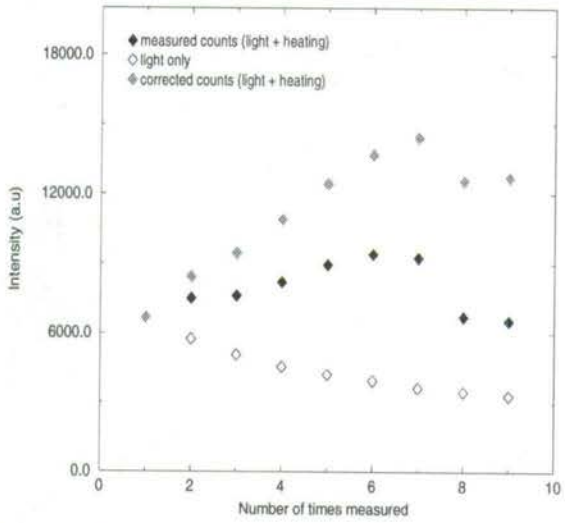

Figure 6.18 A comparison of changes in luminescence intensity due to temperature (for sample 3) and that due to light only.

6.2 Blue light stimulation

The use of blue LEDs for stimulation of luminescence for dosimetry and dating applications is fairly recent [5, 6] . Advantages reported following use of blue LEDs include an increased OSL efficiency per unit power at sample over that obtained using green light stimulation [7], and higher signal to background ratio values and hence more precise equivalent dose values [5]. For this work a blue LED pulsing system was developed from the green LED assembly used for experiments reported in section 6.1. This section reports results of measurements of half life and intensity of luminescence stimulated from quartz by pulsed blue light emitting diodes. The section is organised as follows. Section 6.2.1 reports time-dependent measurements of half life at room temperature. Section 6.2.2 is concerned with measurements of the effect of radiation dose on luminescence half life. Section 6.2.3 presents results of experiments on the influence of preheating procedure on half life values. Section 6.2.4 reports on time–dependent measurements of half life at higher temperatures. Dynamic temperature experiments of half life are reported in section 6.2.5. Section 6.2.6 reports results on temperature–dependent measurements of half life from samples with different initial beta dose. The effect of temperature on luminescence intensity at long stimulation times is reported in section 6.2.7.

6.2.1 Time dependent measurements of half life at room temperature

Time–dependent measurements of half life reported in this section were made at room temperature, typically $20 \pm 2^{o}C$. For all measurements, the pulsing system was operated at a pulse width of 11 μs, a duty cycle of 12.4 %

and a repetition rate of 11 kHz. Time–resolved spectra were recorded over a dynamic range of 64 μs. The increased efficiency of blue LEDs in stimulating luminescence [7], had in this experiment, the effect of producing high counting rates from samples of heated quartz. Therefore in order to avoid distortion to time–resolved spectra and hence spurious half lives, most studies on heated quartz were limited to beta doses between 0 – 4.5 Gy although higher doses, 15 and 150 Gy, were used for studies of luminescence half lives in the slow component region of the OSL. For the comparatively less sensitive daylight bleached quartz e.g [4, 16], the blue LEDs enabled measurements to be made over a wider dose range of 1.5 – 150 Gy.

Fig. 6.19 shows time–dependent change of half life in a sample of heated quartz given a beta dose of 4.5 Gy and preheated at $220^{o}C$ for 5 minutes. It can be observed that the general form of change of half life with time is similar to that in heated quartz under green light stimulation shown in Fig. 6.2. The half life values gradually evolve from an initial value to a final maximum constant value within the time limit studied. In this case, Fig. 6.19, the initial value is 21.0 $\pm$ 0.2 μs and the final value is within 26.3 $\pm$ 0.2 μs, values similar to those calculated for the green LED stimulation (Fig. 6.2) although in that case the sample had been given a larger beta dose of 150 Gy. Although it is difficult to compare directly results for samples under blue and green LED stimulation because of differences in dose used to induce luminescence, the heated quartz appears to retain its characteristic feature in the way the half life values change with stimulation time.

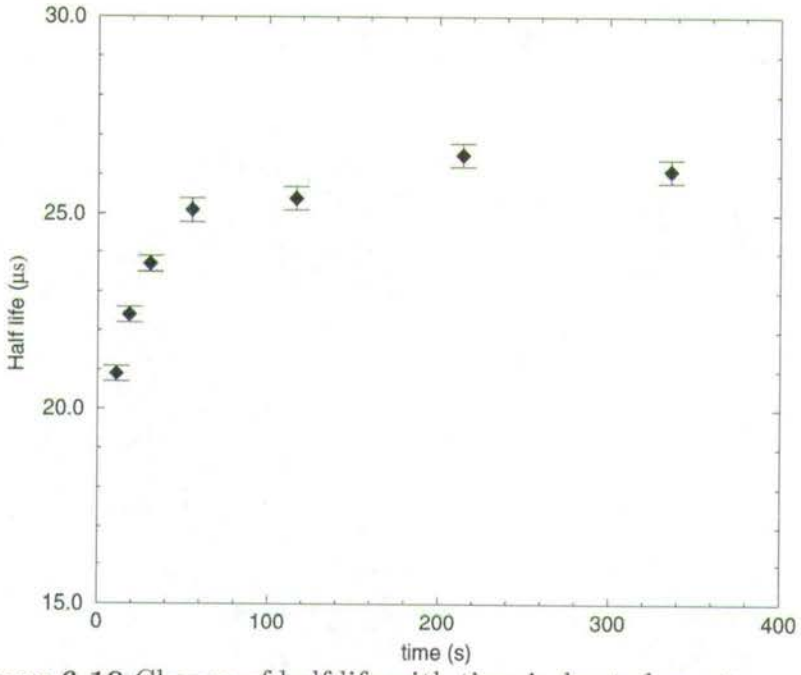

Figure 6.19 Change of half life with time in heated quartz sample dosed to 4.5 Gy and preheated at $220°C$ before measurement of luminescence.

The improved efficiency of the blue LEDs at stimulation of luminescence enabled measurements on daylight bleached quartz for half life analysis at lower doses than was possible with green LED stimulation. Fig. 6.20 shows the change of half life with time for a sample of daylight bleached quartz given a beta dose of 15 Gy and preheated at $220°C$ for 5 minutes before recording of time–resolved spectra at $20°C$. In this case half life values increase from 18.6 ± 0.3 μs to an average final value of about 25 μs.

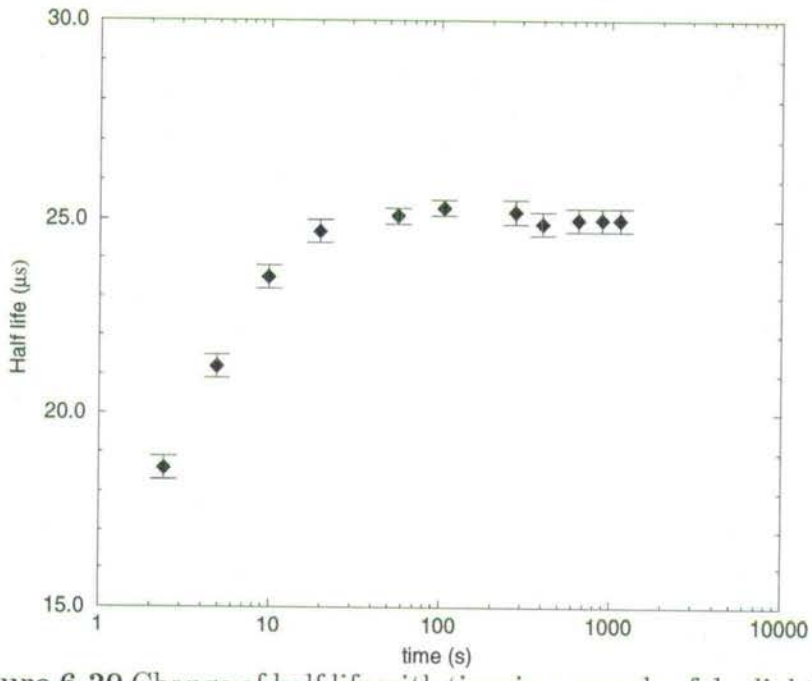

Figure 6.20 Change of half life with time in a sample of daylight bleached quartz dosed to 15 Gy and preheated at $220°C$ before measurement of luminescence.

The rise of half life values from the initial to the maximum value appears to take place in the first 20 s or so or optical exposure while the region of constant half life is comparatively long, 20 – 1000 s. The evolution of half life values may be associated with the changes in the corresponding decay curve, the fast growth of half life values in the first 20 s relate to the fast and medium component regions while the region of constant half life values should be associated with the slow component region, where the optical depletion rate is very slow.

The time–dependent changes of half life for daylight bleached quartz in Fig. 6.20 are in contrast to results obtained with the use of pulsed green LEDs (Fig. 6.4). The main difference is the absence of the 'fast growth' region in the half life vs time graph for green LED stimulation even at a beta dose as high as 1500 Gy. It therefore seems unlikely that the absent initial changes in half life in the green LED case (Fig. 6.4) are subsumed within the first few data points, instead the changes are likely to relate to the ability of the more energetic blue light at inducing variations in half life in comparison with green light.

6.2.2 The effect of radiation dose on luminescence half life

This section reports results of experiments conducted to investigate the effect of radiation dose on luminescence half life. It is an extension of the time–dependent experiments of section 6.2.1 over a wider dose range. Separate samples of daylight bleached quartz were given doses of 1.5, 15 and 150 Gy while samples of heated quartz were given doses of 0.45 and 4.5 Gy before preheating at $220^{o}C$ for 5 minutes.

Fig. 6.21 shows the time–dependent changes of half life for the samples of heated quartz. Both samples show a progressive increase of half life with time to a maximum final value. The initial value for the sample dosed up to 0.45 Gy was measured as 22 ± 1 μs and as 21.0 ± 0.2 μs for the sample dosed up to 4.5 Gy. This is not deemed to be a significant difference given that these half life values are associated with dose values one of which is only a tenth of the other. The difference between these half life values is similar in comparison to that between samples of heated quartz under green LED stimulation shown in Fig. 6.3 where the doses used were larger i.e 1.5 and 15

Gy. As for final half life values, a separation in values is evident in Fig. 6.21 i.e 24 $\pm$ 1 μs for the 0.45 Gy sample and 26.3 $\pm$ 0.2 μs for the 4.5 Gy sample. However, given the size of the uncertainties, the difference is not significant enough to conclude that the final values are influenced by the size of beta dose in the range used (0.45 – 4.5 Gy).

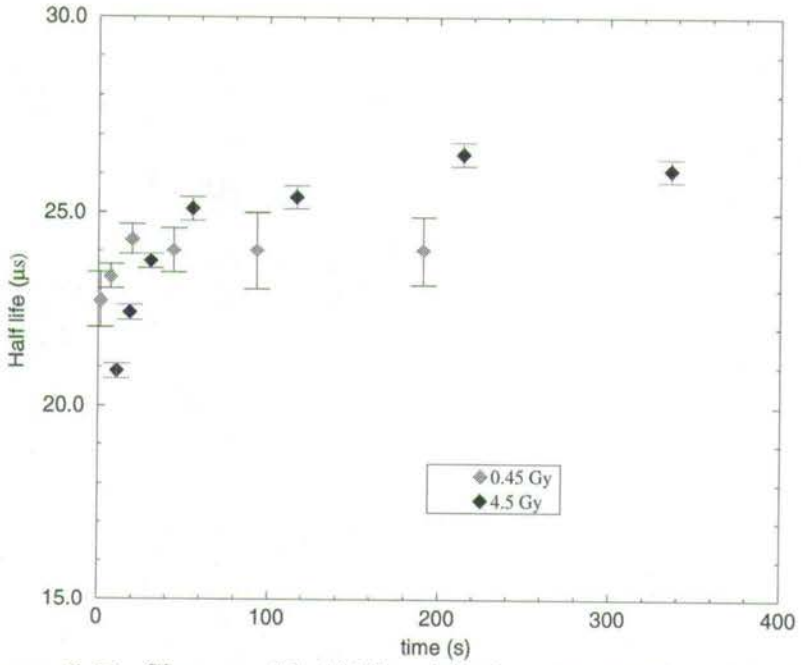

Figure 6.21 Change of half life with time in samples of heated quartz dosed to 0.45 and 4.5 Gy and preheated at 220°C before measurement of luminescence.

Fig. 6.22 compares time–dependent changes in half life in samples of daylight bleached quartz dosed to 1.5, 15 and 150 Gy, and preheated at $220°C$ for 5 minutes prior to recording of time-resolved spectra. It is apparent that the value of dose modifies the way the half lives vary with time. The samples given 1.5 Gy beta dose displays half lives that are constant with time of optical exposure. The average half life value for this sample is 22.2 ± 0.1 μs.

The sample dosed to 150 Gy, on the other hand, represents the opposite extreme; that of high intensity signal at the beginning of the measurement. The values plotted are those calculated from time–resolved spectra determined to be free of distortion due to high counting rates (as discussed in section 4). From an initial half life value of 15.0 ± 0.2 μs, the half lives increase to a constant maximum value within 27.2 ± 0.1 μs. Thus a dose dependence behaviour of initial and final half life values emerges. The largest dose used (150 Gy) is associated with the least initial half life value, 15.0 ± 0.2 μs and the largest final half life value, 27.2 ± 0.1 μs while a lesser dose results in a correspondingly larger initial value and a lower final value e.g 18.6 ± 0.3 μs and 25.0 ± 0.1 μs for the sample irradiated to 15 Gy. This is in contrast to the data for daylight bleached quartz under pulsed green LED stimulation as shown in Fig. 6.4 where half lives were independent of the dose given to samples prior to measurement of time–resolved spectra.

Since the initial half life values may be associated with intense luminescence signals at the beginning of measurement, this raises the concern of whether the clear distinction in half lives as shown in Fig. 6.22 is correlated with particular counting rates. In order to address this question, the half life values of the samples are plotted in Fig. 6.23 against the corresponding counting rates. Comparison of sample to sample half lives show that the same counting rates correspond to different half life values.

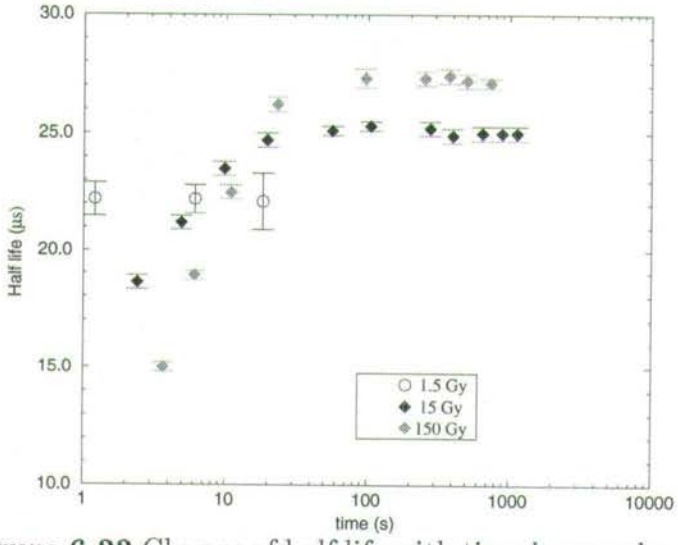

Figure 6.22 Change of half life with time in samples of daylight bleached quartz dosed to 1.5, 15 Gy and 150 Gy and preheated at $220°C$ for 5 minutes before measurement of luminescence.

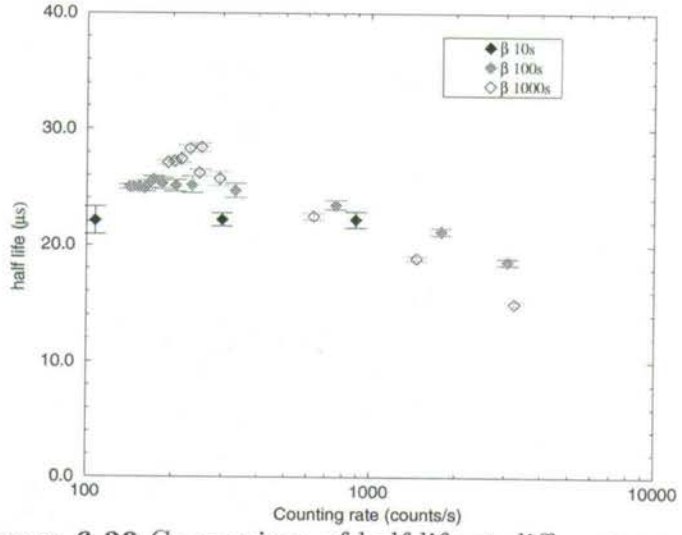

Figure 6.23 Comparison of half life at different counting rates.

The changes in counting rates for any chosen sample reflects the progressive removal of the components of the corresponding decay curve i.e the intense fast component through to the medium and slow components where the sample is well bleached.

It can be concluded that the luminescence half life values are influenced by the amount of beta dose in samples of daylight bleached quartz while in heated quartz, for the dose range used (0.45 – 4.5 Gy), the half life values are not significantly influenced by the size of the beta dose used.

6.2.3 Influence of preheating procedure on half life

For the results presented in sections 6.2.1 and 6.2.2, each sample was preheated at $220°C$ for 5 minutes before recording of time–resolved spectra. The results reported in this section are for a set of experiments conducted to take into account any possible influence the preheating procedure may have on the resulting half life.

For these experiments, samples of heated quartz were given a beta dose of 0.45 Gy and preheated at $220°C$ for 5 minutes, 20 minutes and 1 hour before measurement of luminescence. Samples of daylight bleached quartz were preheated at the same temperature for 1 minute and 5 minutes following beta doses of 1.5, 15 and 150 Gy. There are many possible preheating procedures as discussed previously in section 4.3.1. The procedures selected for use in this work are typical in OSL experiments e.g 5 minutes at $220°C$ is used extensively [48], 1 minute at $220°C$ has also been used [51]. The 20 minute and 1 hour preheating were done to provide comparative data for longer preheating. The longer preheats were chosen instead of possible alternatives which include preheating for 16 hours at $220°C$ [53] and 48 hours at $150°C$ [52].

Fig. 6.24 (a), (b), (c) compares the effect on luminescence half life values in daylight bleached quartz of preheating for 1 and 5 minutes. For this test, the samples were given beta doses of 1.5 Gy (Fig. 6.24 a), 15 Gy (Fig. 6.24 b) and 150 Gy (Fig. 6.24 c).

In Fig. 6.24 (a), the half life values following both 1 minute and 5 minutes preheating are in each case independent of the time of stimulation. Because of low luminescence intensity owing to the small dose used, both sets of data have large uncertainties. However, the half life values for the sample preheated for 1 minute appear to be consistently smaller than those for the sample preheated for 5 minutes. The half life values are within 19.6 $\pm$ 1 μs for the sample given a 1 minute preheat and 22 $\pm$ 1 μs for the sample heated for 5 minutes. There is thus a slight though not significant difference between the two half life values.

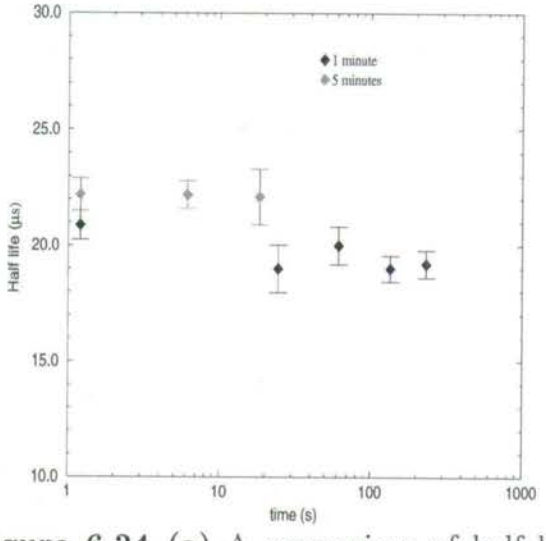

Figure 6.24 (a) A comparison of half lives from samples of daylight bleached quartz preheated for either 1 or 5 minutes after a beta dose of 1.5 Gy.

Half life values from samples given a higher beta dose of 15 Gy and preheated for 1 minute and 5 minutes are compared in Fig. 6.24 (b). In this case, the half life values change with time with most of the change occurring in the first 20s or so of optical stimulation. The half life values in the increasing part of Fig. 6.24 between 0 – 20 s appear to be similar. Thereafter, the half life values for the 1 minute sample at an average of 25.8 $\pm$ 0.1 μs appear to be consistently, although only slightly, larger than values from the sample preheated for 5 minutes whose values are within 25.1 $\pm$ 0.1 μs. Thus in this case, the longer preheating is associated with a shorter half life of luminescence.

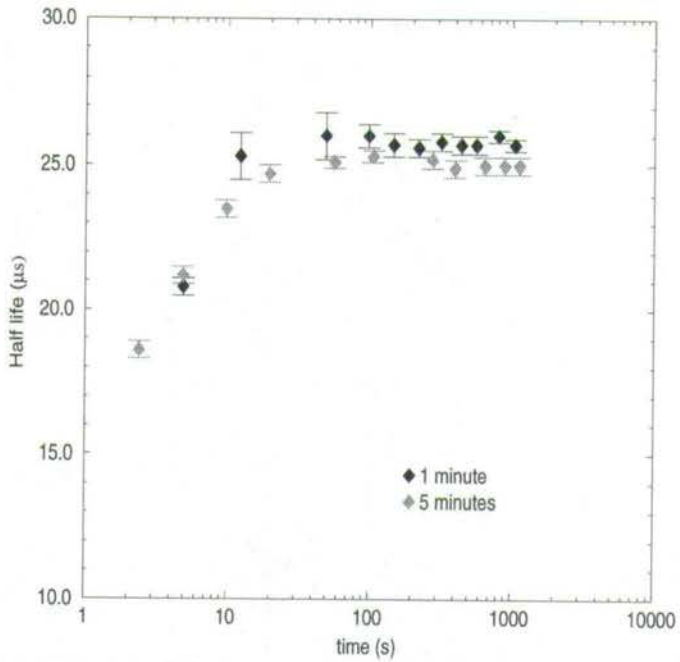

Figure 6.24 (b) A comparison of half lives from samples of daylight bleached quartz preheated for either 1 or 5 minutes after a beta dose of 15 Gy.

The third investigation on the influence of preheating on half life was for samples dosed to 150 Gy and this is shown in Fig. 6.24 (c). The form of the time–dependent changes is similar to that in Fig. 6.24 (b). The one significant change is that the final values have shifted to a higher maximum value of about 28 μs for both samples. Again, it is evident that half lives associated with longer preheating are consistently, although only slightly so, lower than those for the sample preheated for 1 minute.

In general, although there are slight differences in values of half life measured from samples of daylight bleached quartz following preheating for 1 minute or 5 minutes, such differences are not significant.

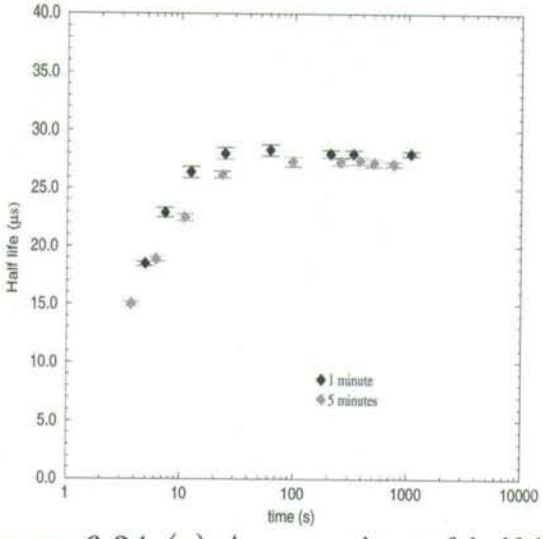

Figure 6.24 (c) A comparison of half lives from samples of daylight bleached quartz preheated for either 1 or 5 minutes after a beta dose of 150 Gy.

Fig. 6.25 compares the time–dependent characteristics of half life in samples of daylight bleached quartz preheated for 1 minute following beta irradiation to 1.5, 15, and 150 Gy. The lowest dose of 1.5 Gy does not appear to have induced any change in half life with time. However, as the dose is increased to 15 Gy and then 150 Gy, there is an observable change in half life with a direct correlation between the size of dose and the half life observed i.e the higher the initial dose, the longer the final half life value. Fig. 6.25 can be compared to Fig. 6.22 where similar dose values were used but samples were preheated for 5 minutes to reveal the fact that the degree of change in half life is influenced significantly only by the size of initial dose (initial charge concentration).

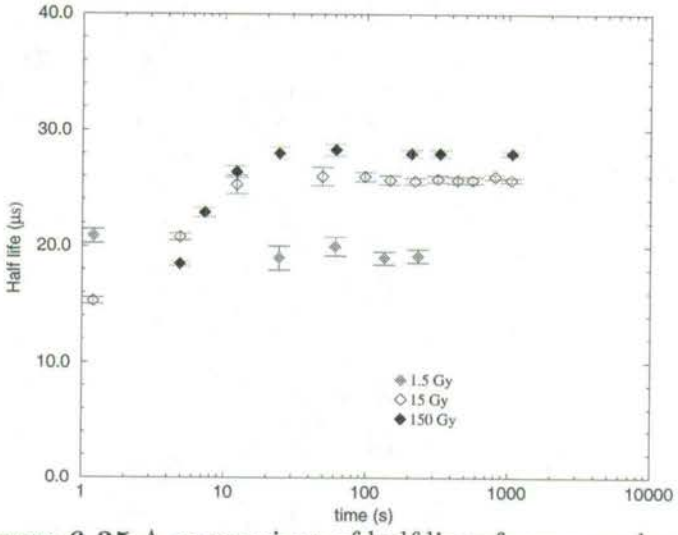

Figure 6.25 A comparison of half lives from samples of daylight bleached quartz preheated for 1 minute after beta irradiation to 1.5, 15 and 150 Gy.

In Fig. 6.26, the time–dependent changes in half life from samples of heated quartz are compared. The preheating times used were 5 minutes, 20 minutes and 1 hour at $220°C$. All samples were given a beta irradiation of 4.5 Gy before preheating and measurement of luminescence time–resolved spectra. The principal distinction in this data, Fig. 6.26, is that half life values for preheating for 5 minutes are consistently less than for values following preheating for 20 minutes and 1 hour. The consequence of preheating for longer than 5 minutes then appears to be a shift in the maximum values to longer half life values. The final values for 20 minutes and 1 hour preheating after about 1000 s and 700 s of optical stimulation are 23.6 $\pm$ 0.1 μs and 23.8 $\pm$ 0.1 μs, respectively, values that are evidently similar. The final value in the measurement rather than the final value is quoted in this case because on close examination, the data points for the 1 hour and 5 minute preheating do not yet seem to be stable within the accuracies shown. The sample preheated for 5 minutes has a lower final value of 22.5 $\pm$ 0.1 μs. Thus in samples of heated quartz, the maximum half life values appear to be influenced by the duration of preheating.

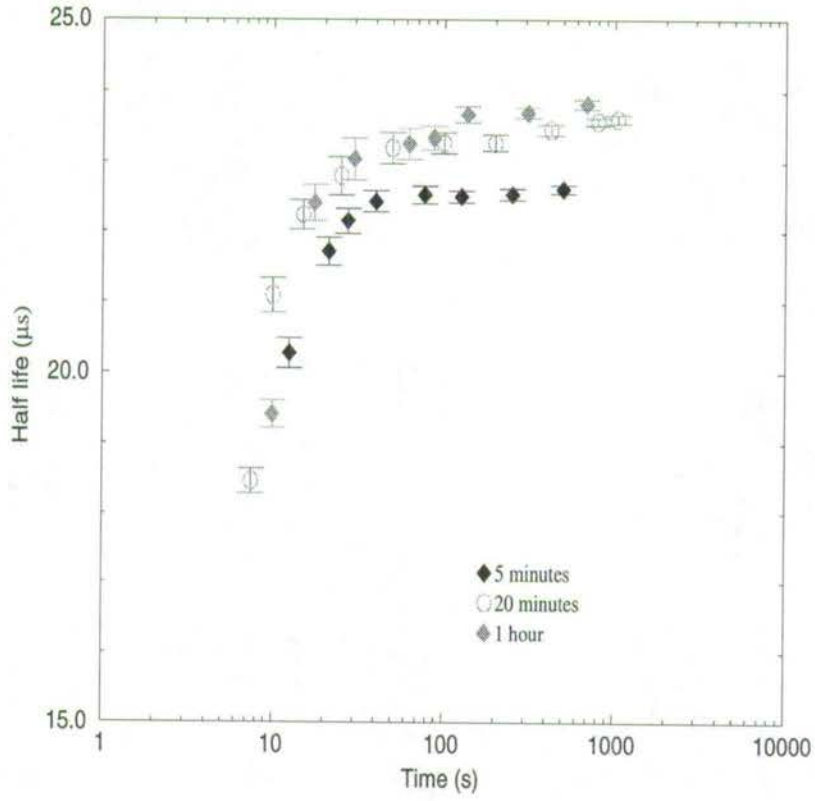

Figure 6.26 A comparison of half lives from samples of heated quartz preheated for 5 minutes, 20 minutes and 1 hour after a beta dose of 4.5 Gy.

6.2.4 Time–dependent measurements of half life at higher temperatures

Time–dependent properties of half life were investigated at 80 and 150°C in addition to experiments conducted at 20°C (Fig. 6.19, Fig. 6.20). An allowance of 2 minutes was made for the samples to come up to temperature. These experiments were made using both heated and bleached quartz. The aim for the choice of the temperatures was to study luminescence half life behaviour above and below 110°C, the temperature position of one of the TL defect centres that influence the emission of optically stimulated luminescence from quartz [16, 20, 22].

Samples of heated quartz were given a beta dose of 4.5 Gy before pre-heating at 220°C after which time–resolved measurements followed. Fig. 6.27 compares the variation in half life with time at 20, 80, and 150°C for samples of heated quartz. The feature of half life values increasing with time from an initial to a maximum value is evidently retained even at higher temperatures.

It can be observed in Fig. 6.27 that the effect of increase in temperature is to reduce the luminescence half life values. This applies to both the initial and final half life values. At 150°C, the half lives are lower than at either 20 or 80°C. At 150, 80 and 20°C, the initial values were calculated as 11.4 $\pm$ 0.1 μs, 17.3 $\pm$ 0.2 μs and 17.0 $\pm$ 0.2 μs in that order. The half lives reach a stable value of about 19 μs at 150°C in comparison with a value of about 25 μs at both 20 and 80°C. There thus appears to be a fundamental difference in half life values above 80°C and at and below 80°C.

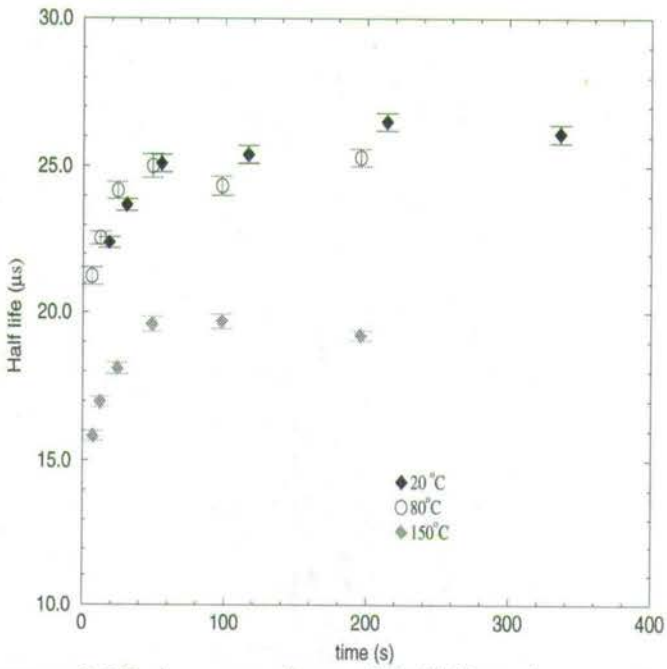

Figure 6.27 A comparison of half lives from samples of heated quartz measured at 20, 80 and 150°C after each sample had been beta dosed up to 4.5 Gy. All samples were preheated at 220°C for 5 minutes prior to measurement of time–resolved spectra.

Fig. 6.28 shows histogram plots of corresponding measurements made on daylight bleached quartz. The samples were given a beta dose of 15 Gy and preheated at 220°C before recording of time–resolved spectra for half life analysis. Because of low intensity there are no data points for half life at low stimulation times for samples measured at 80 and 150°C. The values of half life after 10 s are all independent of stimulation time i.e at 80°C, the values are within 24.6 $\pm$ 0.5 μs and at 150°C the values are at 19.9 $\pm$ 0.2 μs.

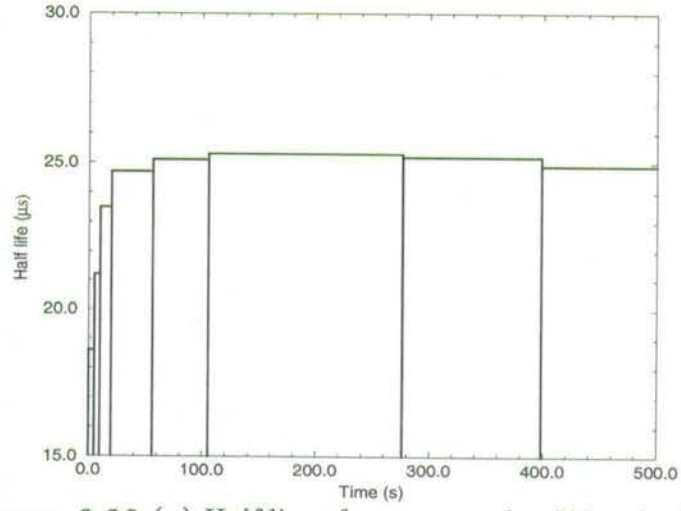

Figure 6.28 (a) Half lives from a sample of bleached quartz measured at $20^{o}C$ after a dose of 15 Gy and preheating at $220^{o}C$ for 5 minutes. Additional measurements at stimulation times of 650, 900 and 1100 s all gave a constant half life of about 25 μs.

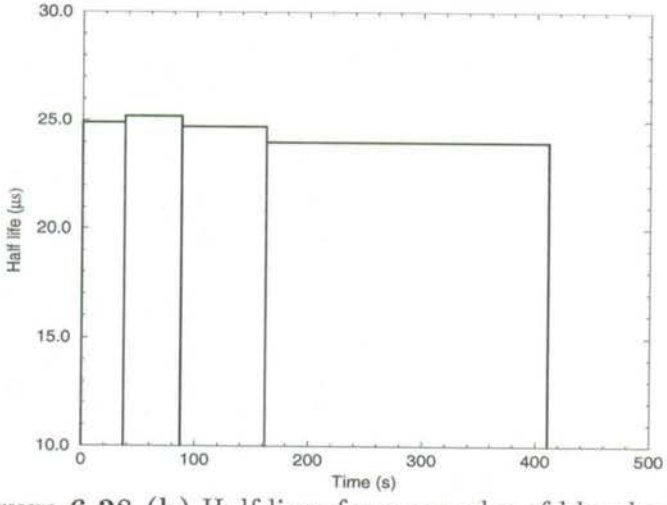

Figure 6.28 (b) Half lives from samples of bleached quartz measured at $80^{o}C$ after a beta dose of 15 Gy and 5 minute preheating at $220^{o}C$.

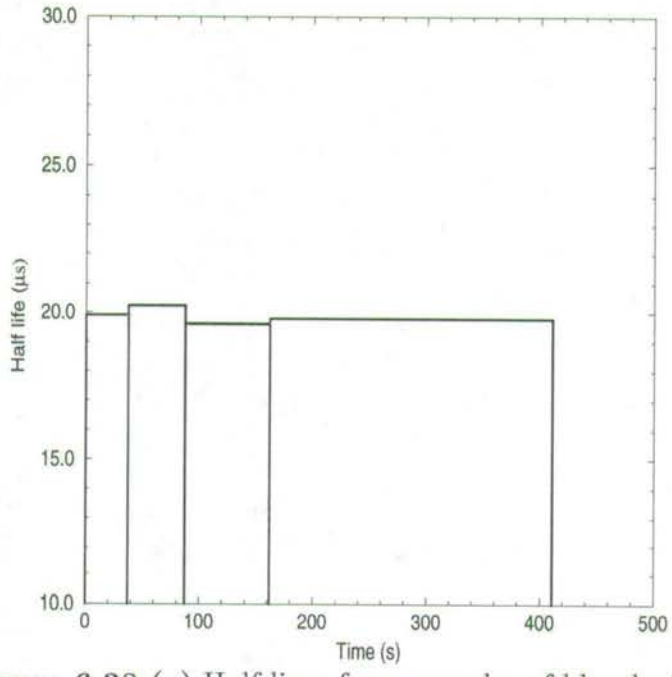

Figure 6.28 (c) Half lives from samples of bleached quartz measured at $150^{o}C$ after each sample had been beta dosed up to 15 Gy.

In general, the changes in this case are similar to those for heated quartz in Fig. 6.27 in that increase in temperature causes a reduction in half life values. It is notable that the case of lower half life values at $150^{o}C$ in comparison with those at 20 and $80^{o}C$ is replicated in daylight bleached quartz. A different experiment was devised to investigate further the association between half life and temperature and this is reported next.

6.2.5 Temperature–dependent measurements of half life at long stimulation times

In this experiment, the effect of temperature on luminescence half lives was studied at temperatures from 20 to 200°C. The method used was to record time–resolved spectra at each temperature from 20 to 200°C in 20°C intervals using the same sample. Each time–resolved spectrum was recorded for a counting time of 12 s. Measurements were made from 20 to 200°C in 20°C steps in cycle 1 and repeated in cycle 2 from 200 to 20°C immediately after cycle 1. Cycle 2 was done as a test of repeatability of results. All measurements on heated quartz were made in the slow component region as otherwise the sample luminescence would produce high counting rates at the beta doses selected for use to sustain repeated measurements.

Fig. 6.29 shows the relationship between half lives and temperature for a sample of heated quartz preheated at 220°C following a beta dose of 4.5 Gy. As can be seen in Fig. 6.29, the half lives hardly changed between 20 and 100°C. In this region, the half life is constant at about 25 μs. This value is consistent with luminescence half life values after long stimulation as shown previously in Fig. 6.19. Then, as the temperature is increased from 100 to 200°C, half life values decrease, reaching a minimum value of 6.5 $\pm$ 0.3 μs at 200°C. In the repeat run from 200 to 20°C, the initial half life as measured at 200°C is 7.2 $\pm$ 0.3 μs which increases as the temperature is decreased to 100°C. Here a half life of 24.4 $\pm$ 0.4 μs was calculated. Below 100°C, the average value of half life is about 26 μs.

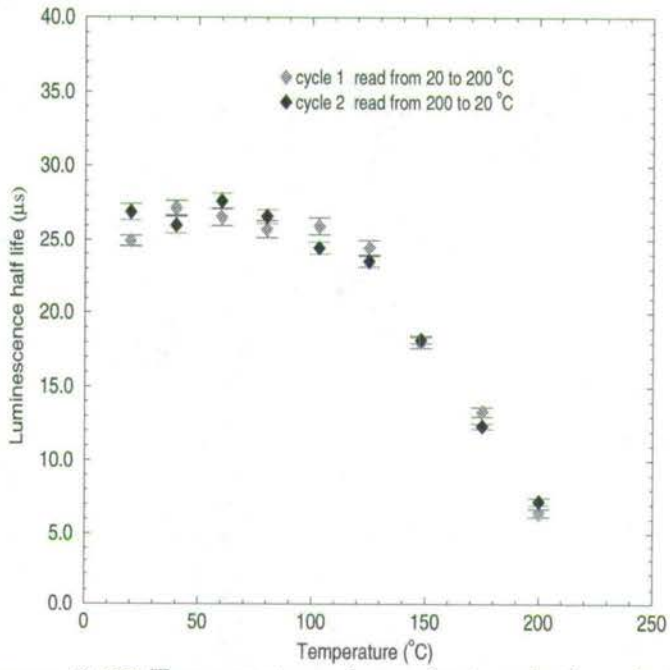

Figure 6.29 Temperature–dependent variations in half life in sample of heated quartz heated at $220°C$ after a beta dose of 4.5 Gy. The measurements were made from 20 to $200°C$ in cycle 1 and repeated in cycle 2 from 200 to $20°C$.

These changes in half life are in agreement with the conclusions drawn from Fig. 6.27 where separate samples were used to determine half lives at 20, 80 and $150°C$. The half life values from 100 to $20°C$ in Fig. 6.29 at about 26 μs again agree with values of half life at long stimulation times for measurements at $20°C$ (Fig. 6.19). The dynamic temperature half life variations of Fig. 6.29 also compare well with values of half life at 80 and $150°C$ as shown in Fig. 6.27. Values at 80 and $150°C$ in Fig. 6.27 reached

after long stimulation were 25.8 ± 0.6 μs and 18.0 ± 0.4 μs respectively which agree with the values, 24.9 ± 0.4 μs at 80°C, and 19.5 ± 0.2 μs at 150°C as found in the data shown in Fig. 6.29.

Temperature–related changes in luminescence half life can be compared with time–dependent changes at constant temperature in order to draw a distinction between the influence of stimulation only and simultaneous optical stimulation and heating. This is shown in Fig. 6.30.

It can be seen that at constant temperature there is a gradual increase of half life from about 22 μs to a maximum of about 26 μs. In contrast, the dynamic temperature measurements plotted on the same relative time scale reveals a sharp decline in half lives originating from the introduction of heating in addition to optical stimulation of luminescence.

In summary, it has been observed that there is good agreement between dynamic temperature measurements with measurements at constant temperatures, 20, 80 and 150°C in heated quartz. Luminescence half life values are constant in the range 20 – 100°C but decrease at a rapid rate from about 125°C. These results repeat when measurements are made from 200 to 20°C. In this case , half life values increase as the temperature is decreased from 200 to 125°C. Below this temperature, half lives are constant, within experimental scatter at about 26 μs. While at 200°C, the value of half life is about 6 μs, the half life value of about 26 μs obtained between 20 and 100°C corresponds to the constant maximum value measured at room temperature.

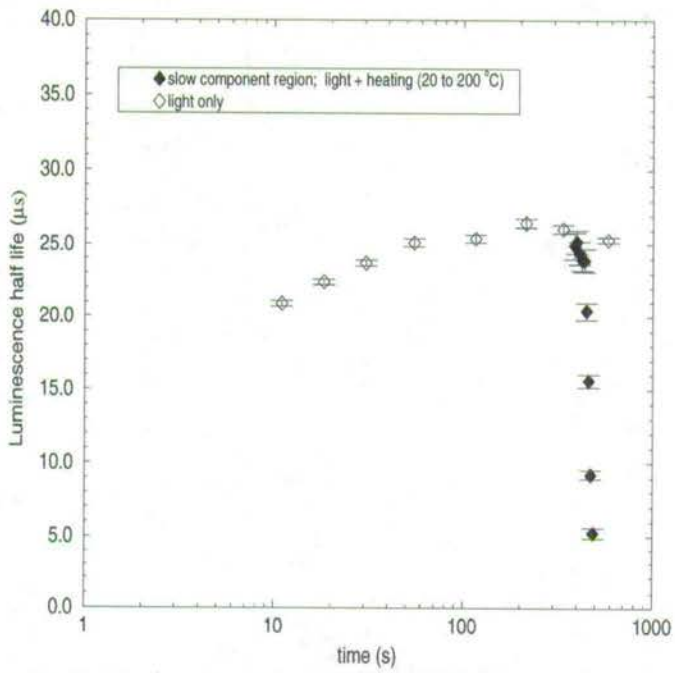

Figure 6.30 A comparison of half life values from a sample under pulsed blue light stimulation to that under optical stimulation while being heated.

6.2.6 Temperature–dependent measurements of half life for samples with different initial doses

This experiment was conducted to investigate whether the size of the initial dose influenced the half lives in the slow component region of quartz. In effect, this checked whether the initial charge concentration affected the value of half lives at long stimulation times. For this experiment three separate samples of heated quartz were given beta doses of 4.5, 15 and 150 Gy, and

then preheated at $220^{o}C$ for 5 minutes before time–resolved spectra were recorded for half life analysis. The samples were then bleached down to the slow component region, measured in the experiment to a known small fraction (1 – 1.5 %) of the initial intensity.

The variation in half life with temperature are compared in Fig. 6.31 (a) for measurements from 20 to $200^{o}C$ and in Fig. 6.31 (b) for measurements from 200 to $20^{o}C$. It can be seen that for all three samples, the half life values are effectively constant between 20 and $100^{o}C$ despite the variation in radiation dose. However, once the measurement temperature is increased above $100^{o}C$, the half life values decrease rapidly. For example, the half life values for the sample irradiated to 4.5 Gy change by as much as 75% between 125 and $200^{o}C$ i.e from about 25 μs at $125^{o}C$ to about 6 μs at $200^{o}C$. In general, there is similarity in half life values for different doses over the whole temperature range (20 – $200^{o}C$). This is even so for half life values measured at $20^{o}C$, the initial measurements, and for values measured at $200^{o}C$ after a full heating cycle. These values are about 25 μs at $20^{o}C$ and about 6 μs at $200^{o}C$. The general conclusion from this set of results (Fig. 6.31 (a)) is that the luminescence half life values decrease with temperature and that the form of the decrease is independent of the amount of the beta irradiation in the range used, 4.5 – 150 Gy.

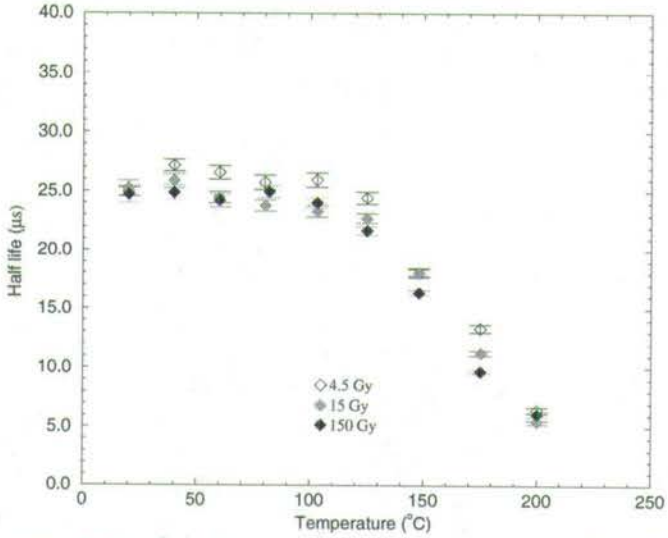

Figure 6.31 (a) Temperature–dependence of half lives measured from 20 to 200°C at 20°C intervals.

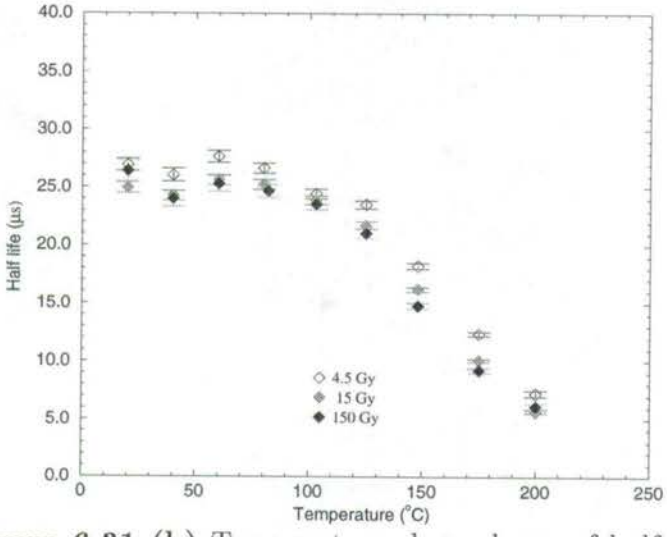

Figure 6.31 (b) Temperature–dependence of half lives measured from 200 to 20°C at 20°C intervals for the sample of Fig. 6.31 (a) above.

The temperature–related changes of half life in the repeat measurements

i.e 200 to 20°C is shown in Fig. 6.31 (b). Evidently there is good agreement between these results with those in Fig. 6.31 (a) for cycle 1 in terms of the change of half life with temperature, and in the values of half life at specific temperatures. Values of half life at any given temperature are also similar regardless of the immediate thermal history of the sample, at least for the two heating cycles used.

The results of Fig. 6.31 (b) confirm the conclusion that half life values in heated quartz under blue light stimulation decrease with temperature for stimulation of luminescence in the slow component region.

6.2.7 The effect of temperature on luminescence intensity at long stimulation times

The relationship between luminescence intensity and temperature has previously been the subject of many studies e.g [22, 46, 70]. However, the studies in this section were devoted to the effect of temperature on the intensity of blue light stimulated luminescence at long stimulation times.

Each sample was given a beta dose and preheated at 220°C for 5 minutes before measurement of luminescence time–spectra. Beta doses used were 4.5, 15 and 150 Gy. Only four of the 470 nm blue light emitting diodes were used for stimulation of luminescence. The LEDs were pulsed at a pulse width and duty cycle of about 11 μs and 12% respectively, and operated with a pulsed current of about 70 mA per LED. The measurements were made from 20 to 200°C in cycle 1 and from 200 to 20°C in cycle 2.

The time–resolved spectra were recorded in 20°C intervals between 20 and 200°C with a delay of 240 s at each temperature for samples to come up to temperature. A stimulation time of about 10 s was used at each measurement temperature. The value of luminescence intensity at each temperature was

obtained by integrating time–spectra over the entire dynamic range.

Figs. 6.32 shows the relationship between luminescence intensity and temperature in the slow component region for a sample of heated quartz dosed to 150 Gy before preheating and measurement of luminescence. It can be observed in this graph that the increase in temperature is accompanied by an increase in luminescence intensity, the maximum of which occurs at about $125°C$. In fact, from 20 to $125°C$, the luminescence intensity has approximately doubled. From 125 to $200°C$, the intensity decreases continuously. When the sequence of measurements is reversed i.e 200 to $20°C$, the form of the intensity – temperature graph is reproduced with the intensity again rising to a peak around $125°C$. The difference in intensity between each of the data points in cycles 1 and 2 represents the loss of luminescence mainly due to temperature. The change in luminescence intensity is easy to observe as any increase in luminescence is over a region of slow optical decay which is essentially flat over the measurement period. Thus in the slow component region, increase in measurement temperature from 20 to $200°C$ leads to a peak in the intensity–temperature graph with the maximum occurring at about $125°C$.

For comparison, measurements were made using dosed but unbleached samples to observe corresponding changes in the fast component region. In this test, the luminescence intensity from a sample under heating was compared to that from a sample under optical stimulation only at room temperature. The changes in luminescence intensity are compared in Fig. 6.33. It can be observed that under continual stimulation the luminescence is decreasing in the sample at constant temperature (as expected) as well as in the sample under heating. Up to about $100°C$ (the first 5 data points), the decrease in luminescence for the samples is similar. Then above $100°C$, the

luminescence for the sample under heating decreases more rapidly. This behaviour can be further clarified if the ratio of intensities from the heated to the unheated sample is plotted against the number of exposures as shown in Fig. 6.45. In this case, the ratio of intensities remains constant for the first 5 data points i.e 20 to $100^{o}C$ for the heated sample showing that the rate of decay of luminescence from the two samples is equivalent. Beyond $100^{o}C$, the faster fall in intensity from the heated sample causes the ratio of intensities to decrease rapidly as well.

Taken together, Figs. 6.33 and 6.34 show that in the fast component region, the decay of luminescence from samples measured with or without heating is virtually indistinguishable for the first $100^{o}C$ or so. Above $100^{o}C$, the decrease of luminescence intensity is more rapid as the temperature at which optical stimulation is made is increased.

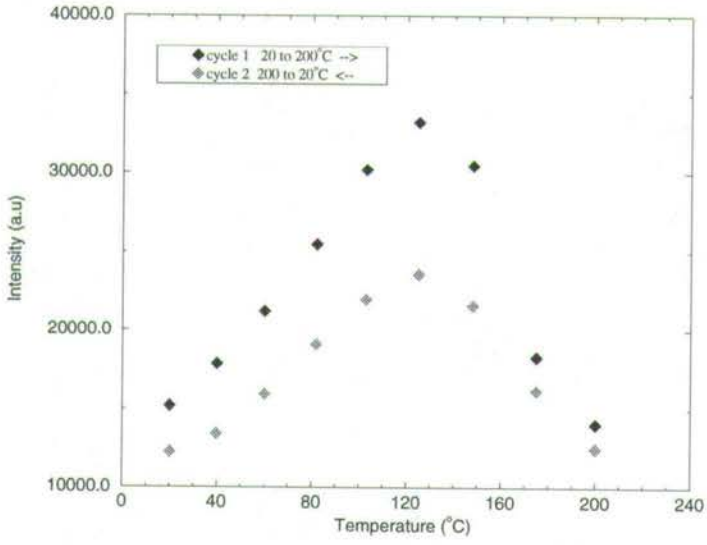

Figure 6.32 Change of luminescence intensity with temperature in the slow component region of quartz under pulsed blue LED stimulation.

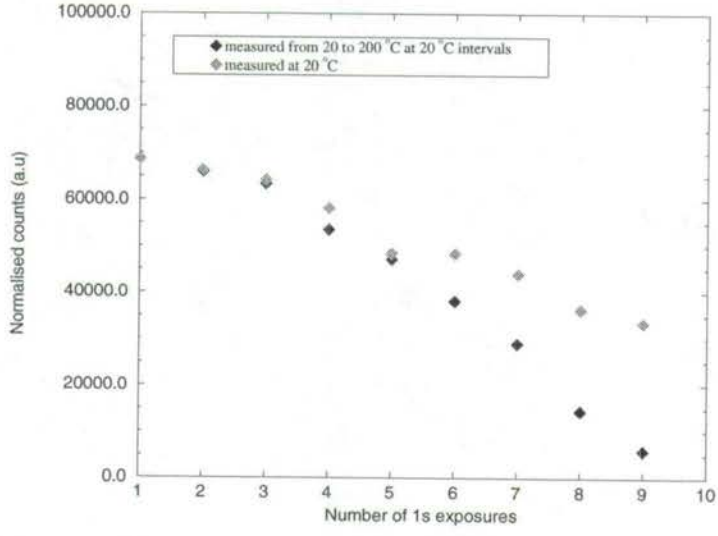

Figure 6.33 A comparison of the fall of luminescence with time in a sample under simultaneous heating and optical stimulation with that under optical stimulation only in the fast component region of heated quartz.

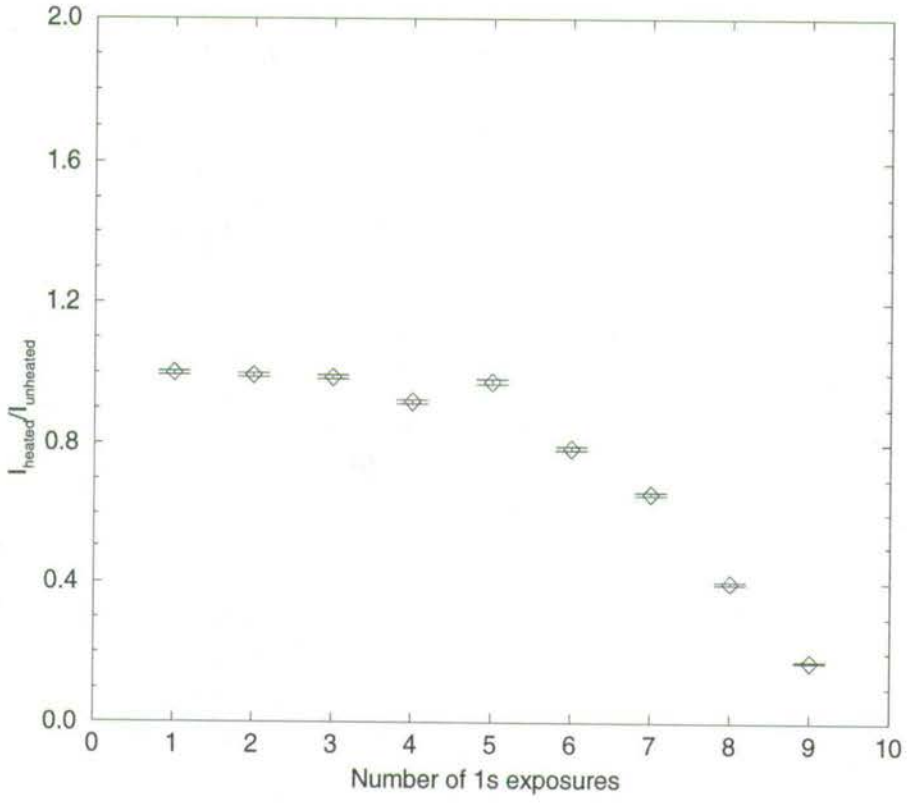

Figure 6.34 Ratio of intensities of luminescence stimulated from a sample under simultaneous heating and optical stimulation to that under optical stimulation only. The ratios are plotted against the number of 1 s exposures. The temperature of the heated sample was increased by $20°C$ per exposure.

Chapter 7

Discussion

This chapter summarises and discusses the experimental observations concerning the instrumentation developed for pulsed optical stimulation of luminescence from quartz and feldspar. The chapter also summarises characteristics of half lives from quartz reported and proposes some explanations to account for results obtained.

7.1 Pulsed optical stimulation of luminescence

The development and implementation of a pulsing system based on light emitting diodes for stimulation of luminescence has advantages of simplicity and economy compared with systems based on lasers [8, 10, 11, 12, 13].

Initially, the performance of the system was assessed by comparing, as shown in table 1 (section 5.5), values of half lives measured with this system with values of half life in published data for microcline and orthoclase [10, 11]. The values compared favourably and indicated that the system could provide reliable data. Half life values measured with the present system range from about 23 ns in feldspar (table 1, section 5.5) to 28 μs in quartz. The system

has been used over a wide range of pulse widths (25 ns (FWHM) – 30 μs) and dynamic ranges (40 ns to 64 μs). A critical factor in the use of pulse widths shorter than 25 ns was the speed with which the light emitting diodes could be switched on and off, the speed being affected by capacitance of the light emitting diodes, stray capacitance in cables and connecting wires, and the pulse rise and fall time of the open collector gates (2N7406) driving the light emitting diodes. For the gates, manufacturers data sheets specify pulse rise and fall times as 2 ns and 6 ns respectively. The overall pulse rise and fall times for a gate–interfaced light emitting diode were estimated to be about 10 and 25 ns respectively.

The luminescence stimulation and detection assembly described in section 3.5.2 and shown in Fig. 3.7 requires that no more than one photon be detected per light pulse. If multiple STOP pulses arrive after a START signal, the resulting time–resolved spectrum will be distorted leading to apparent but spurious half life values. This set–up then imposes a counting rate limitation on time–resolved spectra that can be used for half life analysis. This problem can, however, be overcome by use of a multi channel scaler capable of recording pulses even when more than one STOP pulse arrives after a START pulse. It should be appreciated that the problem of counting rates becomes relevant only at high doses e.g 150 Gy, otherwise the luminescence detection assembly (Fig. 3.7) can be used at doses typical for OSL applications. For example, Fig. 7.1 (a) shows time–resolved spectra recorded after different durations of optical bleaching (12,124, 250 and 750 s) and illustrates that a time–resolved spectrum can be recorded successfully even when the luminescence is only 0.2% of the initial luminescence signal and only a quarter of the scattered light level.

(a) (b)

Figure 7.1 (a) Time-resolved spectra recorded after different exposure time (12, 124, 250, 750 s) compared against the background signal. (b) the corresponding signal-to-background ratio values. The initial beta dose was 150 Gy followed by 5 minute preheating at 220 degrees C.

Fig. 7.1 (b) compares the signal to background ratio during the stimulating light pulse with the ratio after the end of the pulse. The signal–to–background ratio during the pulse is analogous to continuous stimulation since the build–up signal includes a component of the light–emitting–diode emission. The signal–to–background ratio after the pulse relates only to the luminescence and photomultiplier noise. From Fig. 7.1 (b) the signal–to–background ratio after the stimulating light pulse is always at least 12 times better than during the pulse.

The present system can be adapted for use over a wide range of wavelengths by simply fitting appropriate LEDs. Further, since the LEDs are pulsed independently, any number of LEDs can be selected for use.

7.2 Measurements of half life

This section summarises the pattern of results obtained using pulsed green and pulsed blue LED systems. Explanations are proposed to account for the results.

7.2.1 Time–dependent measurements of half life

This sections refers to results reported in sections 6.1.1 for stimulation by green LEDs and in section 6.2.1 for stimulation using blue LEDs. All measurements were made at room temperature. Luminescence half life values measured from samples of heated quartz increase with stimulation time from an initial value to a constant maximum value. This feature is observed under both pulsed green and blue LED stimulation. For the samples used in this test, the initial and final values of half life for both green and blue LED stimulation were about 20 μs and 26 μs respectively. The beta doses used

were 150 Gy for the sample under green LED stimulation and 4.5 Gy for the sample stimulated by blue LEDs.

In samples of daylight bleached quartz, the values of half life were constant with time at about 24 μs for luminescence stimulated by green light following a beta dose of 150 Gy. On the other hand, when using pulsed blue LEDs for stimulation, the luminescence half lives for samples dosed up to 15 Gy increased with time from about 18 to 25 μs. Thus under blue LED stimulation, the change of half life with time in daylight bleached quartz was similar to that observed in heated quartz.

7.2.2 The effect of radiation dose on luminescence half life

In these experiments, reported in sections 6.1.2 and 6.2.2 for green and blue LED stimulation respectively, the relationship of half life and stimulation time was investigated over a wider beta dose range.

The half lives measured from heated quartz increased with time from an initial to a final value. In heated quartz, the beta dose did not significantly influence the behaviour of half lives.

The half lives in samples of daylight bleached quartz under pulsed green LED stimulation were independent of the size of beta dose used. The half lives were constant at about 24 μs over 150 – 1500 Gy. With blue LED stimulation, on the other hand, the value of half life in daylight bleached quartz was constant only for samples dosed to 1.5 Gy. On moving from 1.5 Gy to 15 – 150 Gy, the half life values assumed the form of progressive increase with time from an initial to a final value. The general feature was that the half lives corresponding to the largest beta dose in a set extended from the lowest initial value to the largest final value of half life.

7.2.3 Influence of preheating procedure on half life

This section relates to experimental results reported in sections 6.1.3 (pulsed green LEDs) and in section 6.2.3 (pulsed blue LEDs). The common features of the previous section were, in general, replicated. For example, in all samples of heated quartz under green LED stimulation, half lives increased with time from an initial value to a final constant value. For preheating at $220°C$ for 1 hour, the half lives were constant at about 24 μs.

For stimulation of luminescence using pulsed blue light, half lives were observed to increase from an initial to a final value for all doses used and for preheating at $220°C$ for 5 minutes, 20 minutes and 1 hour.

These results indicated that the form of preheating used, except for preheating at $220°C$ for 1 hour in the green LED case, does not have a major impact on the time dependent characteristics of the half lives measured subsequently.

7.2.4 Time–dependent measurements of half life at higher temperatures

The time–dependent measurements of half life made at 80 and $150°C$ in addition measurements made at $20°C$ revealed how much the temperature of measurement affects the values of luminescence half life.

The characteristic form of half life as a function of stimulation time remained the same at 80 and $150°C$ as at $20°C$. For example, for heated quartz, half life values increased with time from an initial to a constant final value at all three temperatures. Neither did the temperature alter the time–related behaviour of half lives in daylight bleached quartz.

The changes that occurred due to the introduction of a higher measure-

ment temperature were in the values of half lives. Values of half lives calculated at and below $80°C$ differed from those calculated from time–resolved spectra recorded at $150°C$.

In heated quartz, maximum values at 20 and $80°C$ were all within 26 ± 2 μs for stimulation by either blue or green light. At $150°C$, the maximum half life value was lower, within 17 ± 2 μs for both green and blue LED stimulation.

The half life values measured from samples of daylight bleached quartz at both 20 and $80°C$ under both pulsed green and pulsed blue stimulation were dominantly of the order of 25 ± 2 μs. At the higher temperature of $150°C$, the values corresponding to green and blue LED stimulation were about 20 μs and 13 μs respectively.

7.2.5 Temperature dependent measurements of half life at long stimulation times

In order to investigate further the influence of temperature of measurement on half life, time–resolved spectra for half life analysis were recorded from samples held at temperatures in the range $20 - 200°C$ as described in sections 6.1.5, 6.2.5 and 6.2.6. The luminescence from all the samples was bleached down to the slow component region before measurements of time–resolved spectra.

In general, half life values were observed to decrease with temperature from about 20 μs at $20°C$ to about 5 μs at $200°C$. In samples of quartz under green LED stimulation, the decrease was monotonic from 20 to $200°C$. The rate of decrease of half life as a function of temperature of measurement was considerably faster for measurements made above $125°C$ for heated quartz and above $80°C$ for daylight bleached quartz.

For samples of heated quartz in which luminescence was stimulated by pulsed blue LEDs, values of half life were constant at about 26 μs, within experimental scatter, between 20 and 100°C. Above 100°C, half lives decreased at a comparatively faster rate down to about 6 μs at 200°C. However, samples in green LED stimulation had been given a higher dose of 150 Gy in comparison with a dose of only 4.5 Gy for samples measured on the blue LED pulsing assembly. A further investigation using blue LEDs in which samples were dosed to different doses (4.5, 15 and 150 Gy) indicated that the form of half life against temperature was independent of initial dose.

Thus except for differences in the rate at which half lives decreased, the data indicated that increasing the temperature of measurement leads to a decrease in values of half lives. In general, the rate of decrease is greater for temperatures above 100°C.

7.3 Measurements of luminescence intensity

7.3.1 The effect of temperature on luminescence intensity at long stimulation times

The relationship between luminescence intensity and measurement temperature was studied in the slow component region of quartz stimulated by pulsed green LEDs (section 6.1.6) and by pulsed blue LEDs (section 6.2.7).

In the slow component region, the optical depletion rate is so slow that changes in intensity introduced by temperature could easily be monitored. It was observed that the intensity of luminescence increased with temperature initially and as the temperature was increased further, the intensity of the luminescence decreased. It was also observed, using blue LEDs for stimu-

lation, that the intensity of luminescence produced a peak as a function of temperature whether the sequence of measurements were made from 20 to $200°C$ or *vice–versa*. The same form of an intensity peak was obtained when measurements were repeated on the same sample from 20 to $200°C$ using green LEDs for stimulation. The peak temperatures could well be approximated as $148 \pm 10°C$ under pulsed green LED stimulation and $125 \pm 10°C$ under pulsed blue light stimulation.

A comparison was made in the fast component region of the luminescence for two samples; one with stimulation while under heating and the other with optical stimulation only. It was found that in the first $100°C$, the decrease in intensity for the two samples was virtually indistinguishable. Above $100°C$, luminescence for the sample under concurrent heating and optical stimulation decreased at a comparatively faster rate.

7.4 Models

The changes in half life with either temperature or time present a complex problem with multiplicity of factors influencing changes. The emission of luminescence following optical stimulation has been interpreted in various ways. For example the emission has been explained in terms of radiative recombination centres only one of which participates in emission of luminescence [71], or in terms of loss of electrons from an electron trap [20, 21] or loss of electrons from several traps [25]. Thus there is no consensus as to which model describes the process of optical stimulation of luminescence as sometimes the models appear contradictory.

In this thesis, explanations are proposed so as to be consistent with experimental results obtained, namely

1. that half lives increase with time from an initial to a final value
2. that half life values obtained at and below $80°C$ are higher than values obtained at $150°C$
3. that luminescence half lives generally decrease as the temperature of measurement is increased
4. the fact that the intensity of the slow component of luminescence goes through a peak as the temperature is increased in the range $20 - 200°C$.

7.4.1 Changes in half life

The time–resolved spectra in this study measure the delay between stimulation and emission of luminescence. It is assumed in this thesis that luminescence follows the recombination of electrons which have been de–trapped optically. In view of this, a possible schematic diagram for movement of electrons is shown in Fig. 7.2 to explain the changes in half life and intensity of luminescence which were observed experimentally. The energy band diagram has been adapted from that proposed by Murray and Wintle [24] to account for the shapes of decay curves from quartz.

In Fig. 7.2 luminescence is stimulated from the main OSL trap assumed in this case to be the trap usually associated with the emission of TL at $325°C$ [21]. Since continual stimulation of luminescence, leading to a decrease of luminescence, is accompanied by the appearance of photo–transferred thermoluminescence (PTTL) (section 2.1 and also [24]), the model requires traps responsible for the PTTL e.g the $110°C$ trap as well others responsible for re–trapping. PTTL occurs at the $110°C$ TL position as well as at $160°C$ in quartz e.g [24]. For clarity only two traps at which electrons can get re–trapped are shown, one responsible for PTTL at $110°C$ and a second one to

account for other re–trapping processes. Also it was shown that the $110°C$ and the $325°C$ TL peaks are more sensitive to luminescence stimulation by light than the $160°C$ PTTL peak [24].

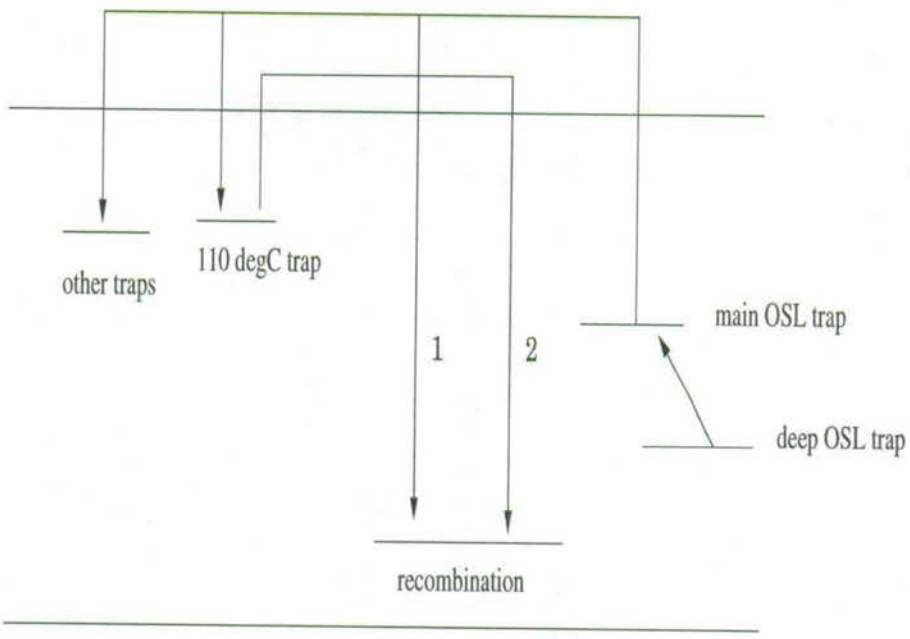

Figure 7.2 A schematic diagram to explain changes in half life and luminescence intensity in quartz.

Thus the process of luminescence emission can then be described simultaneously by process 1 (direct recombination) or process 2 (recombination with a re–trapping stage in between).

Initially, following beta dose and preheating, the main OSL trap has a large concentration of electrons. The lower temperature traps including the $110°C$ TL trap should be empty as the sample would have been held at

$220°C$ before measurement of the first time–resolved spectrum. Thus at the beginning of stimulation, process 1 is dominant. This appears quantitatively as the short half life values. The time (total stimulation time) during which this process is dominant is relatively short in comparison with the total time over which the experiments were made. For example, about 100 s in Fig. 6.7 for heated quartz under green light stimulation and about 30 s for stimulation by blue light (Fig. 6.19). As the total time of optical stimulation increases, the concentration of electrons in the $110°C$ trap builds up due to the phototransfer effect and that in the main OSL trap decreases rapidly. A stage is then reached where electrons are being excited from the $110°C$ trap in addition to a diminishing contribution from the main OSL trap. Presumably because the optical stimulation from the shallow trap is less efficient, the half life is correspondingly longer. As pathway 2 increases in importance the ensuing delay then accounts for the increase in half life values with time. Although both processes occur simultaneously, the measured time–resolved spectra after each count is assumed to represent the average of measured half lives associated with charge transfer from the $110°C$ TL trap or the main OSL trap. The time–resolved spectrum then reflects the dominant one of these effects.

At temperatures above $110°C$, the $110°C$ TL trap and other shallow traps will be kept empty and thus the delay will be avoided. One then expects the half life values at temperatures above $110°C$ to be always shorter than values measured below $110°C$. Thus that half lives at 20 and $80°C$ are longer than values above $110°C$ (e.g Fig. 6.7, Fig. 6.27) is consistent with this argument. It was also observed in Fig. 6.7 and Fig. 6.27 that half life values at $150°C$ also went through an increasing stage before reaching a constant maximum value. This would require presence of re–trapping at other sites to account

for this or presence of some intermediate delaying stage. It is not certain what this would be. It is assumed in Fig. 7.2 that such a delay stage is subsumed in what is labelled 'other traps'.

7.4.2 Decrease of half life with temperature at long stimulation times

The dynamic temperature measurements present a temperature resolved set of half life values. Measurements were made in the slow component region where recombination pathway 2 (recombination via a delay stage) should have applied at the beginning of the measurements. This is because the preceding optical exposure aimed at reducing the luminescence intensity to the slow component will also have led to transfer of charge to shallow traps including the $110°C$ TL trap. If one assumes that the $110°C$ trap is the major trap involved in re–trapping, it would be expected that half lives measured above and below this temperature would differ. Thus below $110°C$, half life values should be of the order of values obtained at room temperature in the slow component region. A possible association therefore emerges between this assumption and values in heated quartz under blue LED stimulation in the slow component region at 20 and $80°C$ i.e 25 ± 1 μs and the value of 26 $\pm$ 1 μs obtained in dynamic temperature recording of time–resolved spectra in a similar temperature range. In general, this comparison should apply for samples bleached to a similar level into the slow component.

Above $110°C$, the continual decrease of half life with temperature should be the result of several effects such as empty shallow traps e.g the $110°C$ which might otherwise trap electrons and delay the subsequent emission of luminescence. The other could be due to thermally assisted optical stimulation which would make the stimulation–emission process more effective.

An alternative model to augment the present one still being explored [72] is concerned with spatial distribution of electron traps each with a cluster of associated recombination centres. Initially, as the rate of charge de-trapping increases due to optical stimulation, the frequency of recombinations at centres in the neighbourhood of the trap are high. This is shown quantitatively as short half lives at the beginning of measurement. With time more and more recombinations occur further out and it is possible that the limiting values of half life observed simply indicate limits of charge movement in the lattice. The decrease of half life with temperature on the other hand could still be associated with such effects as presence of empty shallow traps and thermally assisted optical stimulation which would make the stimulation-emission process more efficient.

7.4.3 Temperature–related changes in luminescence intensity at long stimulation times

The temperature–related changes in luminescence intensity have been discussed by several workers e.g by Spooner [21] who presented luminescence curves as a function of temperature from about $-100^{o}C$ to $200^{o}C$ and by Murray and Wintle [24] who studied decay curves at elevated temperatures. The curves in the earlier work [21] increased with temperature to a maximum and fell again as the temperature was further increased.

In this thesis, temperature–related changes in luminescence intensity were studied in the slow component (Fig. 6.32) and in the fast component (Fig. 6.33). It was found that in the fast component region, increase in temperature above $110^{o}C$ leads to a much more rapid reduction in intensity of luminescence than that observed at room temperature while in the slow component, increase in temperature produces a peak in the intensity measured as a func-

tion of temperature. Further, the nature of half lives in the fast component are different from those in the slow component. These differences suggest that processes of luminescence emission in the fast and the slow component regions may be different.

In a related study, Bailey *et al* [23] measured the luminescence as a function of beta dose from a sample of quartz and extracted growth curves for each of the three components (fast, medium and slow) in addition to studying how bleaching affected each of the three components. Based on this and other past experiments e.g [20] they suggested that the mechanism of luminescence emission applicable to the fast and medium components may be different to that responsible for emission of luminescence in the slow component region. In particular, they suggested that the fast and medium components may be associated with the $325°C$ TL trap and the slow component may not be. Bailey *et al* [23] then proposed an energy band diagram in which luminescence corresponding to each of the three components originates from three different traps.

Alternatively, it is possible to assume the presence of a deep trap from which charge can escape only slowly to the main OSL trap. Thus this trap is assumed to be partly responsible for the emission of luminescence in the slow component region with the total sum measured also including contribution from shallow traps such the $110°C$ TL trap. The relationship of luminescence intensity and temperature i.e the intensity peak, can then be explained on this basis.

The emission of luminescence due to optical stimulation in the slow component proceeds at a slow rate. This rate was estimated for green LED stimulation in section 6.1.6 to be only 0.01% s^{-1}. It is proposed that the electron population responsible for the emission of luminescence in the slow

component originate mostly from a deep trap. This charge has access to the main OSL trap from which it can be stimulated directly to cause luminescence. If it is assumed further that the transfer of charge from the deep trap to the main OSL trap proceeds only inefficiently , then once initial luminescence has been depleted down to the slow component, the electron population in the main OSL trap will remain more or less constant.

As the temperature of the sample is increased, thermal assistance of luminescence stimulation at both the main and the shallow traps becomes important. Most charge would originate from the trap with the larger electron population (in this case the $110°C$ TL trap) in addition to a small but steady contribution from the main OSL trap. As temperature is increased further the contribution from the shallow trap must fall and so that overall the measured luminescence should reach a maximum. Beyond, the maximum, the only contribution should be the small constant emission from the deep trap via the main OSL trap. However, it was observed experimentally that, beyond the maximum, the intensity actually continually decreased. There are several possible explanations for the decrease in luminescence intensity. If the contribution from the main OSL trap is negligible, as it seems, then once the contribution from shallow traps ceases, the luminescence intensity must decrease.

The decrease of luminescence with temperature has also been discussed by other workers e.g Spooner [21] as being due to thermal quenching i.e increased non–radiative de-excitation of a luminescence centre as the temperature is increased. The decrease of luminescence intensity beyond $100°C$ could be evidence for the effect of thermal quenching.

7.5 Thermal quenching

The temperature dependence of luminescence lifetimes can also be explained from thermal quenching of the luminescence at the luminescence centre [73].

The measured lifetimes are closely linked with the emitted luminescence which in turn is affected by probabilities of radiative and non–radiative transitions [73]. If the probability of radiative recombination is assumed to be independent of temperature, and that of non–radiative recombination is related to temperature by the factor exp(−ΔE/kT) [14, 73], the change of luminescence lifetime as a function of temperature may be expressed as:

$$\tau = \frac{\tau_o}{1 + Ce^{\frac{-\Delta E}{kT}}} \tag{7.1}$$

where τ_o is the radiative lifetime which by definition extrapolates to absolute zero of temperature, ΔE is the thermal activation energy of quenching (on transition CE of Fig. 2.5), k is Boltzmann's constant, T is absolute temperature and C is a constant related to the effective density of states [74].

Fig. 7.3 shows the data of cycle 1 in Fig. 6.29 fitted by the thermal quenching function. The values of ΔE and C evaluated from the best fit to the experimental data are 0.64 ± 0.03 eV and 2.72 x 10^7 respectively. These values can be compared with similar values evaluated from temperature related changes in luminescence intensity published elsewhere e.g ΔE = 0.636 ± 0.03 eV, C = 3.4 x 10^7 [24], ΔE = 0.60 eV, C = 7.9 x 10^6 [75].

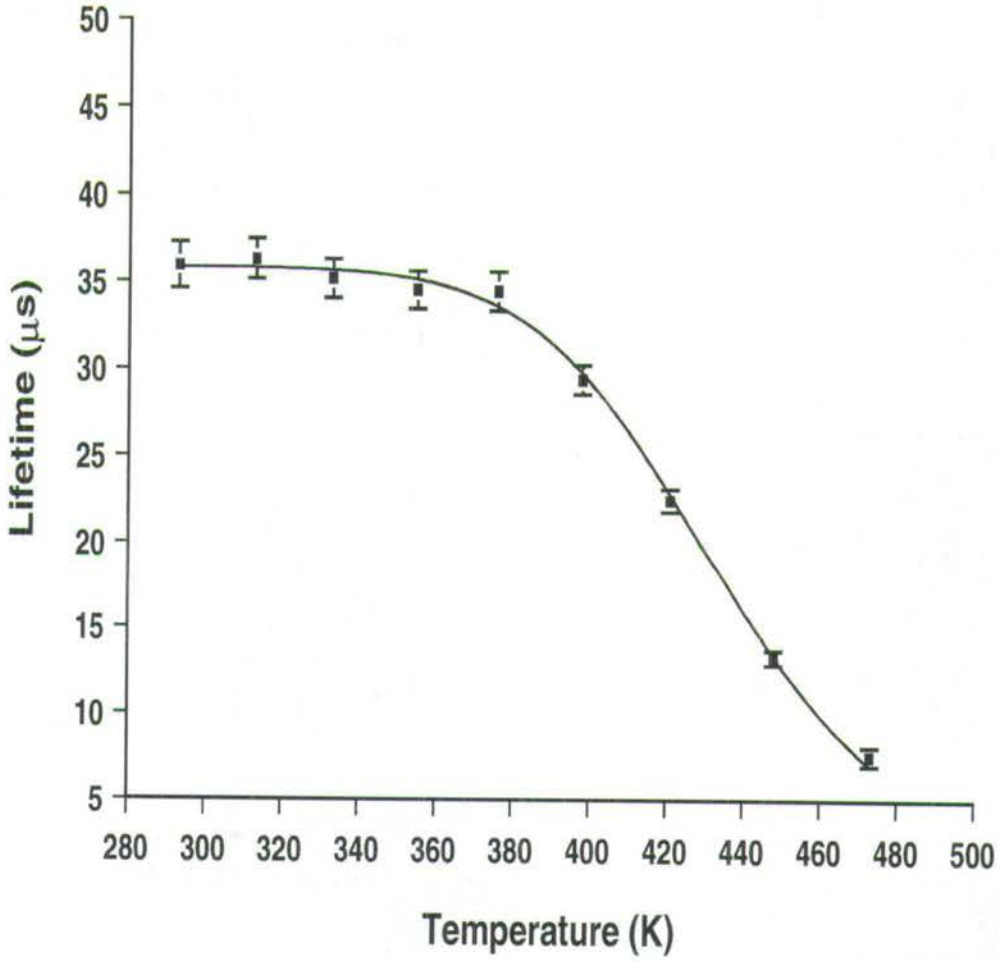

Figure 7.3 Change of luminescence lifetime against temperature (also plotted earlier as cycle 1 of Fig. 6.29). The solid line is the best fit of the thermal quenching equation.

Luminescence half lives measured from quartz have been studied using pulsed green and pulsed blue LED systems. Samples of quartz bleached by heating to $500°C$ and also by exposure to daylight were used in this study. Experimental results show that half lives in quartz are in the range 20 to 30 μs. The values of half lives are considerably shortened at high temperature, reaching for instance about 5 μs at $200°C$.

In general, half lives were observed to increase with stimulation time, for example at room temperature from an initial value within 20 ± 2 μs to a final constant value within 26 ± 2 μs. The exception was in samples of daylight bleached quartz under green light stimulation where half lives were independent of stimulation time (e.g 24 ± 1 μs at room temperature). It was also observed that half lives decreased with temperature. For example, for stimulation using blue LEDs, the values decreased from 24 ± 1 μs to a minimum of 6.5 ± 0.3 μs, and from 20.0 ± 0.3 μs to 5.0 ± 0.2 μs using green light stimulation. The decrease of half lives was independent of the dose that the sample had been given prior to measurement of luminescence.

It is suggested that both time- and temperature–related changes in half life as well as changes in luminescence intensity with time or temperature may be explained in terms of a model in which electron re–trapping, especially by the $110°C$ trap is significant. It is also presumed that luminescence in the slow component of quartz is due to the presence of a deep trap which empties only slowly with the charge having access to the main OSL trap. These explanations are proposed to be consistent with results presented in this thesis.

In conclusion, this thesis has demonstrated that studies of pulsed optical stimulation of luminescence from feldspar and quartz for half life analysis are possible using a light emitting diode based pulsing system.

References

[1] Huntley D J Godfrey-Smith D I and Thewalt M L 1985 Optical dating of sediments *Nature* **313** 105 – 7

[2] Hütt G Jaek I and Tchonka J 1988 Optical dating: K-feldspar optical stimulation response spectra. *Quat. Sci. Rev.* **7** 381 – 6

[3] Poolton N R J and Bailiff I K 1989 The use of LEDs as an excitation source for photoluminescence dating of sediments *Ancient TL* **7** 18 – 20.

[4] Galloway R B 1992 Towards the use of green light emitting diodes for the optically stimulated luminescence dating of quartz and feldspar *Meas. Sci. Technol.* **3** 330 – 5

[5] Hong D G and Galloway R B 1999 Comparison of equivalent dose values determined by luminescence stimulation using blue and green light emitting diodes *Nucl. Instrum. Meth. B* 59 – 64

[6] Bøtter-Jensen L, Mejdahl V and Murray A S 1999 New light on OSL *Quat.Sci. Rev.* **18** 303 – 309

[7] Bøtter-Jensen L 1997 Luminescence techniques: Instrumentation and methods. *Radiat. Meas.* **27** 749 – 768

[8] McKeever S W S Alkselrod M S and Markey B G 1996 Pulsed optically stimulated luminescence dosimetry using α-Al_2O_3 *Radiat. Prot. Dosim.* **65** 267 – 272

[9] Bulur E and Göksu H Y 1997 Pulsed optically stimulated luminescence from α-Al_2O_3 using green-light-emitting diodes. *Radiat. Meas.* **27** 479 – 488

[10] Clark R J Bailiff I K and Tooley M J 1997 A preliminary study of time-resolved luminescence in some feldspars *Radiat. Meas.* **27** 211–220

[11] Clark R J and Bailiff I K 1998 Fast time-resolved luminescence spectroscopy in some feldspars *Radiat. Meas.* **29** 553 – 560

[12] Sanderson D C W and Clark R J 1994 Pulsed photostimulated luminescence of alkali feldspars *Radiat. Meas.* **23** 633–9

[13] Markey B G Colyott L E and McKeever S W S 1995 Time-resolved optically stimulated luminescence from α-Al_2O_3 *Radiat. Meas.* **24** 457 – 463

[14] McKeever S W S 1985 *Thermoluminescence of solids* (Cambridge: Cambridge University Press)

[15] Aitken M J 1985 Thermoluminescence dating (London: Academic Press)

[16] Aitken M J 1998 An Introduction to Optical dating (Oxford: Oxford Science Publications)

[17] Chen R and McKeever S W S 1997 Theory of thermoluminescence and related phenomena (Singapore: World Scientific Publishing)

[18] McKeever S W S and Chen R 1997 Luminescence models *Radiat. Meas.* **27** 625 – 661

[19] Smith B W, Aitken M J, Rhodes E J, Robinson P D and Gerald D M 1986 Optical dating:methodological aspects *Radiat. Prot. Dosim.* **17** 229 – 233

[20] Smith B W and Rhodes E J 1994 Charge movements in quartz and their relevance to optical dating *Radiat. Meas.* **23** 329 – 333

[21] Spooner N A 1994 On the optical dating signal from quartz *Radiat. Meas.* **23** 593 – 600

[22] Wintle A G and Murray A S 1997 The relationship between quartz thermoluminescence, photo-transferred thermoluminescence, and optically stimulated luminescence *Radiat. Meas.* **27** 611 – 624

[23] Bailey R M, Smith B W and Rhodes E J 1997 Partial bleaching and the decay form characteristics of quartz OSL *Radiat. Meas.* **27** 123 – 136

[24] Murray A S and Wintle A G 1998 Factors controlling the shape of the decay curve *Radiat. Meas.* **29** 65 – 79

[25] Huntley D J, Short M A and Dunphy K 1996 Deep traps in quartz and their use for optical dating *Can. J. Phys.* **74** 80 – 91

[26] Milanovich–Reichhalter I and Vana N 1990 Phototransferred thermoluminescence in quartz *Radiat. Prot. Dosim.* **33** 211 – 213

[27] Chithambo M L and Galloway R B 2000 A pulsed light emitting diode system for stimulation of luminescence. *Meas. Sci. Technol.* **11** 418 – 424

[28] Galloway R B Unpublished notes and Private communication

[29] Bailiff I K Private communication

[30] Bube R H 1992 *Electrons in solids* (Boston: Academic Press)

[31] Kirsh Y 1992 Kinetic analysis of thermoluminescence *phys. stat. sol.* **129** 15 – 48

[32] Galloway R B 1990 Notes on a recently constructed TL system *Ancient TL* **8**, 10 – 1

[33] Galloway R B 1991 A versatile 40–sample system for TL and OSL investigations *Nucl.Tracks. Radiat. Meas.* **18** 265 – 271

[34] Galloway R B, Hong D G and Napier H J 1997 A substantially improved green-light-emitting diode system for luminescence stimulation *Meas. Sci. Technol.* **8** 267 – 271

[35] Mills A A, Sears D E and Hearsey R 1977 Apparatus for the measurement of thermoluminescence *J. Phys. E: Scientific Instruments* **10** 51 – 6

[36] Huntley D J, Godfrey–Smith D I and Thewalt M L W 1988 Some quartz thermoluminescence spectra relevant to thermoluminescence dating *Nucl. Tracks. Radiat. Meas.* **14** 27 – 33

[37] Liritzis Y and Galloway R B 1990 Bremsstrahlung from a shielded beta irradiator *J.Radioanal.Nucl.Chem.,Letters* **146** 333 – 345

[38] Wintle I K 1997 Luminescence dating: Laboratory procedures and protocols *Radiat. Meas.* **27** 769 – 817

[39] Spooner N A, Prescott J R and Hutton J T 1988 The effect of illumination wavelength on the bleaching of thermoluminescence (TL) of quartz *Quat. Sci. Rev.* **7** 325 – 330

[40] Bøtter-Jensen L, Duller G A T and Poolton N R 1994 Excitation and emission spectrometry of stimulated luminescence from quartz and feldspars *Radiat. Meas.* **23** 613 – 6

[41] Bøtter-Jensen L and Duller G A T 1992 A new system for measuring OSL from quartz samples *Nucl. Tracks. Radiat. Meas.* **20** 549–553

[42] Bailiff I K 1993 Measurement of the stimulation spectrum (1.2–1.7 eV) for a specimen of potassium feldspar using a tunable solid state laser *Radiat. Prot. Dosim.* **47** 649–653

[43] Bailiff I K and Barnett 1994 Characteristics of infrared-stimulated luminescence from a feldspar at low temperatures *Radiat. Meas.* **23** 541–545

[44] Kleitz W 1996 *Digital Electronics* (New Jersey: Prentice Hall) p 504

[45] Short M A and Huntley D J 1992 Infrared stimulation of quartz *Ancient TL* **10** 19 – 21

[46] Galloway R B 1993 Stimulation of luminescence using green light emitting diodes *Radiat. Prot. Dosim.* **47** 679 – 682

[47] Wintle A G 1993 Recent developments in optical dating of sediments *Radiat. Prot. Dosim.* **47** 627 – 635

[48] Rhodes E J 1988 Methodological considerations in the optical dating of quartz *Quat. Sci. Rev.* **7** 395 – 400

[49] Wintle A G and Murray A S 1998 Towards the development of a preheat procedure for OSL dating of quartz *Radiat. Meas.* **29** 81 – 94

[50] Li S H 1991 Removal of the thermally unstable signal in optical dating of K – feldspar *Ancient TL* **9** 26 – 9

[51] Galloway R B and Hong D G 1996 Concerning the normalization of additive dose optically stimulated luminescence from quartz *Ancient TL* **14** 1 – 5

[52] Wolfe S A, Huntley D J and Ollerhead J 1994 Recent and late Holocene sand dune activity in Southern Saskatchewan. In *Current Research 1995-B; Geological Survey of Canada* 131 – 140

[53] Stokes S 1992 Optical dating of young (modern) sediments using quartz: results from a selection of depositional environments *Quat. Sci. Rev.* **11** 153 – 9

[54] Murray A S, Roberts R G and Wintle A G 1997 Equivalent dose measurements using a single aliquot of quartz *Radiat. Meas.* **27** 171 – 184

[55] Stokes S 1996 Preheats, palaedoses and paradigms in the optical dating of quartz *Ancient TL* **14** 5 – 8

[56] Duller G A T 1991 Equivalent dose determination using single aliquots. *Nucl. Tracks. Radiat. Meas.* **18** 371 – 8

[57] Godfrey–Smith D I, Huntley D J and Chew W 1988 Optical dating studies of quartz and feldspar sediment extracts *Quat. Sci. Rev.* **7** 373 – 380

[58] Ditlefsen C and Huntley D J 1994 Optical excitation of trapped charges in quartz, potassium feldspars and mixed silicates: the dependence on photon energy. *Radiat. Meas.* **23** 675 – 682

[59] Huntley D J, McMullan W G, Godfrey-Smith D I and Thewalt M L W 1989 Time-independent recombination spectra rising from optical ejection of trapped charges in feldspars *J.Lumin.* **44** 41 – 6

[60] Jungner H and Huntley D J 1991 Emission spectra of some potassium feldspars under 633 nm stimulation. *Nucl. Tracks. Radiat. Meas.* **18** 125 – 6

[61] Barnett S M and Bailiff I K 1997 Infrared stimulation spectra of sediments containing feldspars *Radiat. Meas.* **27** 237 – 242

[62] Huntley D J, Godfrey-Smith D I and Haskell E H 1991 Light–induced emission spectra from some quartz and feldspars *Nucl. Tracks. Radiat. Meas* **18** 127 – 131

[63] Scholefield R B, Prescott J R, Franklin A D and Fox P J 1994 Observations on some thermoluminescence emission centres in geological quartz *Radiat. Meas.* **23** 409 – 412

[64] Krbetschek M R, Rieser U and Stolz W 1996 Optical dating: some dosimetric properties of natural feldspars *Radiat. Meas.* **66** 407 – 412

[65] Galloway R B 1996 Equivalent dose determination using only one sample: alternative analysis of data obtained from infrared stimulation of feldspars *Radiat. Meas.* **26** 103 – 6

[66] Galloway R B 1994a On the stimulation of luminescence with green light emitting diodes *Radiat. Meas.* **23** 547 – 550

[67] Galloway R B 1994b Comparison of the green and infrared stimulated luminescence of feldspar *Radiat. Meas.* **23** 617 – 620

[68] Galloway R B and Napier H J 1994 The influence of sample treatment on feldspar dose response *Ancient TL* **12** 43 – 8

[69] Cutter J Galloway R B Hodgson J C and Napier H J 1994 A test of the single aliquot method of dose determination for feldspar stimulated by green light *Ancient TL* **12** 24– 7

[70] Smith B W, Rhodes E J, Stokes S, Spooner N A and Aitken M J 1990 Optical dating of sediments: Initial quartz results from Oxford. *Archaeometry* **32** 19 – 31

[71] McKeever S W S 1994 Models for optical stimulation of thermoluminescence in sediments *Radiat. Meas.* **23** 267 – 276

[72] Chithambo M L and Galloway R B Temperature dependence of luminescence time–resolved spectra from quartz *Radiat. Meas.* In press

[73] Swank R K and Brown F C 1963 Lifetime of the excited F center *Phys. Rev* **130** 34 – 41

[74] Liu J P, Kong M Y, Si J J, Huang D D, Liu J P, Sun D Z 1988 *J.Phys.D: Appl. Phys.* **31** 85 – 87

[75] McKeever S W S, Bøtter-Jensen L, Agersnap Larsen N, and Duller G A T 1997 *Radiat. Meas.* **27** 161 – 170